Treball de Fi de Màster

MÀSTER UNIVERSITARI EN ENGINYERIA NUCLEAR

Thermal-hydraulic analysis of the ITER Electron Cyclotron Upper Launcher Antenna

MEMÒRIA

Autor: Roger Pijoan Fusté
Director: Alfredo de Blas del Hoyo

Convocatòria: Juny 2018

Escola Tècnica Superior
d'Enginyeria Industrial de Barcelona

Index

Table of Figures

Table of Tables

ABSTRACT

Master thesis about the study of the behaviour of the cooling performance of the ITER Electron Cyclotron Upper-Launcher Antenna, through CFD (Computational Fluid Dynamics) simulations with Ansys Fluent, trying to reproduce in 3D and in real scale its operation.

Two different analyses have been done. On the one hand a steady-state thermal-hydraulic CFD analysis, in order to study and analyse the behaviour of the Antenna under its operation conditions, to detect the critical zones where the material limits are reach and where the requirements from ITER Organisation are not fulfilled. On the other hand, a thermal-mechanical transient analysis in order to detect possible temperature inertia between pulses on the ITER inductive operation, and to verify that using an steady-state CFD analysis the results are good enough, and there is no need to use a transient analysis where the complexity of the simulation I highly increase.

Based on the results obtained in this project, it is concluded that the cooling performance of the BSM works properly except some temperature peaks, which ones with simply design modifications or material changes are expected to be mitigated. Moreover, the possibility of temperature inertia has been refused and that a steady-state analysis represents a conservative approach compere with a transient one.

The studies in CFD increasingly are gaining more prominence in the world of industry thanks to its great reliability and precision of its results while simulating the different phenomena that occur in reality, in a fast and economical way. However, it should be noted that these studies are not 100% reliable and it is recommended validate and verify them with sensitivity analysis and experimental data.

RESUM

Treball de fin de màster sobre l'estudi del sistema de refrigeració de " ITER Electron Cyclotron Upper-Launcher Antenna", a través de simulacions CFD amb Ansys Fluent, intentant reproduir en 3D i a escala real el seu funcionament.

S'han realitzat dos anàlisis diferents. D'una banda, un anàlisi de CFD tèrmic-hidràulic estacionari per estudiar i analitzar el comportament de l'antena en les seves condicions d'operació, amb l'objectiu de detectar les zones crítiques on els límits de materials son excedits i on els requisits de "ITER Organisation" no són complerts. D'altra banda, una anàlisi transitòri termo-mecànic per detectar possibles acumulacions de temperatura entre polsos durant l'operació inductiva d'ITER. La finalitat d'aquest darrer anàlisis és verificar que els resultats en estat estacionari són suficientment bons, i per tant, no hi ha necessitat d'utilitzar un anàlisi transitori on la complexitat de la simulació augmenta considerablement.

En base els resultats obtinguts en aquest projecte, es conclou que el el sistema de refrigeració de la BSM funciona correctament, excepte per alguns pics de temperatura, els quals amb modificacions del disseny o canvi de materials s'espera que es mitiguin. A més a més, s'ha refusat la possibilitat d'acumulacio de temperatura en una operació pulsativa, un anàlisi estacionari representa un enfocament conservador i coherent amb un de transitori.

Els estudis de CFD cada vegada són més destacats en el món de la indústria, gràcies a la seva gran fiabilitat i precisió en els resultats, de forma ràpida i econòmica. No obstant això, cal assenyalar que aquests estudis no són 100% fiables i es recomana validar-los i verificar-los amb anàlisis de sensibilitat i dades experimentals.

RESUMEN

Trabajo de final de máster sobre el estudio del sistema de refrigeración de "ITER Electron Cyclotron Upper-Launcher Antenna", a través de simulaciones CFD con Ansys Fluent, intentando reproducir en 3D y en escala real su funcionamiento.

Se han realizado dos análisis diferentes. Por un lado, un análisis CFD térmico-hidráulico estacionario, para estudiar y analizar el comportamiento de la antena en sus condiciones de operación con el objetivo de detectar las zonas críticas donde los límites de materiales son excedidos y donde los requisitos de "ITER Organisation" no son cumplen. Por otro lado, un análisis transitorio termo-mecánico para detectar posibles acumulaciones de temperatura entre pulsos durante la operación inductiva de ITER con la finalidad de verificar que los resultados en estado estacionario son suficientemente buenos y por lo tanto no hay necesidad de utilizar un análisis transitorio donde la complejidad de la simulación aumenta considerablemente.

Basándose en los resultados obtenidos en este proyecto, se concluye que el sistema de refrigeración de la BSM funciona correctamente, excepto por algunos picos de temperatura, los cuales con modificaciones del diseño o cambio de materiales se espera que se mitiguen. Además, se ha rechazado la posibilidad de acumulación de temperatura debido a una operación pulsativa, un análisis estacionario representa un enfoque conservador y coherente con uno transitorio.

Los estudios de CFD cada vez son más destacados en el mundo de la industria, gracias a su gran fiabilidad y precisión en los resultados, de forma rápida y económica. Sin embargo, hay que señalar que estos estudios no son 100% fiables y se recomienda validarlos y verificarlos con análisis de sensibilidad y datos experimentales.

DEDICATION AND ACKNOWLEDGMENTS

First of all, I would like to thank my TFM tutor, Alfredo de Blas del Hoyo, for his help and cooperation at all times, whenever I need it, he has not hesitated to take care of me and to help me in the best way possible . It has been a great guide for the realization of the TFM.

Secondly, I would like to thank my colleagues from Fusion for Energy, mainly to my both supervisors, Ferran Albajar Viñas and Francesca Cau for their help and guidance during my traineeship. And thank the Antennas and Plasma Engineering Unit, mainly to Jose Miguel Pacheco Cansino, to let me used the work that I did for them during my traineeship program at F4E as my final master thesis. And thanks the other trainees of F4E, we have created a strong relation during this 9 month of traineeships, it has been an unforgettable experience.

And finally, thank my family and friends, to be during my whole university stage by my side supporting me at all times.

Thanks to all of you for your time and your help.

CHAPTER 1: INTRODUCTION

Nowadays, obtaining electricity from alternative sources is becoming an indispensable factor for sustaining humanity in the future, in a world where fossil fuels have an expiry date, energy CO_2 free emissions is a goal and reliable energy sources is a necessity.

Nuclear fusion energy is becoming more and more a solution to escape from this dependence that traps humanity to fossil fuels. However, still a lot of research is needed to make nuclear fusion a reality.

The development of CFD simulations, have transferred the industry and research to a new era. CFD allows the realization of very accurate and reliable studies of the behaviour of fluids under complex environments, in a fast and in an economic way. The use of CFD is increasingly becoming a vital component in the design of industrial products and processes.

Four Electron Cyclotrons Launchers will be installed in ITER. Their main purpose is to counteract plasma instabilities by injecting up to 24 MW of microwave power at a frequency of 170 GHz at dedicated positions into the plasma.

The present master thesis is based on the analysis of the behaviour of the ITER Gyrotron Upper-Launcher Antenna, under working conditions in order to verify its design and study its performance during ITER operation by thermal-hydraulic simulations.

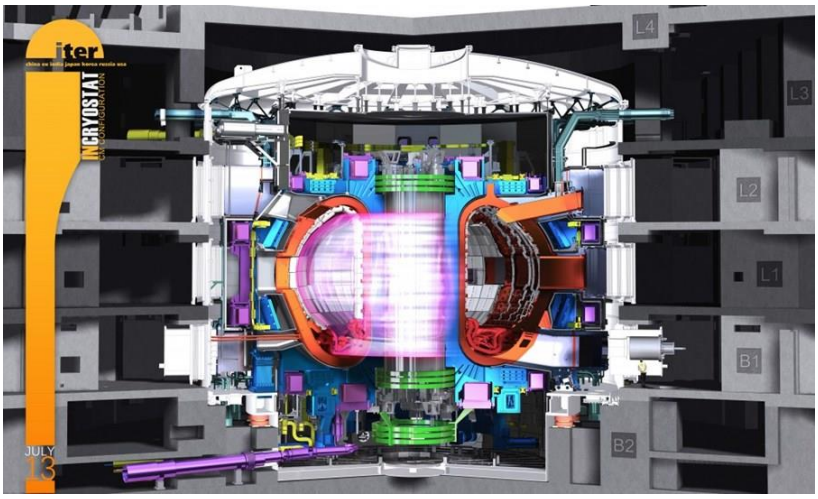

Figure 1: ITER Tokamak [16]

CHAPTER 2: OBJECTIVES AND PROJECT SCOPE

The goal of this analysis is to study the Upper-Launcher Gyrotron Antenna cooling performance. From a hydraulic point of view the main points to be checked are the resultant pressure drop and the cooling fluid velocities. From a thermal point of view, are the resultant temperature's maps that later will be used as an input for the thermal mechanical analysis in order to obtain the stresses that shall meet the operational material limits, in order to ensure its proper operation on ITER.

The object to be analysed, is the ITER European Upper-Launcher Gyrotron Antenna (Figure 2) that is being designed following the IETR Organization requirements and that has to be used on the ITER project.

The first step will be the generation of a main mesh to be used for a steady-state CFD analysis. A sensitivity analysis with a refine mesh will be done in order to discard mesh dependent results.

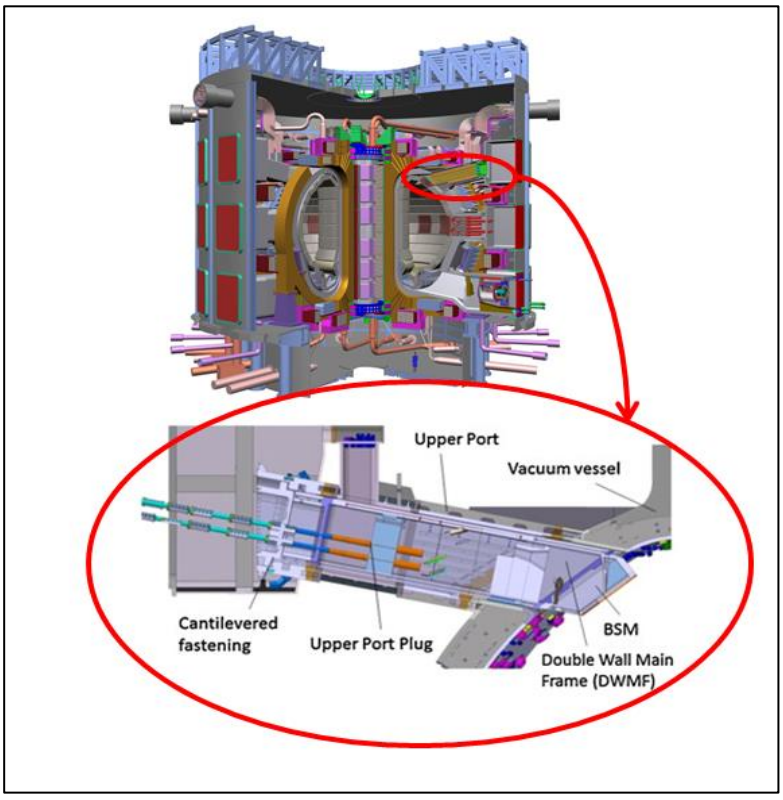

Figure 2:Electron Cyclotron Upper Launcher [6]

The next step will be the performance of a transient analysis in order to simulate the real operation of the antenna on ITER, to study mainly temperature inertia problems and verify that with a steady-state simulation we are achieving similar results.

CHAPTER 3: THEORETICAL ASPECTS

3.1. What is Fusion?

Without fusion, there would be no life on Earth [1].

What we see as light and fell as warmth is the results of a fusion reaction in the core of our Sun: hydrogen nuclei collide, fuse into heavier helium atoms and release tremendous amount of energy in the process.

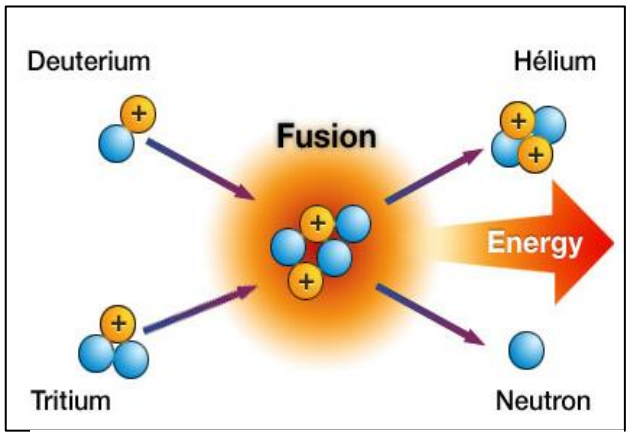

Figure 3: Iter Fusion Reaction [1]

Atoms never rest: the hotter they are, the faster they move. In the Sun's core, where temperatures reach 15,000,000 °C, hydrogen atoms are in a constant state of agitation. As they collide at very high speeds, the natural electrostatic repulsion that exists between the positive charges of their nuclei is overcome and the atoms fuse. The fusion of light hydrogen atoms produces a heavier element, helium.

The mass of the resulting helium atom is not the exact sum of the initial atoms, however—some mass has been lost and great amounts of energy have been gained. This is what Einstein's famous formula $E=mc^2$ describes: the tiny bit of lost mass (m), multiplied by the square of the speed of light (c^2), results in a very large figure (E), which is the amount of energy created by a fusion reaction.

Every second, our Sun turns 600 million tonnes of hydrogen into helium, releasing an enormous amount of energy. But without the benefit of gravitational forces that work in our Universe, achieving fusion on Earth has required a different approach.

Twentieth-century fusion science identified the most efficient fusion reaction in the laboratory setting to be the reaction between two hydrogen (H) isotopes deuterium (D) and tritium (T) (Figure 3). The DT fusion reaction produces the highest energy gain at the "lowest" temperatures. It requires nonetheless temperatures of 150,000,000 degrees Celsius—ten times higher than the hydrogen reaction occurring in the Sun.

3.2. ITER Project

3.2.1. ITER

ITER ("The Way" in Latin) is one of the most ambitious energy projects in the world today [2].

In southern France, 35 nations are collaborating to build the world's largest tokamak, a magnetic fusion device that has been designed to prove the feasibility of fusion as a large-scale and carbon-free source of energy based on the same principle that powers our Sun and stars.

The experimental campaign that will be carried out at ITER is crucial to advancing fusion science and preparing the way for the fusion power plants of tomorrow.

Thousands of engineers and scientists have contributed to the design of ITER since the idea for an international joint experiment in fusion was first launched in 1985. The ITER Members—China, the European Union, India, Japan, Korea, Russia and the United States—are now engaged in a 35-year collaboration to build and operate the ITER experimental device, and together bring fusion to the point where a demonstration fusion reactor can be designed.

3.2.2. ITER Goals

The amount of fusion energy a tokamak is capable of producing correlates directly to the number of fusion reactions taking place in its core. Scientists know that the larger the vessel, the larger the volume of the plasma, and therefore the greater the potential for fusion energy.

With ten times the plasma volume of the largest machine operating today, the ITER Tokamak will be a unique experimental tool, capable of longer plasmas and better confinement. The machine has been designed specifically to [3]:

1. Produce 500 MW of fusion power for pulses of 400 s

ITER is designed to produce a ten times return on invested energy: 500 MW of fusion power from 50 MW of input power (Q=10). It will be the first of all fusion experiments in history to produce net energy.

2. Demonstrate the integrated operation of technologies for a fusion power plant

ITER will bridge the gap between today's smaller-scale experimental fusion devices and the demonstration fusion power plants of the future.

3. Achieve a deuterium-tritium plasma in which the reaction is sustained through internal heating

4. Test tritium breeding

One of the missions for the later stages of ITER operation is to demonstrate the feasibility of producing tritium within the vacuum vessel. The world supply of tritium (used with deuterium to fuel the fusion reaction) is not sufficient to cover the needs of future power plants. ITER will provide a unique opportunity to test mock-up in-vessel tritium breeding blankets in a real fusion environment.

5. Demonstrate the safety characteristics of a fusion device

6. Set the basis for DEMO (DEMOnstration Power Station)

DEMO is the machine that will bring fusion energy research to the threshold of a prototype fusion reactor. After ITER, the machine that will demonstrate the technological and scientific *feasibility* of fusion energy, DEMO will open the way to its industrial and commercial exploitation.

ITER will be the school where physicists and engineers will learn to build DEMO. In fact, it's the essence of the international collaboration that has formed behind the project: in ITER, each participating member will acquire the experience that will allow it to proceed, back home, with the next step.

3.3. Plasma Heating

One of the main requirements for achieving fusion is to heat the plasma particles to very high temperatures. In ITER, several heating methods will work concurrently to bring the plasma in the core of the machine to 150 million °C [4].

3.3.1. Ohmic heating

Within the tokamak, the changing magnetic fields that are used to control the plasma produce a heating effect (Joule effect). The magnetic fields create a high-intensity electrical current through induction, and as this current travels through the plasma, electrons and ions become energized and collide. Collisions create "resistance" that results in heat, but paradoxically as the temperature of the plasma rises, this resistance, and therefore the heating effect, decreases. Heat transferred through high-intensity current, known as ohmic heating, is limited to a defined level. In order to obtain still higher temperatures and reach the threshold where fusion can occur, heating methods must be applied from outside of the tokamak.

3.3.2. External heating

Two families of external heating methods will be applied and studied on ITER, neutral beam injection and high-frequency electromagnetic wave, and will complement ohmic heating to bring the ITER plasma to temperature.

Neutral beam injection consists in shooting high energy particles into the plasma. Outside of the tokamak, charged deuterium particles are accelerated to the required energy level. These accelerated ions then pass through an "ion beam neutralizer" where their electrical charge is removed. The high velocity neutral particles can then be injected into the heart of the plasma where, by way of rapid collision, they transfer their energy to the plasma particles.

Millions of watts of heating power can be delivered to the plasma using this technique, bringing its temperature closer to the level where fusion can occur. A third source of heat, high frequency electromagnetic waves, is planned into the design of the ITER Tokamak to boost temperatures to the required 150 million °C.

In the same way that microwaves transfer heat to food in a microwave oven, the energy carried by high-frequency waves introduced into the plasma is transferred to the charged particles, increasing the velocity of their chaotic motion, and at the same time their temperature. Following this principle two types of waves will be employed in ITER, matching frequency of plasma ions and electrons in the interior of the ITER machine to maximize heat transfer. The Ion Cyclotron Resonance Heating (ICRH) and the Electron Cyclotron Resonance Heating (ECRH).

3.4. Electron Cyclotron Resonance Heating (Gyrotron)

To heat up ITER's plasma to approximately 150 million °C various powerful heating systems will need to be deployed. The Electron Cyclotron (EC) is one of them. Try to think of it a bit like a powerful microwave oven that will heat up the super-hot gas. How? Basically, the EC will convert electricity from the grid and supply it to the gyrotrons, devices that generate strong electromagnetic waves, which in turn, will transfer their energy to the electrons of the ITER plasma to heat it up and confine it better.
The ITER Gyrotron (Figure 4) is a vacuum electron tube in a strong magnetic to deliver up to 1 MW of continuous wave at 170 GHz with an efficiency around 50% (2 MW input power) [5].

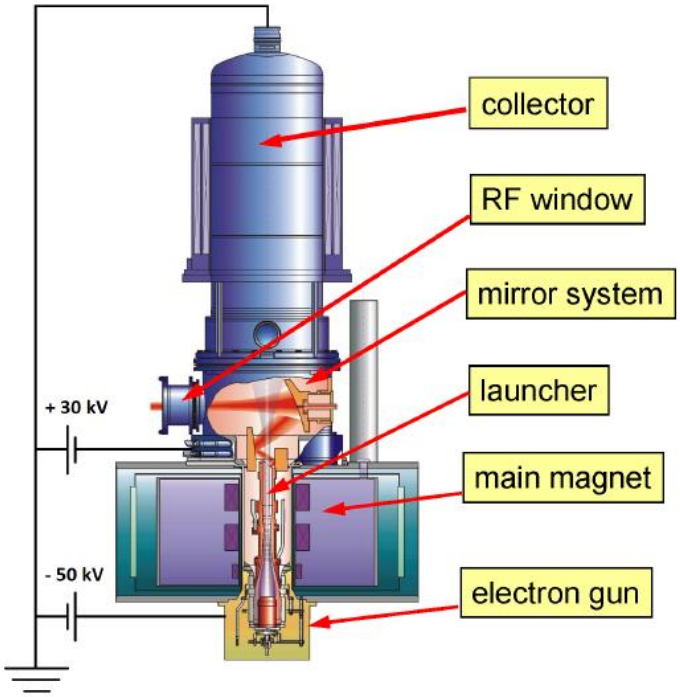

Figure 4: Gyrotron [5]

3.5. Electron Cyclotron Upper Launcher

Four EC H&CD (Electron Cyclotron Heating and Current Drive) launchers will be installed in ITER. Their main purpose is to counteract plasma instabilities by injecting up to 24 MW of microwave power at a frequency of 170 GHz at dedicated positions into the plasma. The microwave power is transmitted into the dedicated ports by 8 waveguide lines per launcher. Inside the launcher the microwaves are guided into the plasma quasi-optically by an adjusted set of mirrors (Figure 5). These mirrors and also the foremost segments of waveguides are mounted into the Upper Port Plug (UPP), which is a massive steel structure capable to dissipate up to 800 kW heat and to withstand strong

mechanical loads induced mainly from plasma disruptions. The UPP also provides shielding to protect the port cell area and sensitive components from neutrons [6].

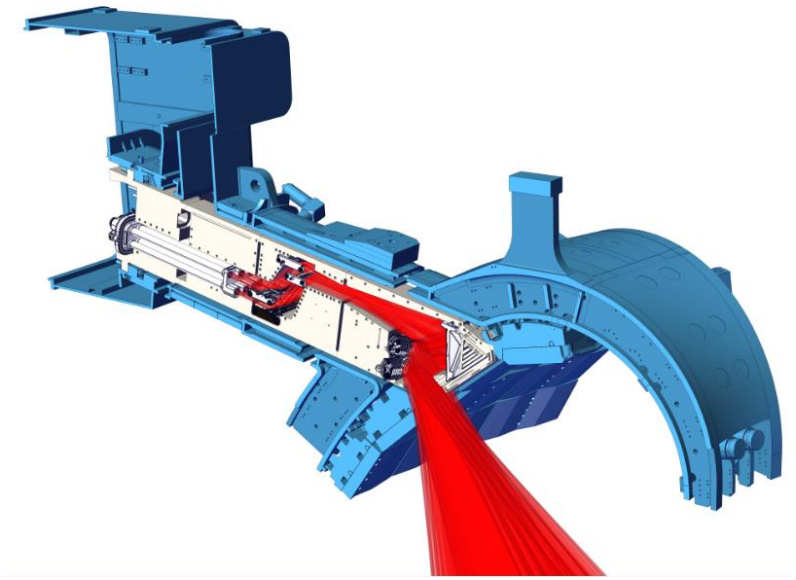

Figure 5: Electron Cyclotron Upper Launcher [6]

3.6. CFD

3.6.1. What is CFD?

Computational Fluid Dynamics (CFD) is the simulation of fluids engineering systems using modelling (mathematical physical problem formulation) and numerical methods (discretization methods, solvers, numerical parameters, and grid generations, etc.) [7]. The process is as figure 6.

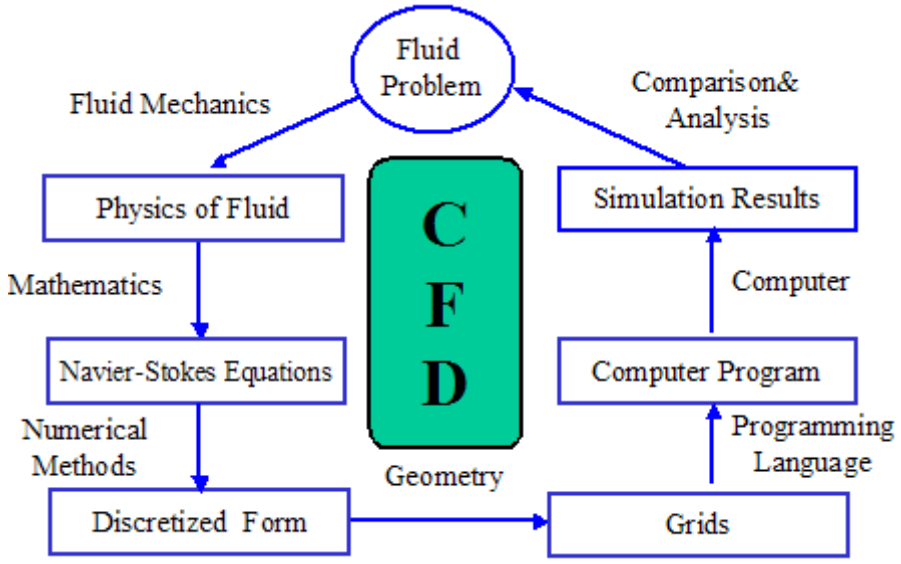

Figure 6: Process of Computatiopnal Fluid dynamics [7]

Computational Fluid Dynamics (CFD) provides a qualitative (and sometimes even quantitative) prediction of fluid flows by means of:

- Mathematical modelling (partial differential equations)
- Numerical methods (discretization and solution techniques)
- Software tools (solvers, pre- and post-processing utilities)

CFD enables scientists and engineers to perform "numerical experiments" (i.e. computer simulations) in a 'virtual flow laboratory'.

3.6.2. How does CFD work?

Computational fluid dynamics is based on the Navier-Stokes equations. These equations describe how the velocity, pressure, temperature, and density of a moving fluid are related.

These equations are very complex, and in practice, these equations are too difficult to solve analytically. In the past, engineers made further approximations and simplifications to the equation set until they had a group of equations that they could solve. Recently, high speed computers have been used to solve approximations to the equations using a variety of techniques like finite difference, finite volume, finite element, and spectral methods. This area of study is called Computational Fluid Dynamics or CFD.

The Navier-Stokes equations consist of a time-dependent continuity equation for conservation of mass, three time-dependent conservation of momentum equations and a time-dependent conservation of energy equation.

Navier-Stokes Momentum Equation

$$\rho \frac{\partial v}{\partial t} + (\rho v \cdot \nabla) v = -\nabla p - \nabla \cdot \tau + \rho g$$

$\rho \frac{\partial v}{\partial t}$ → Transient term

$(\rho v \cdot \nabla) v$ → Convective term

∇p → Pressure term

$\nabla \cdot \tau$ → Diffusion term

$\rho g \ \nabla \cdot \tau$ → External forces term

Where:

- "ρ" is the density.
- "v" is the flow velocity.
- "∇ " is the divergence.
- "p" is the pressure.
- "t" is time.
- "τ" is the stress tensor.
- "g" represents body accelerations, for example gravity, inertial accelerations, electrostatic accelerations, etc.

Convection is a physical process that occurs in a flow in which some property is transported by the ordered motion of the flow.

Diffusion is a physical process that occurs in a flow in which some property is transported by the random motion of the molecules of the gas. Diffusion is related to the stress tensor and to the viscosity of the gas.

To solve a flow problem, you have to solve all five equations simultaneously; that is why we call this a coupled system of equations. There are actually some other equations that are required to solve this system because of we only have five equations for six unknowns (three velocities, the pressure, the density and the temperature). Therefore, an extra equation is needed, the equation of state that relates the pressure, temperature, and density of the fluid. Moreover, we need to specify all of the terms of the stress tensor. In CFD the stress tensor terms are often approximated by a turbulence model [8].

I have listed below the most commonly used Viscosity turbulence models over the past ten or so years and the intended use behind their development:

- Spalart-Allmaras: One equation model for attached aerodynamic analysis.
- k-epsilon: Two equation model for free shear and non-wall bounded flow behaviour. Was the previous industrial standard.
- k-omega: Two equation model for wall bounded flows, not commonly used.
- SST (Shear Stress Transport): Two equation model blending the freestream advantages of the k-epsilon model with the wall bounded advantages of the k-omega model. This is the new industrial standard and should be the default choice for most applications.

3.7. Environmental Impact

As the world's largest tokamak and the first to produce net energy, ITER will play an important role in demonstrating to the world that fusion technology is not only scientifically viable, but also safe and environmentally responsible [9].

3.7.1. Regulatory Body

Throughout construction, commissioning and operation, ITER's safety processes will comply with French regulations, as verified regularly through audit and inspection by the French nuclear authorities.

In accordance with the 2006 French law on Transparency and Nuclear Security, a **Local Information Commission** (*Commission locale d'information*, or CLI) was created for ITER in 2009. This independent body acts as an interface between the ITER Organization and the local population for questions of nuclear safety, radioprotection and the installation's impact on personnel and the environment. The ITER Organization and the French Nuclear Safety Agency (ASN) provide the ITER CLI with any information necessary to the exercise of its mission. The group, which meets regularly, is composed of representatives from local government, environmental groups, trade unions, businesses and health professionals.

3.7.2. Accidents

Can a Fukushima-type accident happen at ITER? Absolutely not. The fundamental differences in the physics and technology used in fusion reactors make a fission-type nuclear meltdown or a runaway reaction impossible. The fusion process is inherently safe.

In a fusion reactor, there will only be a limited amount of fuel (less than four grams) at any given moment. The reaction relies on a continuous input of fuel; if there is any perturbation in this process, the reaction ceases immediately. Even in the event of the total loss of the cooling function, ITER's confinement barriers would not be affected. The temperatures of the vacuum vessel that provides the first confinement barrier would under no circumstances reach the melting temperatures of the materials.

3.7.3. Radioactive materials

The fusion process at ITER requires tritium, a radioactive form of hydrogen with a half-life of 12.3 years. Although the amount of tritium used during plasma pulses is very small, only a few grams at any one time, the confinement of this radioelement within the fuel cycle is one of the most important safety objectives at ITER.

A multiple-layer barrier system has been designed to protect against the spread or release of tritium into the environment.

Even in the event of a cataclysmic breach in the tokamak, the levels of radioactivity outside the ITER enclosure would remain very low. The ITER Preliminary Safety Report presents an analysis of risks that demonstrates that during normal operation, ITER's radiological impact on the most exposed populations will be one thousand times less than natural background radiation. For postulated "worst-case scenarios," such as fire in the Tritium Plant, the evacuation of neighbouring populations would not be necessary.

3.7.4. Radioactive waste

Fusion reactors, unlike fission reactors, produce no high activity/long life radioactive waste. The "burnt" fuel in a fusion reactor is helium, an inert gas. Activation produced in the material surfaces by the fast neutrons will produce waste that is classified as very low, low, or medium activity waste. All waste materials (such as components removed by remote handling during operation) will be treated, packaged, and stored on site.

Because the half-life of most radioisotopes contained in this waste is lower than ten years, within 100 years the radioactivity of the materials will have diminished in such a significant way that the materials can be recycled for use in other fusion plants. This timetable of 100 years could possibly be reduced for future devices through the continued development of 'low activation' materials, which is an important part of fusion research and development today.

CHAPTER 4: METHODOLOGY AND PROJECT PHASES

The methodology and the phases of project to carry out the study of the electron cyclotron upper launcher in working conditions, through CFD simulations are presented below:

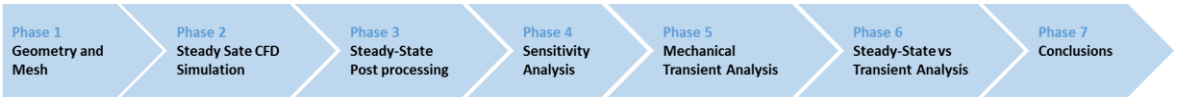

Phase 1. Geometry and Mesh

At this stage, the geometry and mesh of the CAD model is designed. This phase takes place before the CFD simulation phase, and it is the basis of any simulation. It is very important to get an optimal design of the mesh, a balance between a mesh sufficiently simple to guarantee a rapid convergence of results, and sufficiently complex to obtain reliable results.

This phase consists of the following activities or sub-phases:

- Design of geometry
- Mesh design

Phase 2. Steady Sate CFD Simulation

This phase explains the input parameters and configuration used in Ansys Fluent to set-up the simulation. This phase consists of the following activities or sub-phases:

- Choose the flow type (compressible or incompressible, laminar or turbulent, etc.)
- Choose the calculation model and type of problem (turbulence model)
- Establish boundary conditions
- Establish study monitors

Phase 3. Steady-State Post processing

This phase consists of analysing the results obtained from the CFD simulation. This phase consists of the following activities or sub-phases:

- Extraction and study of contour graphics of pressure, velocity, temperature, etc.
- Detect the critical points
- Analyse the distribution of the water inside the channels

- Analyse if the cooling system is working properly
- Study the possibility to improve the design to enhance the results

Phase 4. Sensitivity Analysis

This phase consist of verify that the previous simulation results don't depend on the number of mesh elements, by refining the mesh. This phase consists of the following activities or sub-phases:

- Generate a new mesh with more elements and more complexity
- Repeat exactly the same simulation performed on phase 2 with the new refine mesh
- Extract the results of the new simulations
- Compere the results with the ones obtained on phase 3

Phase 5. Mechanical Transient Analysis

This phase consist of analyse the electron cyclotron upper launcher antenna cooling performance along time, during ITER pulse operation. This phase consists of the following activities or sub-phases:

- Set-up a mechanical transient analyses
- Extract results of the evolution of the temperature vs time
- Study the presence of temperature accumulation between pulses

Phase 6. Steady-State vs Transient Analysis

This phase consist of comparing the results of the steady state CFD simulation with ones from the mechanical transient simulation. This phase consists of the following activities or sub-phases:

- Results comparison
- Analyse if the use of a steady-state CFD simulation it is good enough

Phase 7. Conclusions

This phase consist on the extraction of conclusions from the project. This phase consists of the following activities or sub-phases:

- Asses the cooling performance of the electron cyclotron upper launcher antenna
- Expose the critical points found after the analysis
- Suggest improvements to enhance the system behaviour
- Set the mesh and the type of analysis for future simulations

CHAPTER 5: GEOMETRY AND MESH

5.1 CAD Model

On figure 7 it is shown the CAD model of the BSM that has been analysed.

(Geometry designed by Fusion for Energy)

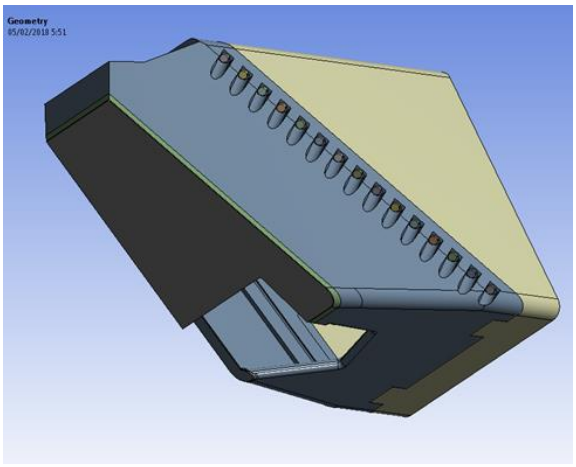

Figure 7: CAD Model of the Gyrotron Antenna

The part under study is the "grey part" (Figure 7), that part it is called Blanket Shield Module (BSM), is a removable part that goes attached at the end of the upper launcher by bolts. The BSM is the part of the upper launcher that will be facing the plasma; therefore it is a high critical part that it is supposed to receive important amount of thermal and neutronic loads coming from the plasma.

In order to simulate properly the hole BSM, part of the upper launcher where the BSM it is attached by bolts "yellow-brown part" (Figure 7) will be also analyse to performed a good simulation of the interface between the BSM and the upper launcher.

5.2 Materials and components

The model analysed is formed by five different components and four different materials:

1. BSM → Stainless Steel 316L (N)-IG
2. Double Wall → Stainless Steel 316L (N)-IG
3. Bolts → Inconel (Alloy 718)
4. Heat Sinks → CuCrZr Alloy
5. Hydraulic Part → Liquid Water (H2O)

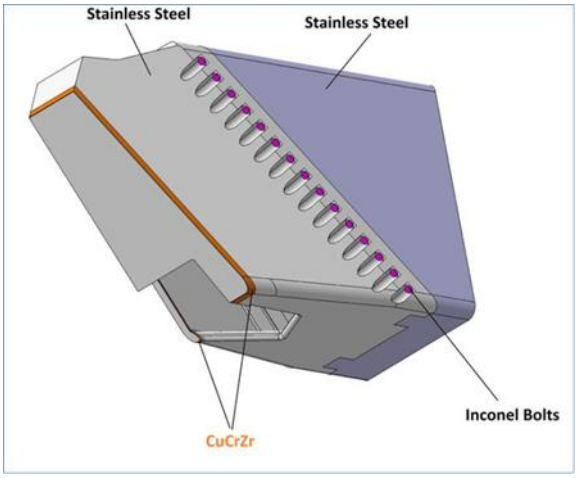

Figure 8: Solid Part

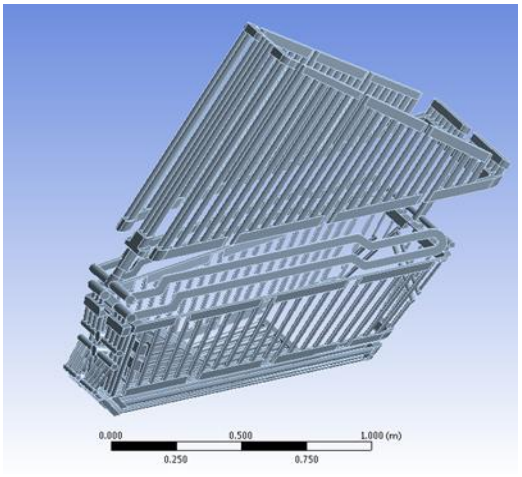

Figure 9: Hydraulic Part

Solid materials properties have been extracted from the SDC-IC Appendix A (ITER_D_222RLN - Appendix A, Materials Design Limit Data) as temperature dependent properties (Polynomial), except density that has been set as a constant value.

Water properties have been set as temperature dependent in fluent (Polynomial) using data from (https://webbook.nist.gov/chemistry/fluid/) for the corresponding temperature range, except density that has been set as a constant value.

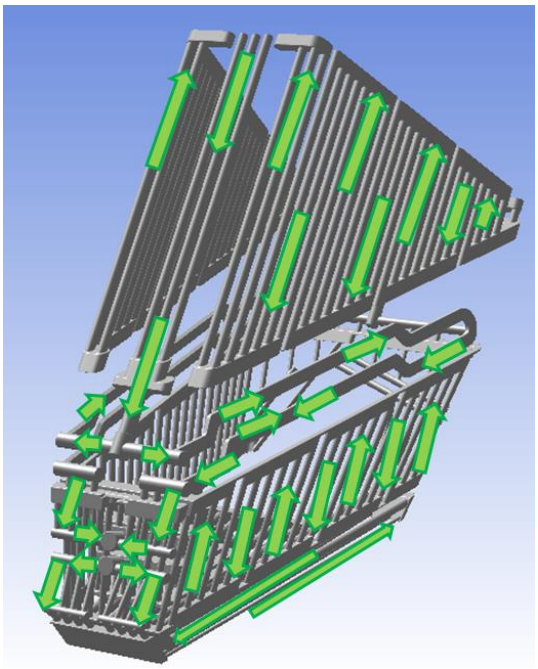

Figure 10: Water direction

5.3 Mesh

In order to design the mesh of the CAD model, the model has been imported on Ansys Meshing, software selected to perform the mesh.

The generation of a mesh, it is one of the most crucial steps on a CFD simulation. The use of a good mesh has an uncountable number of advantages, such as better results convergence, more reliable results, less computational time, etc. The crucial point for a good mesh it is to find the appropriate balance of mesh complexity, the number of mesh elements, depending on the CPU power that it is available to perform the analysis, in order to have a reasonable simulation time and to obtain reliable results that are not dependent to the mesh. In order to find that balance the methodology followed, was to generate an initial mesh, good but not too complex, to allow a fast simulation. After, by refining that mesh, through the increase of the number of mesh elements and introducing an specific mesh for the boundary layer, perform a sensitivity analysis by comparing the results of the two meshes, the initial one vs the refine one, if the results are different means that we have not found yet the proper number of mesh elements that ensure an independence on the results from the mesh, so an iterative process starts till the improve mesh have the same or similar enough results that the previous one.

Once the methodology followed on the mesh design is known, an explanation of the factors that have allowed the creation of a personalized and optimal mesh are explained. Basically, four factors have been controlled:

- **Body Sizing:** It allows to generally control the size of the block cells of an entire volume block.
- **Face Sizing:** It allows to refine specific surfaces where finer mesh is required, such as cooling tubs with small diameters.
- **Edge Sizing:** It allows to refine the mesh around specific edges.
- **Inflation:** It allows to perform a detailed control of the mesh in the boundary layer, where a high-precision mesh is needed to capture the large changes that takes place in the fluid boundary layer.

By controlling the four factors described above, the mesh has been built. A thinner meshfor that zones where is required, such as the boundary layer, aorund the tubes with small diameteres, etc.. In contrast, in those simpler and non-hydraulic parts, such as the interior of the big solid parts, the mesh has been desogn simpler to reduce the degree of complexity of the mesh.

The mesh created is a tetrahedral mesh, which presents a refinement in those areas where more precision is required.

Below is a more detailed explanation of the caracteristics of the mesh builded (Table 1):

Table 1: Main Mesh parameters

Hydraulic Body Sizing: 10 mm	
Hydraulic Face Sizing: 4 mm	

FWP Front Pipes Face Sizing: 3 mm	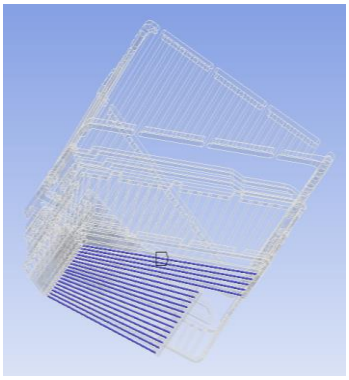
General Body Sizing: 15 mm	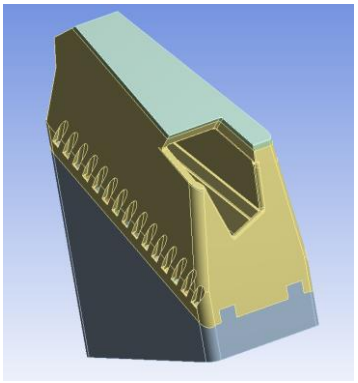
CuCrZr Body Sizing: 9 mm	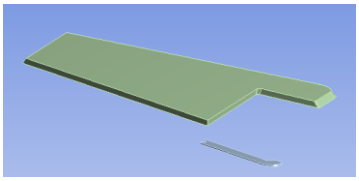
Upper SS Plate Body Sizing: 5 mm	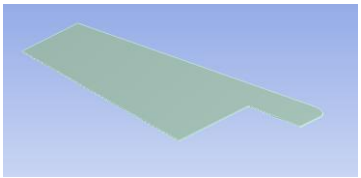
Inconel Bolts Face Sizing: 5 mm	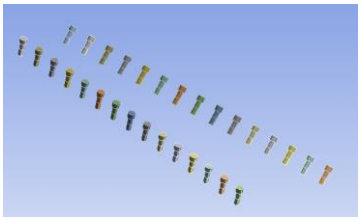

Once the tetrahedral mesh is done on Ansys meshing (Figure 11), the mesh is imported on Ansys Fluent where the simulation will take place and be set-up, although before that, the mesh is converted to a polyhedral mesh on

Ansys Fluent. The reason of that conversion to a polyhedral mesh, is that in general for a thermal-hydraulic CFD simulations the polyhedral mesh works better, mainly due to the fact that a polyhedral mesh needs a high degree of quality, it is often that the conversion to a polyhedral mesh fails, although if the conversion succeeds that means that the resultant mesh has a good quality (Figure 12).

Tetrahedral Mesh (17.220.627 elements)	Polyhedral Mesh (6.659.315 elements)
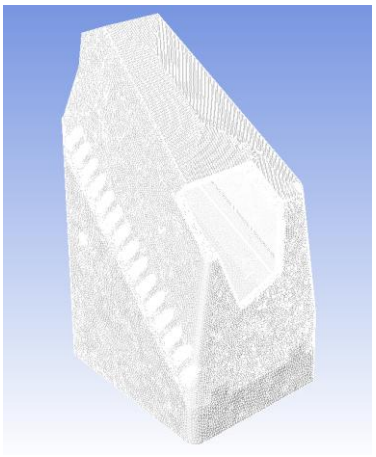 *Figure 11: Tetrahedral mesh*	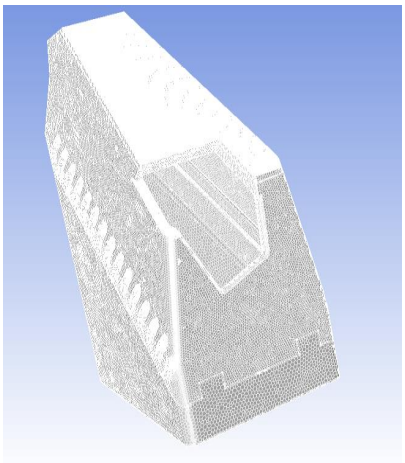 *Figure 12: Polyhedral mesh*

5.3.1 The advantages of a polyhedral mesh

Comparisons in many practical tests have verified that with polyhedral meshes, one needs about four times fewer cells, half the memory and a tenth to fifth of computing time compared to tetrahedral meshes to reach solutions of the same accuracy. In addition, convergence properties are much better in computations on polyhedral meshes, where the default solver parameters usually do not need to be adjusted. An example is presented below to demonstrate this [10].

The test case represents a water jacket of an engine; the pressure drop between inlet and outlet is the relevant engineering quantity that is monitored. Computations were performed on six polyhedral and six tetrahedral grids, with numbers of cells ranging between 21.872 and 593.888 (polyhedral) and between 39.587 and 2.322.106 (tetrahedral). Prismatic layers along walls were generated in all cases.

In order to determine the mesh dependency of the solutions, the pressure drops computed on all grids are compared in Figure 13. This figure shows that the results from both grid types are indeed, as required, converging to a grid independent value. In all cases, the same discretization and solution method was used (second-order upwind differencing scheme for convective fluxes).

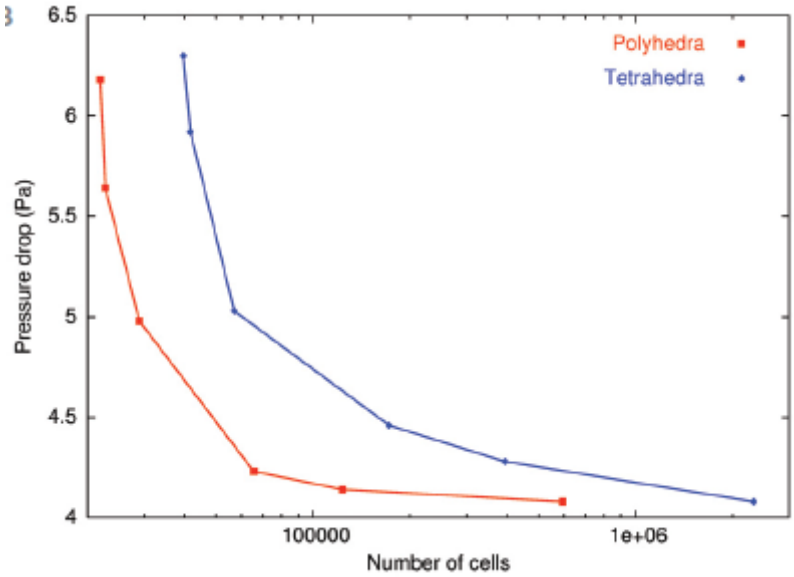

Figure 13: Mesh convergence graph [10]

It is important to note that the results obtained on any polyhedral mesh are more accurate than the results obtained on a tetrahedral mesh with a comparable number of cells. Actually, the result from polyhedral mesh with 65.513 cells is slightly more accurate than the result from a tetrahedral mesh with 393.273 cells (about 6 times more). The computing time on this polyhedral mesh is less than one tenth of the computing time for the tetrahedral mesh that would deliver the same accuracy.

CHAPTER 6: STEADY STATE CFD SIMULATION

In this section, the different steps followed in Ansys Fluent will be explained in detail, about how to set-up and initialize the CFD simulation.

Step 1. Mesh import and mesh conversion

The first step was to import the tetrahedral mesh from Ansys Meshing to Fluent. Once imported, using the automatic mesh convertor in Fluent (Figure 14), the tetrahedral mesh is converted into a polyhedral mesh (Figure 15).

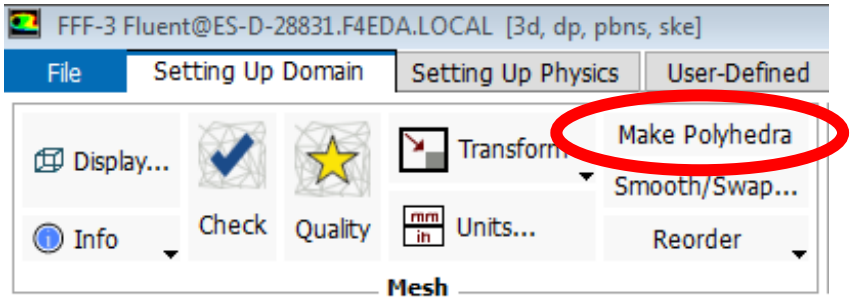

Figure 14: Automtic Fluent plyhedral mesh convertor

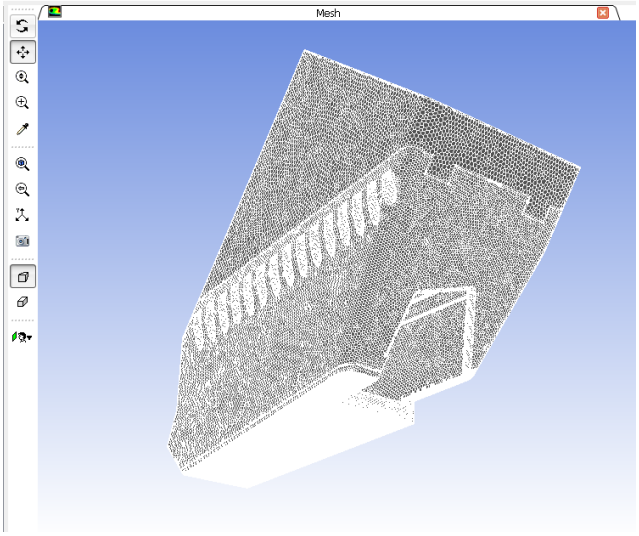

Figure 15: Mesh already converted into a polyhedral mesh

Step 2. Model selection

Knowing that we have a fluid with a Reynolds number higher than 4000, means that we have turbulent fluid. So, the next step is to choose the turbulence model that will be used. The model selected is the k-ω SST (Figure 16).

The based Shear-Stress-Transport (SST) model was designed to give highly accurate predictions of the onset and the amount of flow separation under adverse pressure gradients by the inclusion of transport effects into the formulation of the eddy-viscosity. This results in a major improvement in terms of flow separation predictions. The superior performance of this model has been demonstrated in a large number of validation studies.

Moreover, in order to apply the energy equation and taking into account the effect of temperature and thermal loads, it is need to activate the energy model (Figure 17).

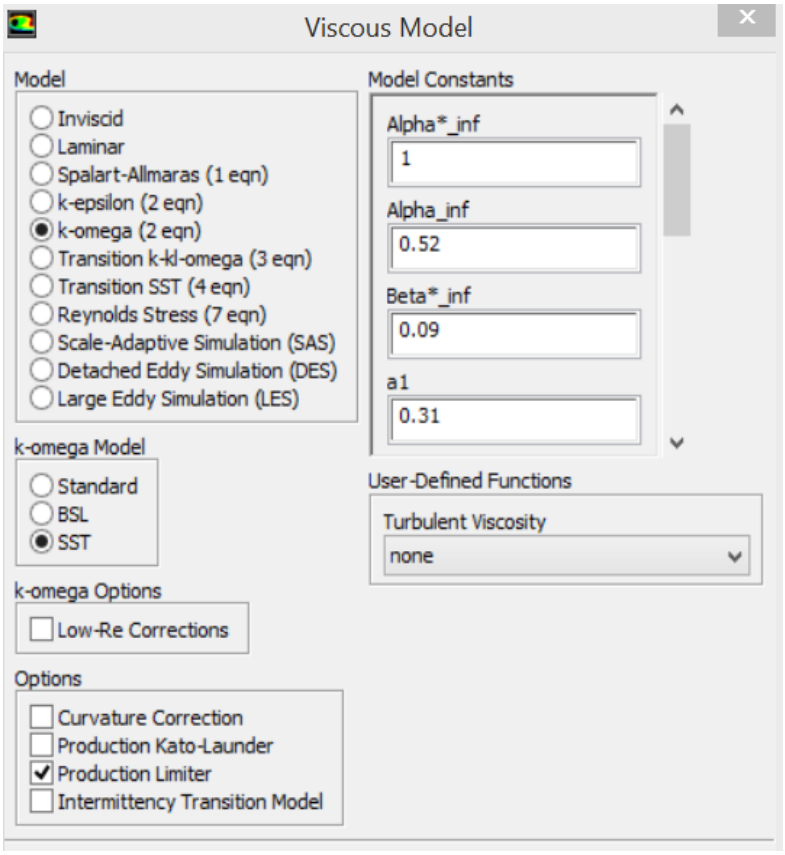

Figure 16: Turbulence model selection

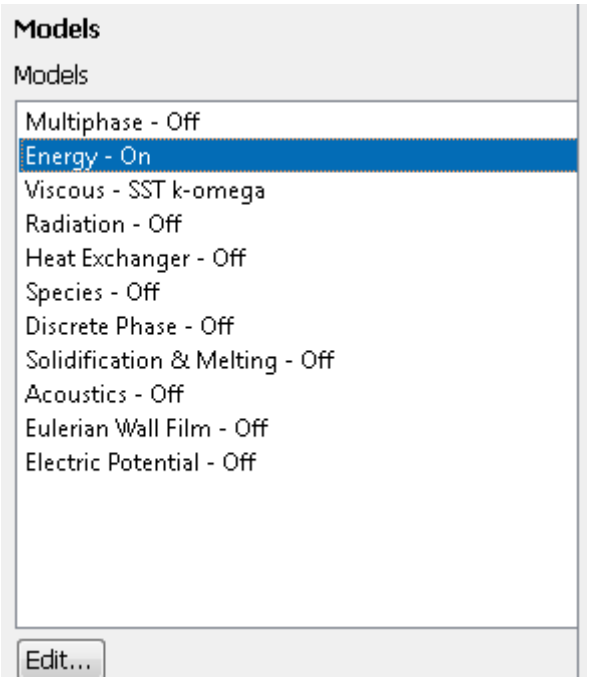

Figure 17: Energy equation activation

Step 3. Materials specifications

On this step the materials specifications have to be set and apply in the different components (Figure 18):

1. BSM → Stainless Steel 316L (N)-IG
2. Double Wall → Stainless Steel 316L (N)-IG
3. Bolts → Inconel (Alloy 718)
4. Heat Sinks → CuCrZr Alloy
5. Hydraulic Part → Liquid Water (H2O)

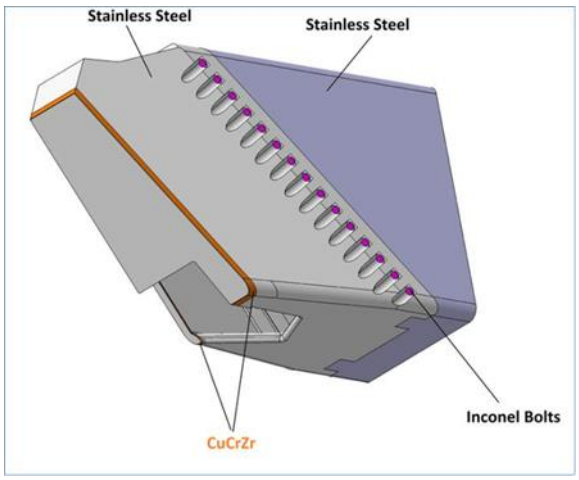

Figure 18: BSM Materials

Solid materials properties have been extracted from the SDC-IC Appendix A (ITER_D_222RLN - Appendix A, Materials Design Limit Data) as temperature dependent properties (Polynomial), except density that has been set as a constant value.

Water properties have been set as temperature dependent in fluent (Polynomial) using data from (https://webbook.nist.gov/chemistry/fluid/) for the corresponding temperature range, except density that has been set as a constant value (Figure 19).

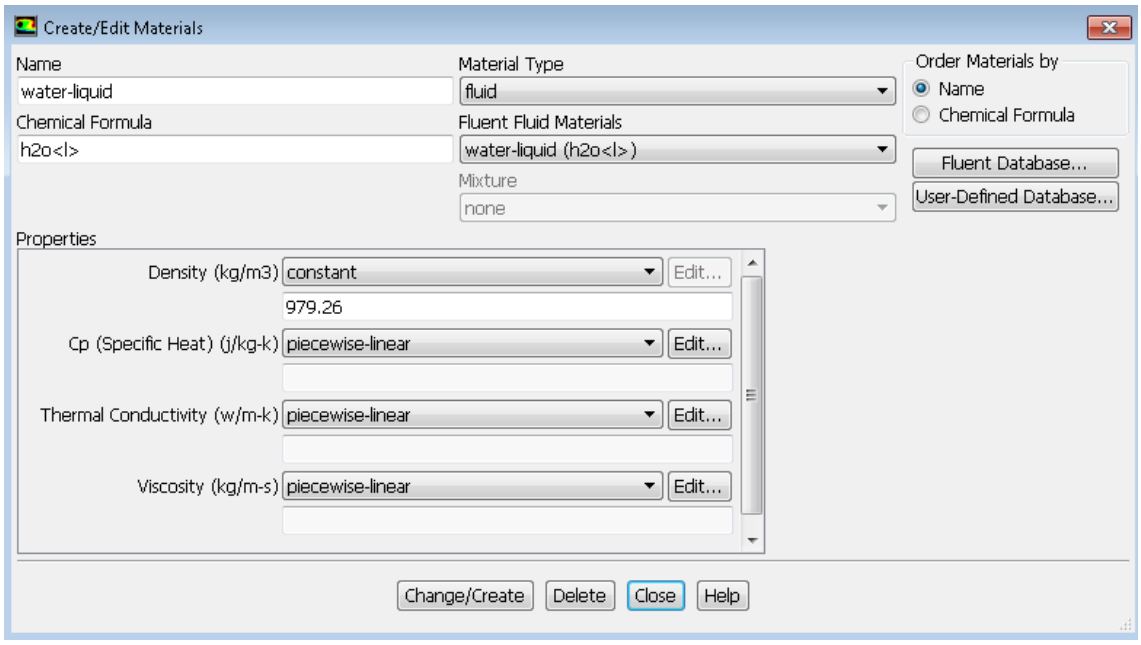

Figure 19: Materials properties

Step 4. Boundary Conditions

The next step is the introduction of the boundary conditions:

Hydraulic part

The hydraulic part BC used on the analysis are the following ones:

- Mass Flow Inlet: 4.5 kg/s
- Outlet pressure: 0 Pa
- Operating Pressure: 40 bar
- Operating Temperature: 70 ºC
- Gravity: -9.81 m/s on z-axis

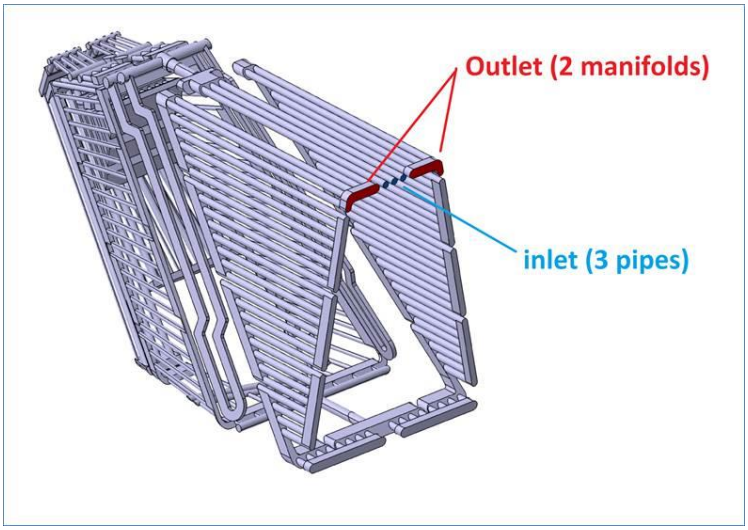

Figure 20: Inlet and Outlet BC location

Solid part

The solid parts BC used on the analysis are the following ones:

- Adiabatic Walls

- Source term: Nuclear volumetric heating (Figure 21).

(Source term calculated by Fusion for Energy Neutronic team)

The steps followed and the macros used in order to use a .vtk file as nuclear heating on Ansys Fluent, are shown on the Annex section 15.3.

The nuclear loads (.vtk file), were calculated previously using the MCNP (Montecarlo) method and are provided as a volumetric discrete distribution (3-D grid with cubic cells) with a resolution of 1 cm in all directions. This distribution is directly interpolated on the FEM model's mesh.

- Surface Thermal loads (Figures 22 and 23) calculated using the Plasma View Factor (ANSYS radiosity). This view factor was calculated taking into account a max surface heating value of 0.35 MW/m2 at the front surface of the BSM First Wall Panel.

(Surface Thermal loads calculated by Fusion for Energy)

The view factor F_{12} is the fraction of energy exiting an isothermal, opaque, and diffuse surface 1 (by emission or reflection), that directly impinges on surface 2 (to be absorbed, reflected, or transmitted). View factors depend only on geometry.

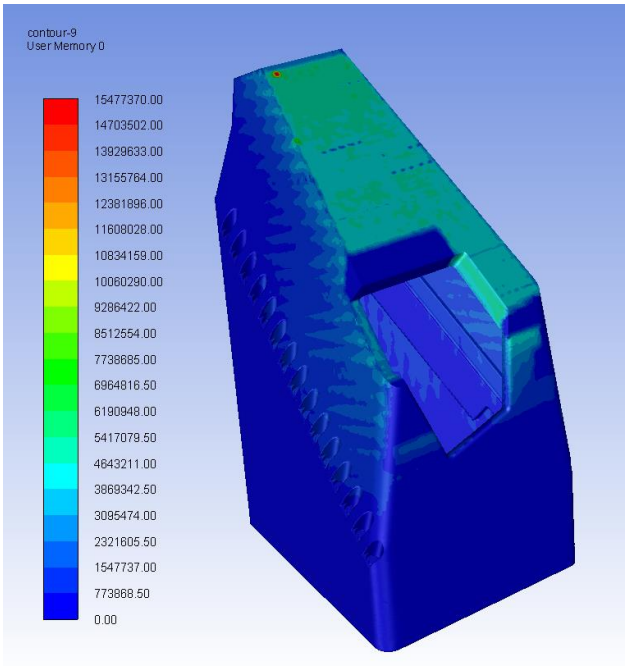

Figure 21: Nuclear heating (W/m3)

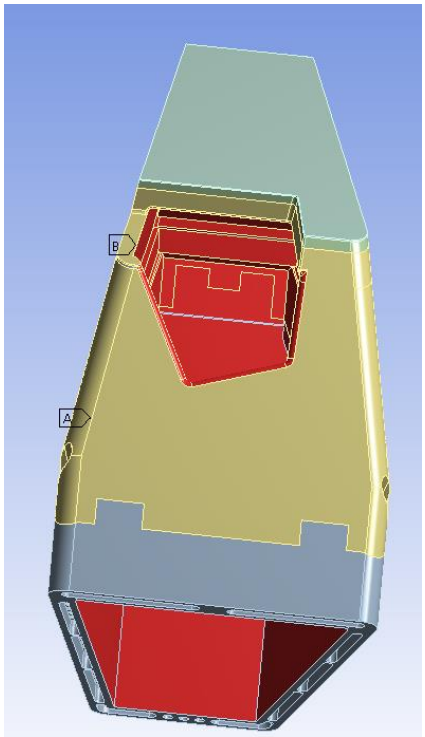

Figure 22: Internal surfaces Thermal Load

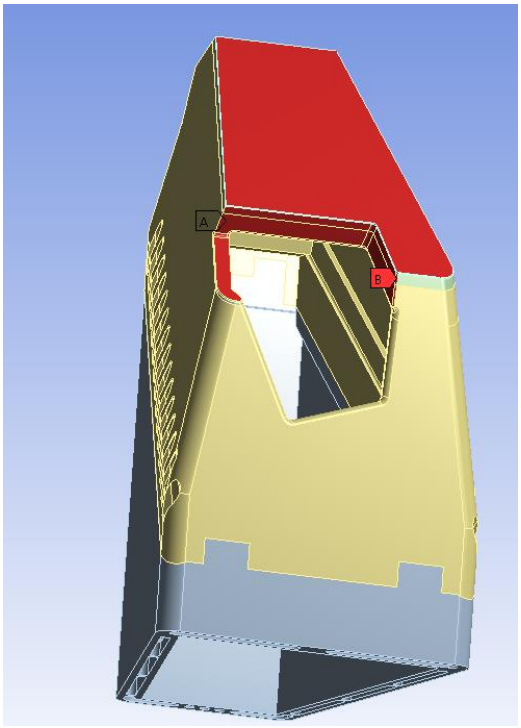

Figure 23: External Surfaces Thermal Load

Step 4. Solution Methods selection

Now it is time to set the solution method (Figure 27).

As it has been explained on section 3.6.2

The partial differential equations shown earlier in this section must be discretized or transformed into a set of algebraic equations which can be solved digitally. There are numerous methods available to do this discretization. The three most popular (based on the number of commercial computational fluid dynamics (CFD) codes available) are [11]:

1. **Finite Differences (Figure 24)**
2. **Finite Volumes (Figure 25)**
3. **Finite Elements (Figure 26)**

In the **finite difference method**, the partial derivatives are replaced with a series expansion representation, usually a Taylor series. The series is truncated usually after 1 or 2 terms. The more terms you include, the more accurate the solution. However, more terms in the expansion causes the complexity and number of discrete points or nodes of the solution to increase dramatically. Applying this method to a regularly shaped geometry is straightforward. However, for irregularly shaped geometries, the equations must be transformed before the Taylor series can be applied. This transformation introduces all sorts of problems in terms of additional cross-coupling of equations, mesh generation and general convergence.

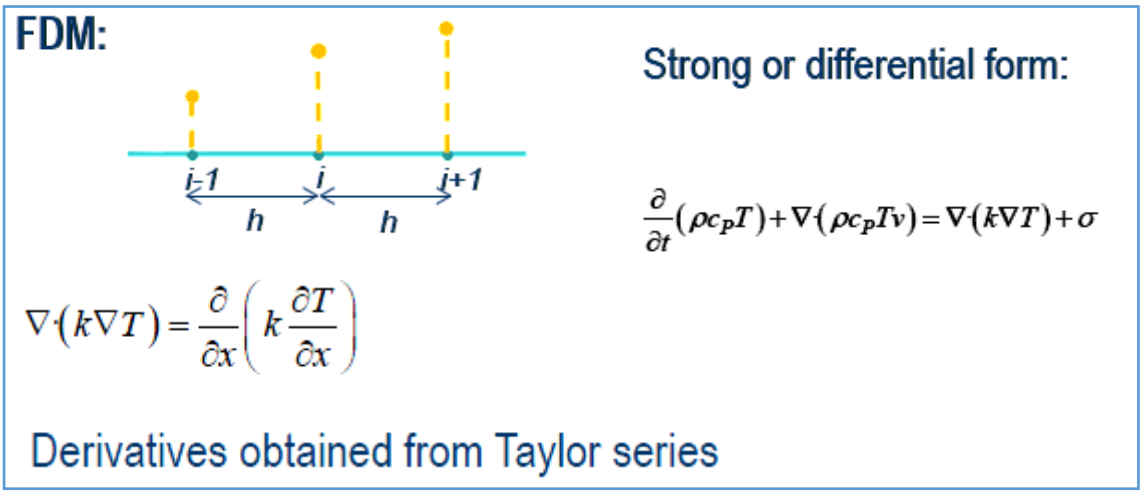

Figure 24: Finite Differences Method [15]

In the **finite volume method**, the governing equations are integrated over a volume or cell assuming a piece-wise linear variation of the dependent variables (u, v, w, p, T). Again the piece-wise linear variation determines both the accuracy and the complexity. Using these integrations, you essentially

balance fluxes across the boundaries of the individual volumes. The flux is calculated at the mid-point between the discrete nodes in the domain.

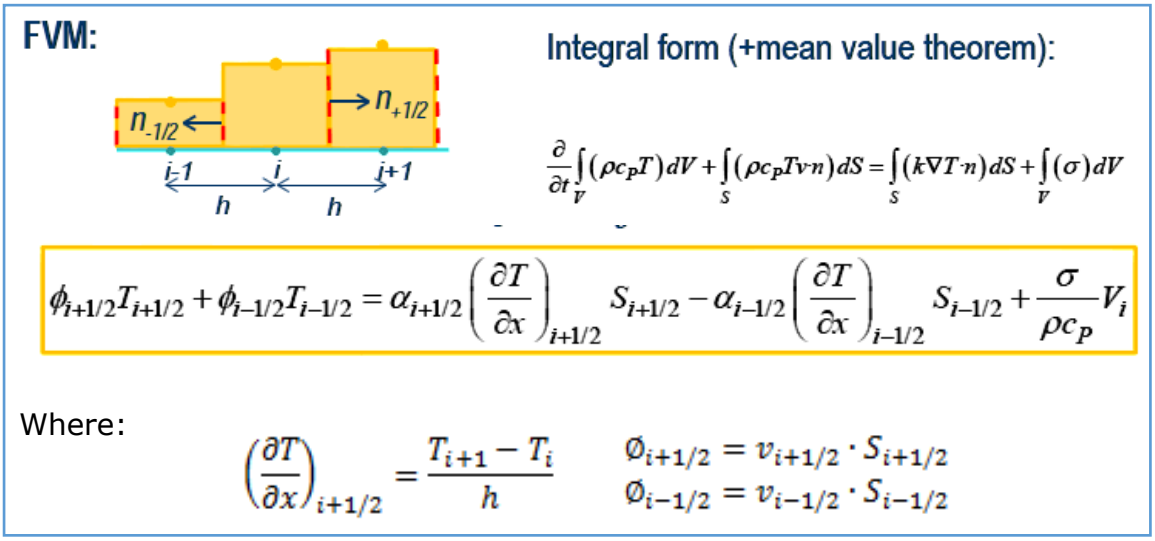

Figure 25: Finite Volumse Method [15]

The numerical schemes more used are the following ones:

- Central Differences → $\begin{cases} T_{i+1/2}=\frac{T_{i+1}-T_i}{h} \\ T_{i-1/2}=\frac{T_i-T_{i-1}}{h} \end{cases}$

- Upwind → $\begin{cases} if\ \emptyset_{i\pm1/2}>0 \begin{cases} T_{i+1/2}=T_{i+1} \\ T_{i-1/2}=T_i \end{cases} \\ if\ \emptyset_{i\pm1/2}<0 \begin{cases} T_{i+1/2}=T_i \\ T_{i-1/2}=T_{i-1} \end{cases} \end{cases}$

In the **finite element method**, Galerkin's method of weighted residuals is generally used. In this method, the governing partial differential equations are integrated over an element or volume after having been multiplied by a weight function. The dependent variables are represented on the element by a shape function, which is the same form as the weight function.

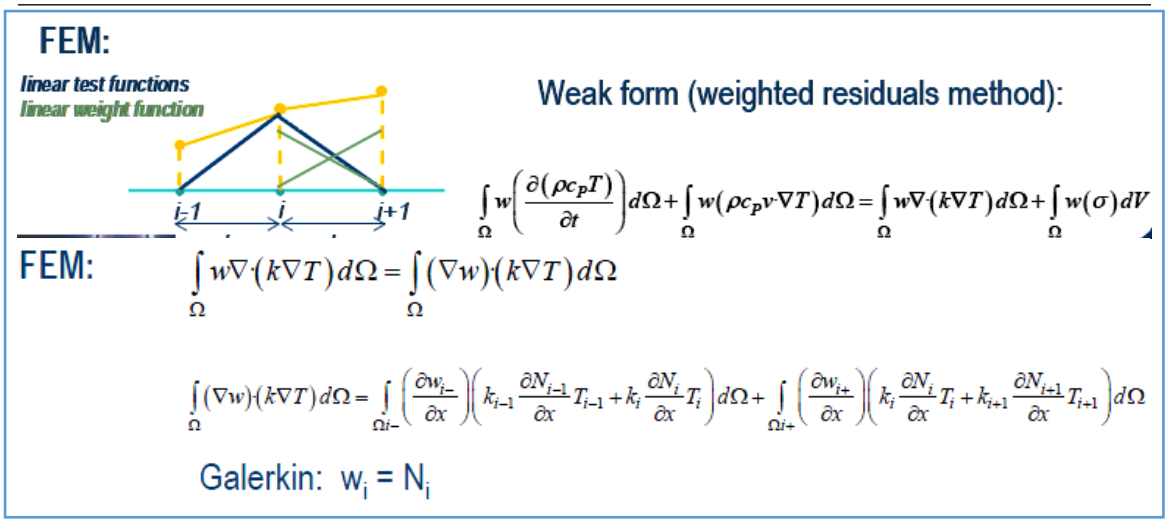

Figure 26: Finite Elements Method [15]

In our case, Ansys Fluent uses a Finite Volume Method (FVM) with Upwind as a numerical scheme.

First level classification of algorithms:

Density-based

In density-based solver, the energy, momentum, continuity and species transport equations are solved simultaneously. Mainly used for compressible flows.

Pressure-based

In the pressure-based solver, the governing equations are solved sequentially. Mainly used for incompressible flows.

In our case, our working fluid is liquid water, meaning that we have a incompressible flow, so a pressure-based algorithm is chosen.

There is mainly three solution scheme PRESSURE-BASED [12]:

1. **SIMPLE algorithm**
2. **PISO algorithm**
3. **COUPLED algorithm**

The **Semi-Implicit Method for Pressure Linked Equations (SIMPLE algorithm)** uses a relationship between velocity and pressure corrections to enforce mass conservation and to obtain the pressure field. Velocity does not account for the effect of actual neighbour values.

The **Pressure-Implicit with Splitting of Operators (PISO)** pressure-velocity coupling scheme, part of the SIMPLE family of algorithms, is based on the higher degree of the approximate relation between the corrections for pressure and velocity. One of the limitations of the SIMPLE algorithms is that

new velocities and corresponding fluxes do not satisfy the momentum balance after the pressure-correction equation is solved. As a result, the calculation must be repeated until the balance is satisfied.

The **Coupled algorithm** solves the momentum and pressure-based continuity equations together. Using the coupled approach offers some advantages over the non-coupled or segregated approach. The coupled scheme obtains a robust and efficient single phase implementation for steady-state flows, with superior performance compared to the segregated solution schemes. Linearization is also needed; all algorithms need to linearize the momentum equation.

The solution schemes chosen for our simulation, has been the Coupled algorithm, in order to get a strong coupling between equations and a more stable calculations, although a coupled scheme requires more CPU requirements.

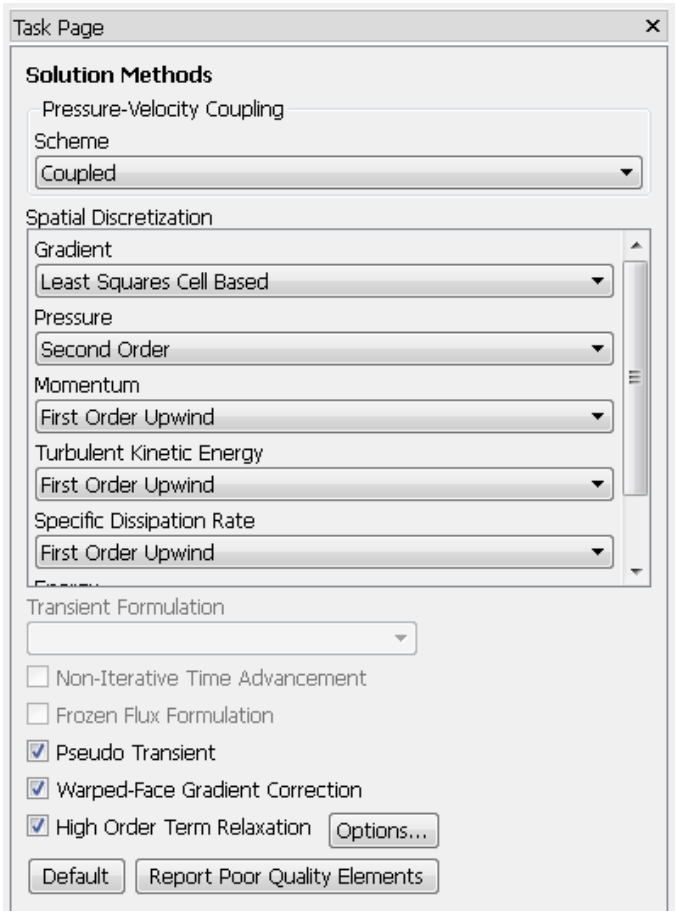

Figure 27: Solution Methods Selection

Step 5. Initialization and Convergence criteria

The simulation converges when the following criteria are reached:

- Residuals lower than 10^{-3} or stable values* of inlet pressure, outlet mass-flow, maximum water velocity and maximum temperature of the different components.
  *(variation between ten iteration lower than 10^{-2})

As far as the case initialization is concerned, a hybrid initialization from the boundary conditions has been use, in order to optimize the convergence.

Step 6. Monitors

In order to know when the simulation has converged, 8 monitors have been created:

1. Inlet Pressure
2. Outlet Mass Flow
3. Maximum water velocity
4. Maximum BSM temperature
5. Maximum Double Wall temperature
6. Maximum Bolts temperature
7. Maximum CuCrZr temperature
8. Maximum Water Temperature

When the variation of this 8 monitors during ten consecutive iterations is lower than10^{-2}, it is when we can say that the simulation has converge. It is also helpful to display the monitors results vs iteration while the simulations is running in order to have an idea about what is going on, such as to detect when the simulation is diverging.

Step 7. Simulation Launching

On this step the simulation is ready to be launched. Before that is recommended to use the "Check Case" option (Figure 28). In order to performed a quick and automatic validation of the simulation set-up.

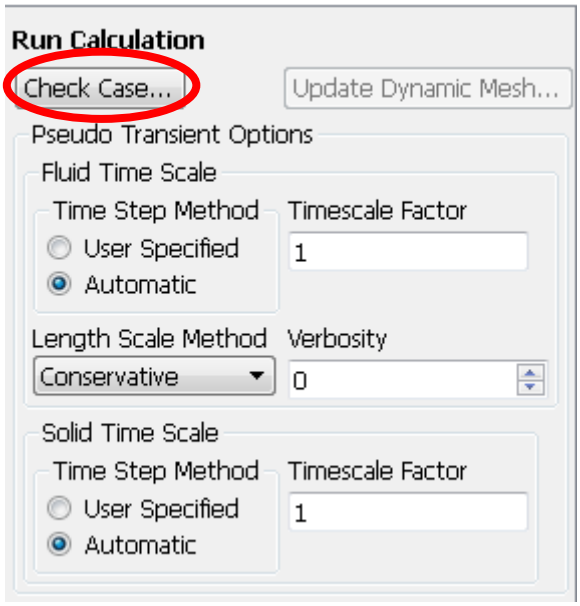

Figure 28: Check Case

CHAPTER 7: STEADY-STATE POSTPROCESSING

7.1. Numerical Results

On this chapter the main results extracted from the thermal hydraulic CDF simulation are exposed:

Table 2: Numerical results from CFD steady-state simulation

Software	FLUENT 18.0
Mesh Type	Poly
Mesh elements	6,659,315
Turbulence model	k-ω SST
P_in [bar]	3.13
P_out [Pa]	0
Vel_in [m/s]	3.17
Vel_out [m/s]	0.48
Max_vel [m/s]	9.81
Mass Flw_in [kg/s]	4.5
Mass Flow_out [kg/s]	4.5
Avg Wall Y+	168.67
Avg Temperature Water [◦C]	87.85
Max Temperature Water [◦C]	131.19
Avg Temperature DW SS [◦C]	143.01
Max Temperature DW SS [◦C]	460.09
Avg Temperature SS [◦C]	136.79
Max Temperature SS [◦C]	434.53
Avg Temperature CuCrZr [◦C]	119.17
Max Temperature CuCrZr [◦C]	173.13
Avg Temperature Inconel [◦C]	271.02
Max Temperature Inconel[◦C]	389.7
Avg Temperature Inlet [◦C]	70
Avg Temperature Outlet [◦C]	98.54
Total Pressure drop [bar]	3.36
Total Temp. difference In/Out [◦C]	28.54

In order to perform a fast an easy validation of the results, an energy balance has been calculated in order to check that all the energy that goes in the system is the same that is going out, as in a steady-state the thermal balance has to be always 0.

Energy Balance

Knowing the energy that we are introduction in the system by the boundary conditions:

- **Energy In** → $\boxed{538.94\ kW}$

  Nuclear heating → 255.7kW

  Surface heat loads → 283.24kW

The only way possible to extract energy from the system is by the water, due to the fact that all the walls of the system are adiabatic, using the following equation we are able to compute the energy extracted out of the system by the water, by the temperature difference between inlet and outlet.

- **Energy Out**

$$Q = \dot{m}\, cp\, \Delta T$$

$$Q = 4.5\frac{kg}{s} * 4182.7\frac{J}{kg\ K} * 28.54K$$

$$\boxed{Q = 537.18\ \text{kW}}$$

The result of the energy balance is a difference of 1.76 kW, a 0.33% of error, error that is totally inside the expected error bar.

7.2. Contour maps

7.2.1. Thermal results on solids

Table 3: Temperature contour maps on the solid part

Temperature [ºC]	**Temperature [ºC]**
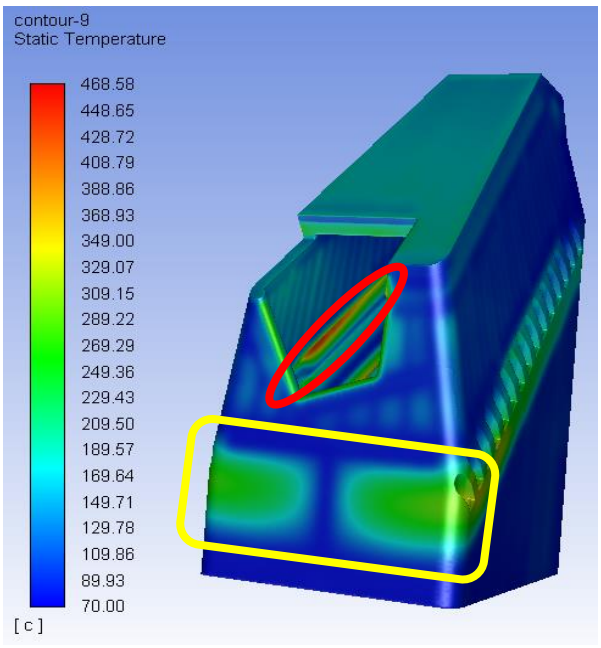	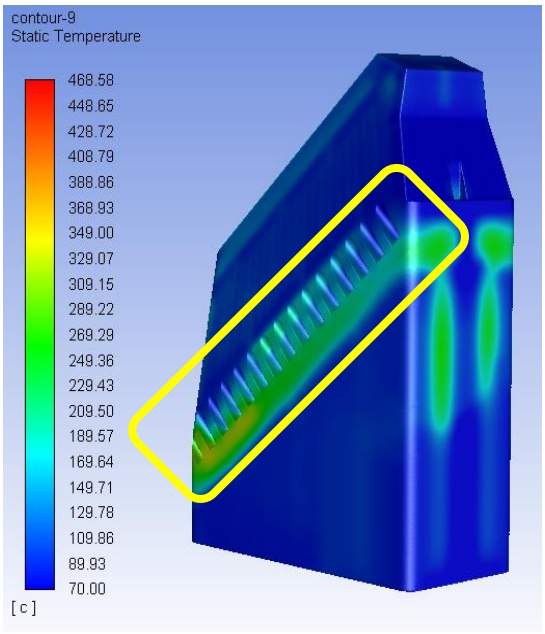
Temperature [ºC]	
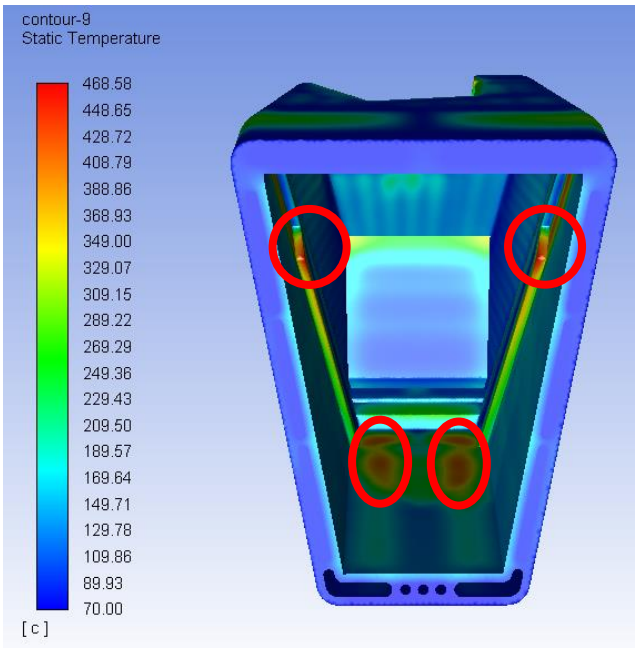	

Overall the cooling performance of the BSM seems to be good, and with an expected behaviour, where the coldest parts are the closest ones to the cooling pipes. However, five critical zones have been detected ("in red") (Table 3), where temperatures are higher or quite close to 450ºC, which is a temperature limit for Stainless Steel 316L (N)-IG under irradiating conditions.

Moreover, other critical zones ("in yellow") (Table 3) have been detected near the bolts, where the BSM is attached to the rest of the Upper Launcher. Where due to lack of cooling pipes, we are generating quite important ΔT that could lead to undesirable thermal stresses.

7.2.2. Hydraulic Results

Table 4: Contour maps of the hydraulic part

Pressure [Pa]	**Wall Y+**
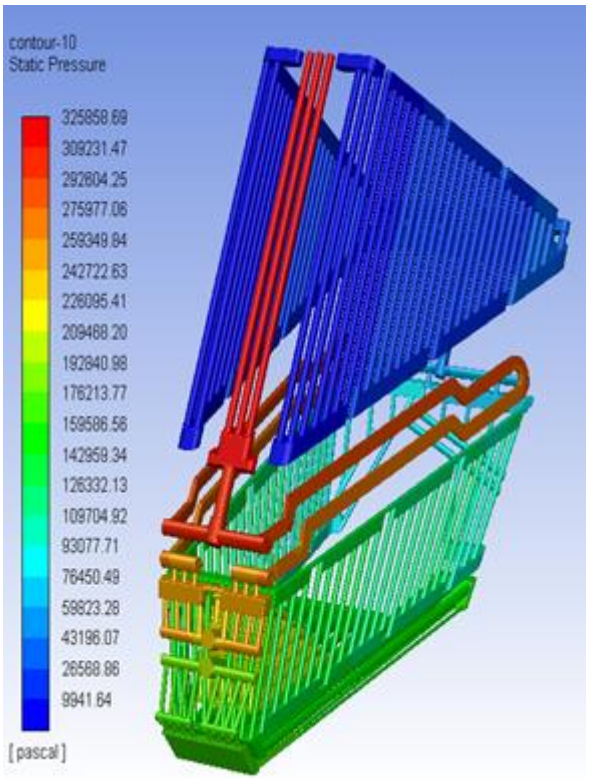	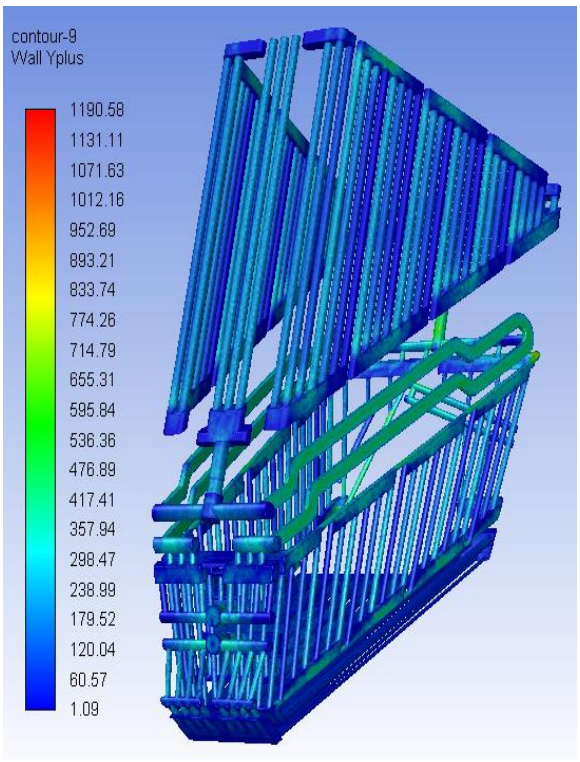

Heat transfer coefficient [w/m²K]	**Heat transfer coefficient [w/m²K]**
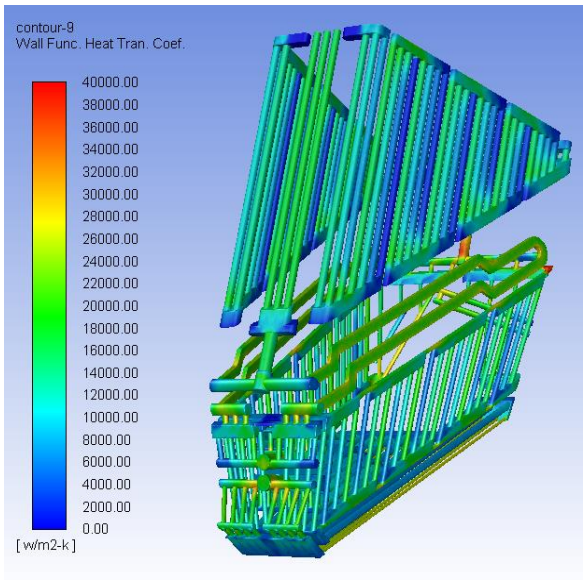	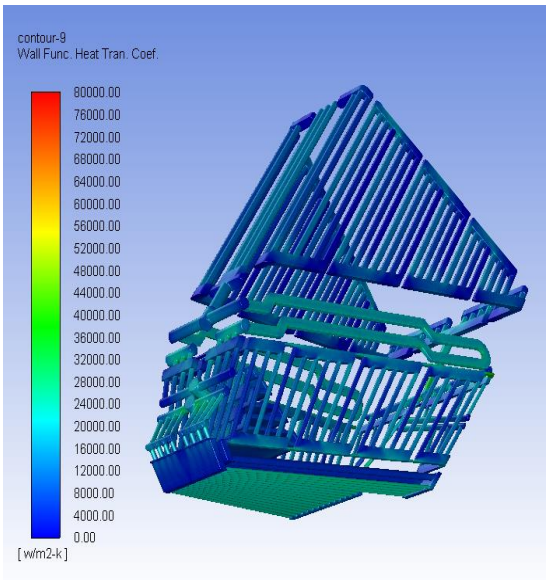
Temperature [ºC]	**Temperature [ºC]**
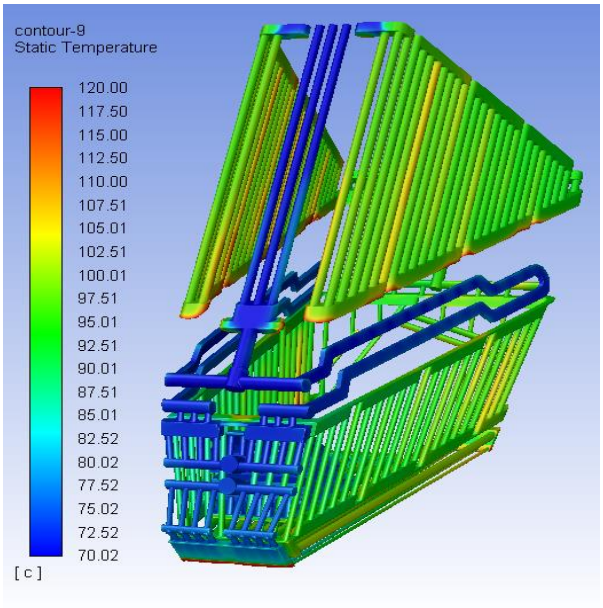	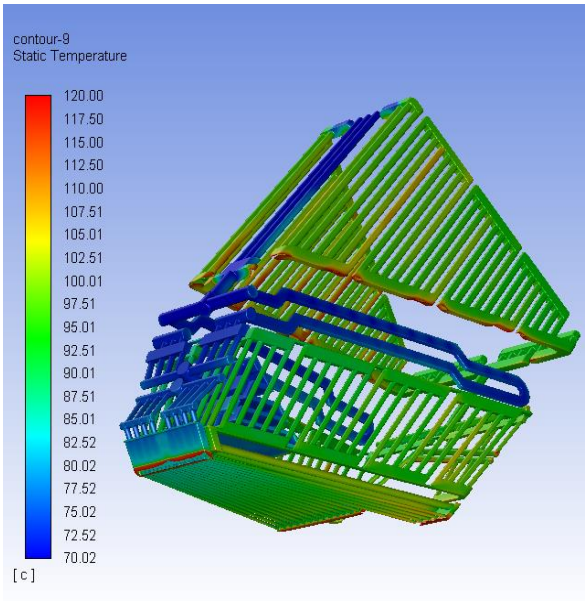

The pressure follows an expected behaviour (Table 4), where the highest values are found on the inlet, and while the water is going through the pipes is losing pressure, till the 0Pa boundary condition is achieved on the outlet. Just remember that the pressure map shown on (Table 4), represents relative pressures, the real pressure is the operating pressure (40 bar) plus the relative one.

Moreover, the maximum temperature on the water is ~130ºC (Table 4) meaning that in a system where the working pressure is 40bar, the saturation temperature is ~250 ºC; therefore we are quite far from having evaporation on the pipes, what is highly undesirable.

7.2.3. BSM Shell Side

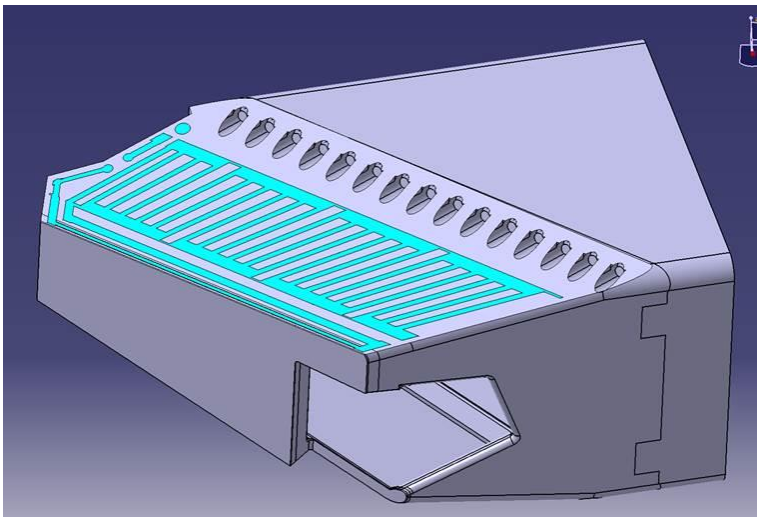

Figure 29: BSM Shell Side cutting plane location

Table 5: Internal contour maps on the BSM Shell Side

Temperature [ºC]	**Temperature [ºC] only water**
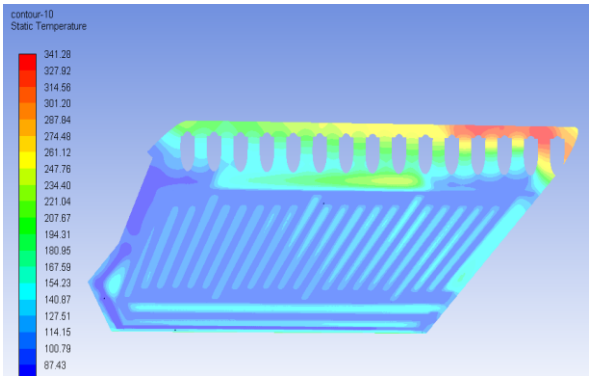	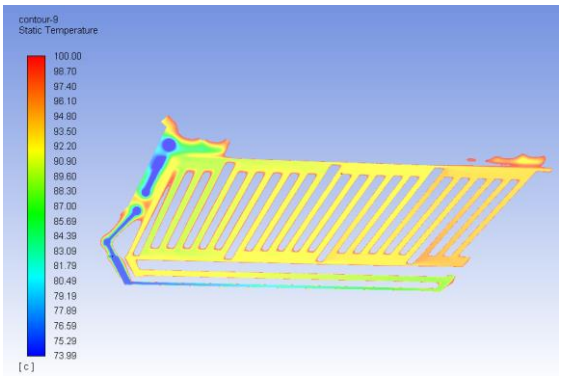
Velocity [m/s]	**Pressure [Pa]**
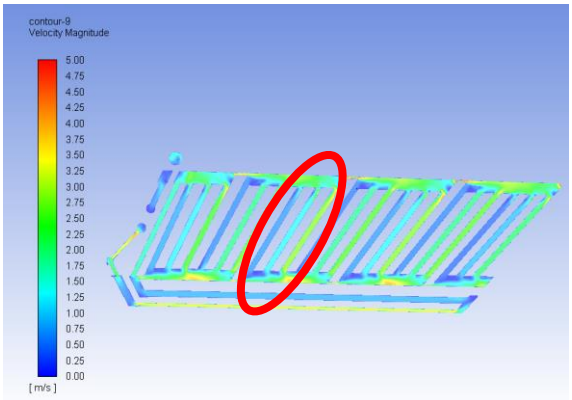	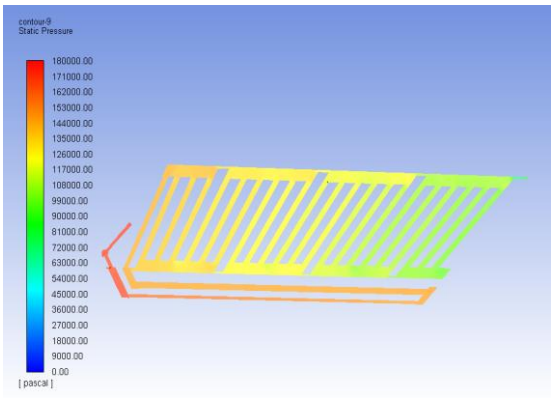

An import undesired behaviour has been detected, on the BSM Shell Side pipes (Figure 29), the water is not well distributed inside the pipes ("in red") (Table 5), the water inside that pipes follows a three parallel pipes path (Figure 30), and it was expected a distributed fluid on the three parallel pipes, although it is not what we see. The water mostly goes through the last third pipe, and almost avoiding the first pipe. This effect is not desirables, because could generate a non-uniform cooling of that region leading to important ΔT on the material between pipes, generating in that way undesired thermal stresses.

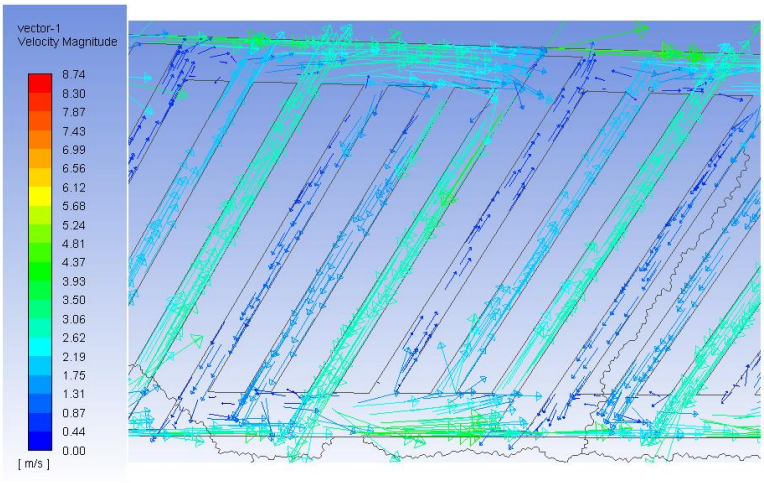

Figure 30: Velocity vectors map on the BSM Shell side

7.2.4. BSM Shell Bottom

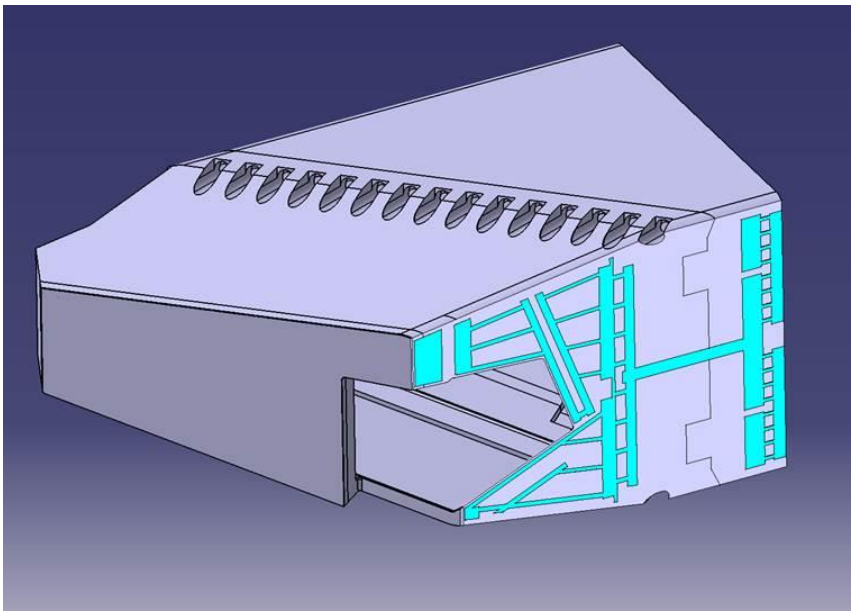

Figure 31: BSM Shell Bottom cutting plane location

Table 6: Internal contour maps on the BSM Shell Bottom

Temperature [ºC]	Temperature [ºC] only water
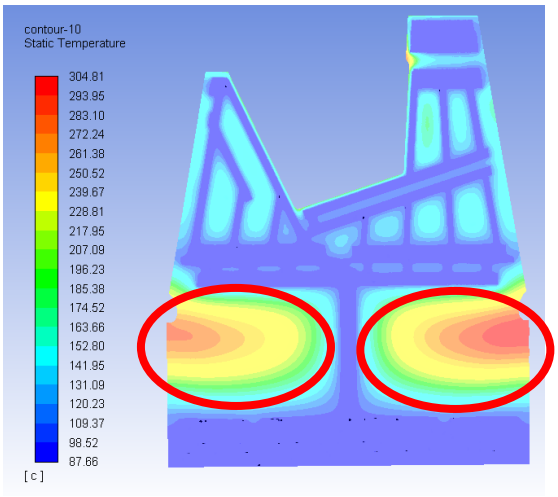	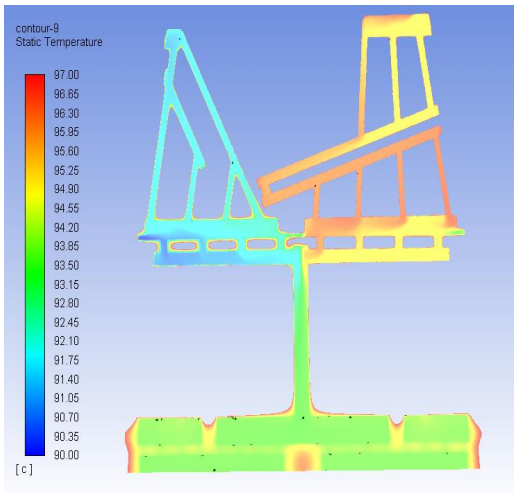
Velocity [m/s]	**Pressure [Pa]**
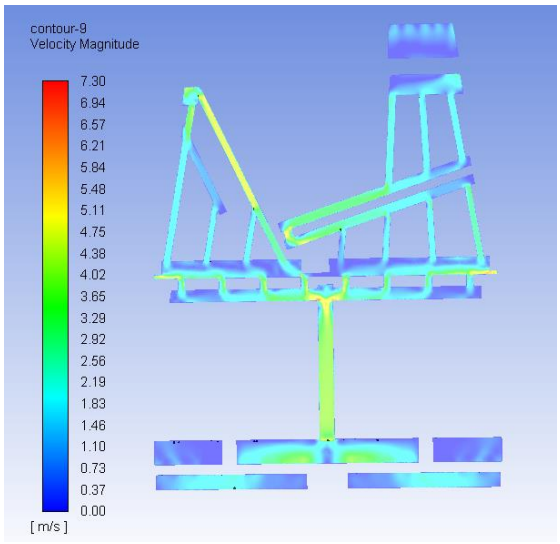	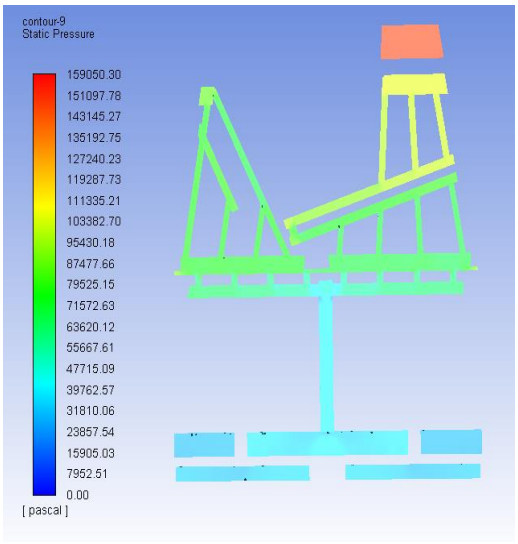

On this section plane on the bottom BSM shell pipes (Figure 31), it can be observed clearly, the region ("in red") (Table 6) where the BSM is attached through bolts to the rest of the Upper Launcher, that due to a lack of cooling pipes on that region the heat is not extracted properly, and two important focus of heat are generated.

7.2.5. Front Wall Panel Front Pipes

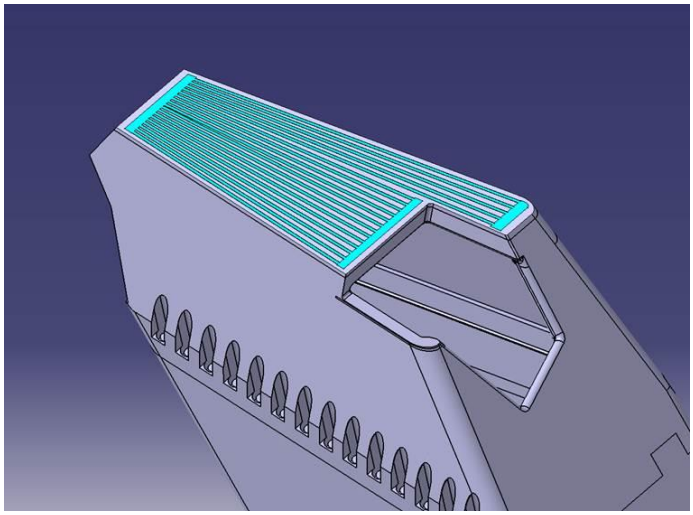

Figure 32: FWP Front Pipes cutting plane location

Table 7: Internal contour maps on the FWP Front Pipes

Temperature [ºC]	Temperature [ºC] only water
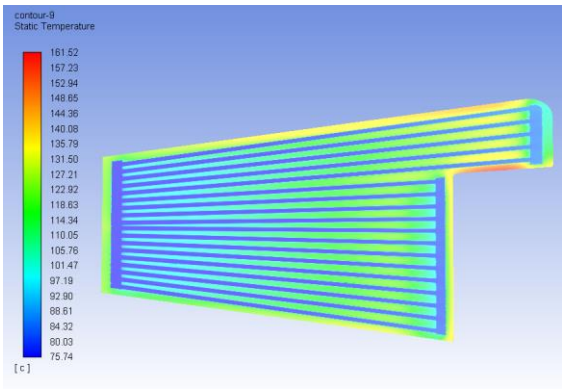	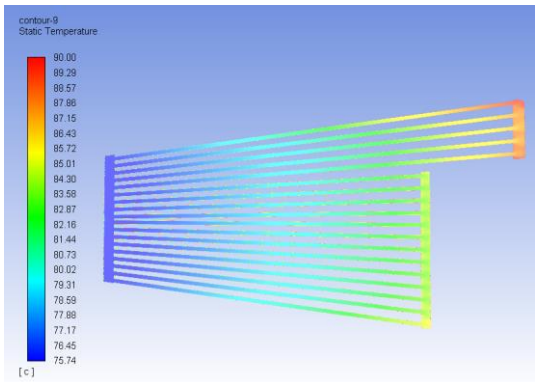
Velocity [m/s]	**Pressure [Pa]**
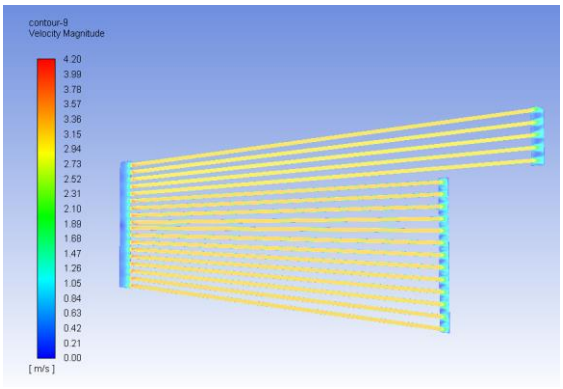	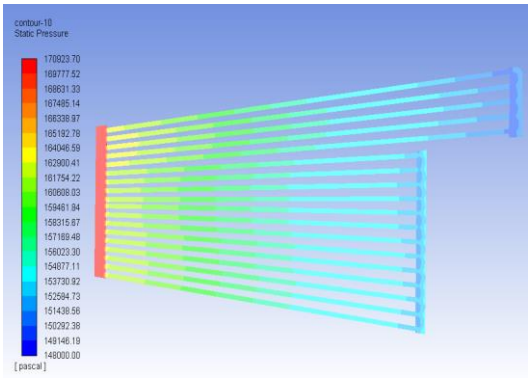

In relation with the BSM plate pipes that are facing directly the plasma (Figure 32), we can see that they perform perfectly its cool job due to that the cooling pipes system on that zone is working as properly. It is important to check that we are always far from the temperature limit for the Stainless Steel (450ºC) and from the water temperature limit (250ºC). Moreover, in order to avoid problems of oxidation is recommended to avoid velocities inside the pipes higher than 10 m/s, value never exceed on this analysis.

7.2.6. Front Wall Panel Plate Pipes

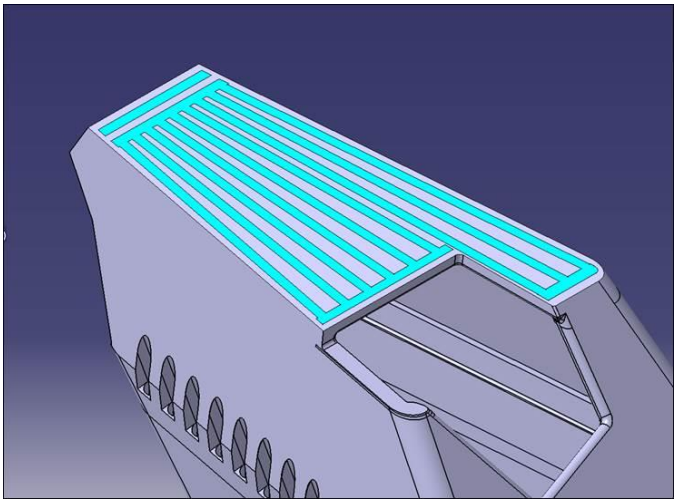

Figure 33: FWP Plate Pipes cutting plane location

Table 8: Internal contour maps on the FWP Plate Pipes

Temperature [ºC]	Temperature [ºC] only water
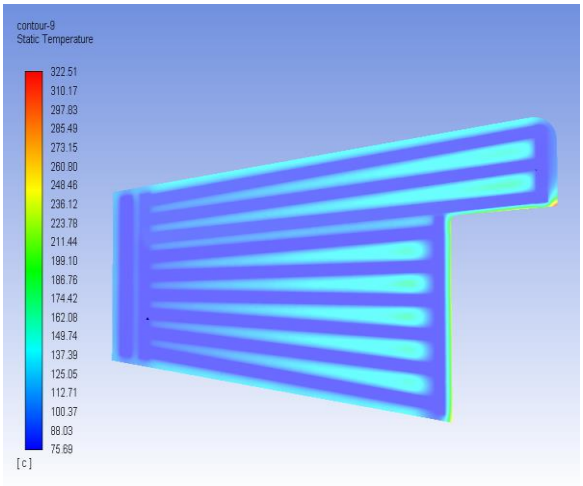	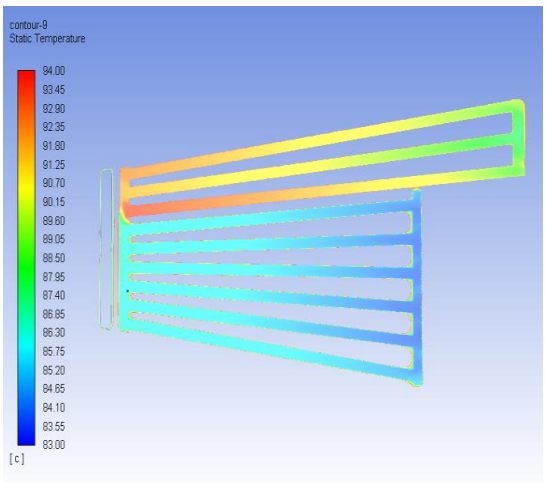

Velocity [m/s]	Pressure [Pa]
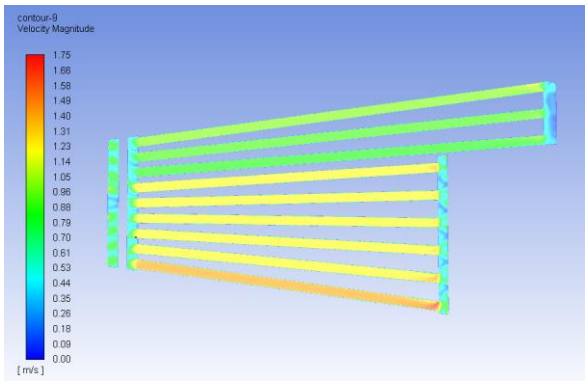	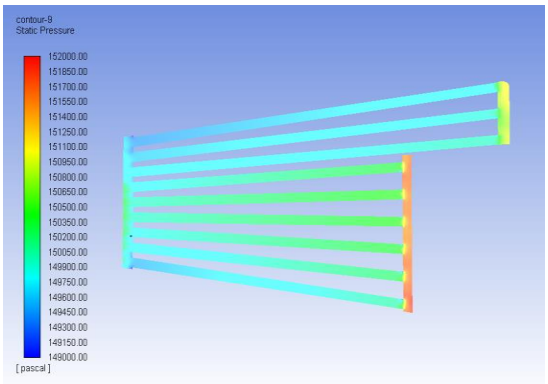

The main concern for the Plate pipe (Figure 33), the ones just above the Front pipes, is that due to its higher diameter compere with the Front pipes an average of 1m/s is achieved, leading to a quite low velocity for a proper heat extraction on that zone. However, seems that in that zone being just above the Front pipes that work perfectly as we could see on section 7.2.5, the Plate pipes are not facing an important heat load, therefore even with that quite low velocity we are not reaching any critical situation, nowhere the limits are exceed.

7.2.7. Central XZ Plane

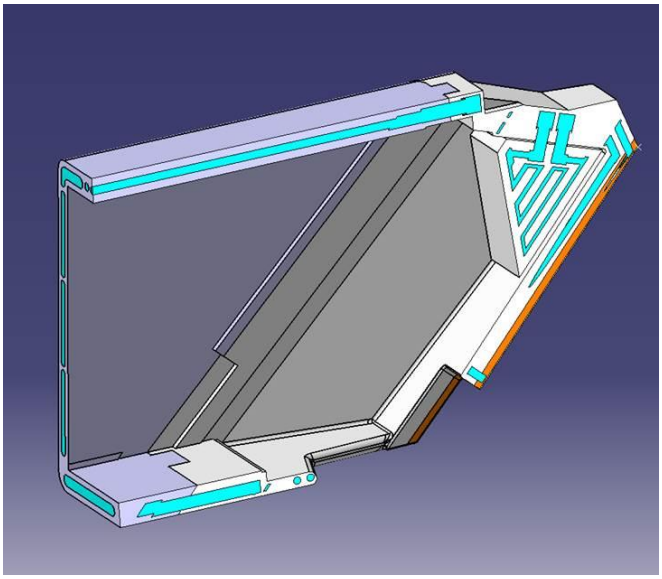

Figure 34: Central XZ cutting plane location

Table 9: Internal contour maps on the Central XZ Plane

Temperature [ºC]	**Temperature [ºC] only water in upper shield**
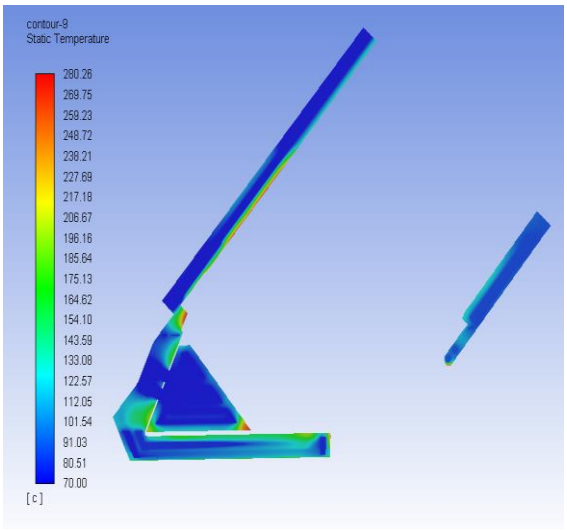	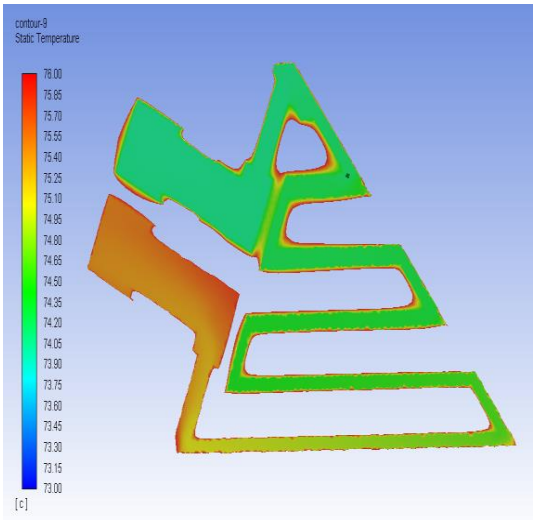
Velocity [m/s]	**Pressure [Pa]**
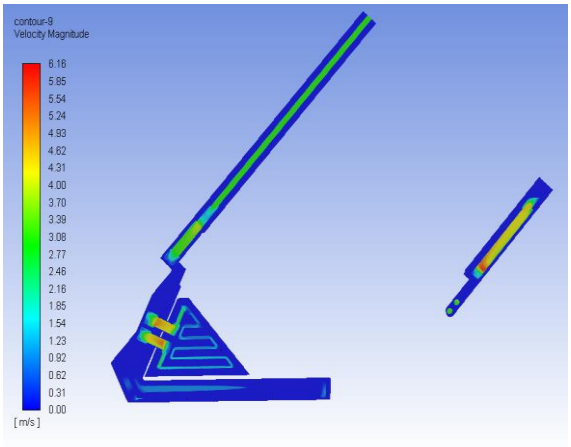	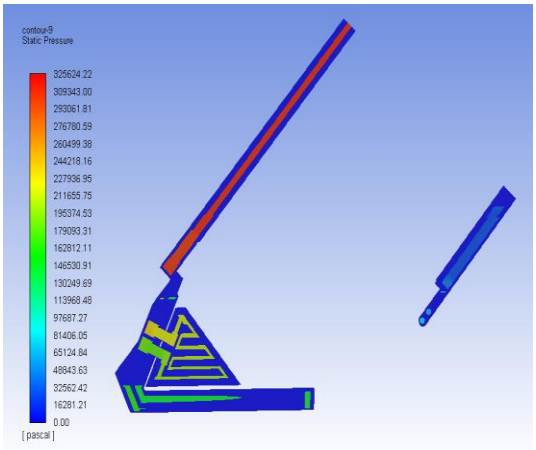

The upper-shielding (Figure 34) receives an important amount of thermal loads as its function is to be an internal shield for the BSM, although we can appreciate on Table 9 that its cooling system is working properly and keeping it under reasonable temperatures.

7.2.8. Bolts

Table 10: Internal contour maps on the Bolts

Temperature [ºC]	Temperature [ºC]
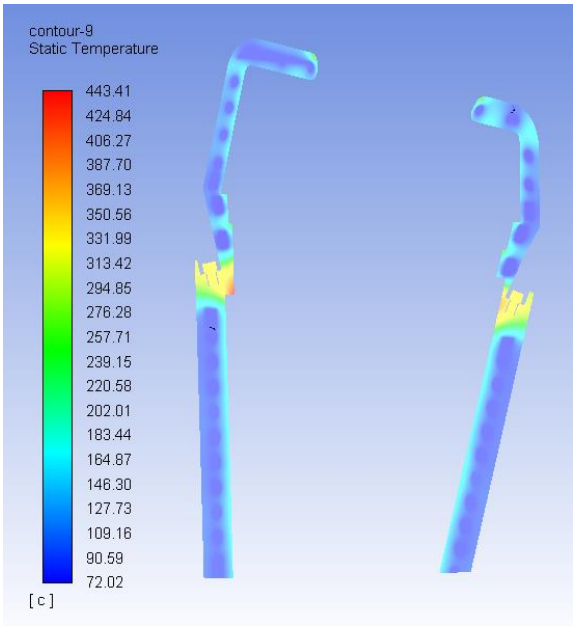	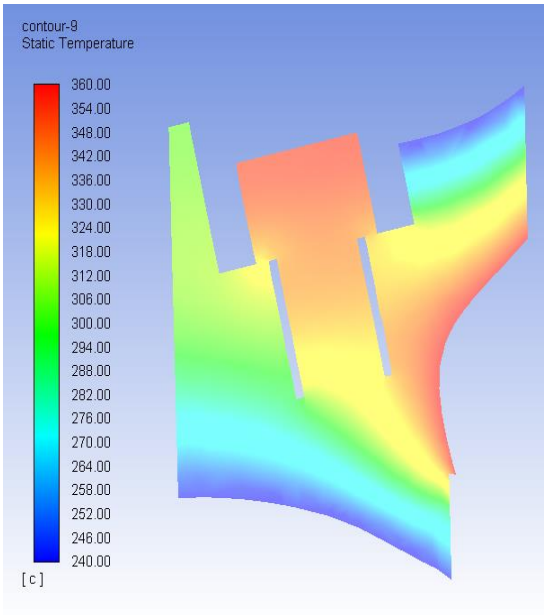

The bolts that joined the BSM to the rest of the Upper-Launcher are made of Inconel (Alloy 718), which have a temperature limit of 300ºC under irradiating conditions. Therefore, a critical point has been found on the bolts where a maximum temperature of 360 ºC is reached.

CHAPTER 9: SENSITIVITY ANALYSIS

In order to verify that the previous results don't depend on the number of mesh elements, a sensitivity analysis has been done by refining the mesh.

9.1. Refine Mesh

The methodology applied for the creation of the refine mesh (Figure 35) is the same that the one used to create the main mesh (Section 5.3) but this time a smaller sizing and a boundary layer mesh (inflation) have been used in order to increase the number of mesh elements.

Polyhedral Refine Mesh (52.369.975 elements)

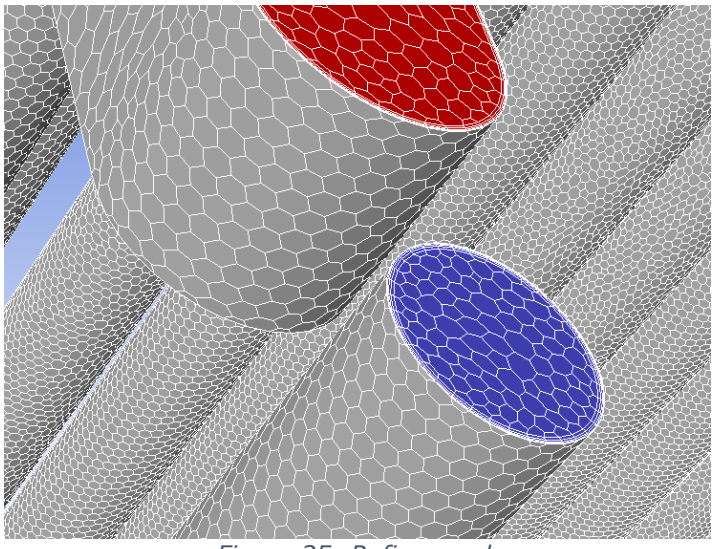

Figure 35: Refine mesh

Boundary layer mesh

In general, in order to obtain more reliable results, it has been chosen to use a specific refinement of the mesh on the boundary layer, meaning that a finer and more controlled mesh has been used, in those areas where the water is in contact with solid walls, the walls of the cooling tubes. Doing that, the wall y+ will decrease considerably, ensuring that the wall y+ requirements for the turbulence model selected will be fully complied.

The fluid boundary layer due to its viscosity has a different velocity profile than outside it. This fact explains that in the narrow layer there are great

changes in speed in very short distances, this is why a mesh small enough it is needed to capture those great changes that takes place in such a small area.

In order to generate that specific mesh on the boundary layer, on Ansys Meshing exists a mesh control method, called Inflation. This method allows to build a fully controlled mesh on the boundary layer by setting three input parameters:

- The distance of the first cell of the boundary layer
- The number of cells in the boundary layer
- The factor of cell growth of the boundary layer

Therefore, the first step is to calculate how large the first cell has to be. In order to find this value, you need to know what y+ is the desired one.

The y+ is a non-dimensional distance. It is often used to describe how coarse or fine a mesh is for a particular flow pattern on the boundary layer. It is important in turbulence modelling to determine the proper size of the cells near domain walls. The turbulence model wall laws have restrictions on the y+ value at the wall. For instance, the K-omega SST model with standard wall function requires a wall y+ value between approximately 300 and 30. A faster flow near the wall will produce higher values of y+, so the grid size near the wall must be reduced [13].

There are two different ways to solve the boundary layer:

On the one hand there is the way that requires a proper mesh at that zone and it simply solve that zone as any other, calculating for each cell its value.

On the other hand there is the way called "wall functions model", where there is no need to make a super-refine mesh on that zone, that model approaches by means of a logarithmic curve the speed profile that the working fluid has

in the boundary layer without having to calculate cell by cell what happens in the boundary layer.

The wall y+ recommended on Ansys Fluent to use a cell by cell calculation, is a y+≤5 and to use the wall functions model a 30≤y+≥300.

On Figure 36, it can be seen on the left image a boundary layer mesh using the wall functions method, and on the right image can be observed a boundary layer mesh using the cell by cell calculation.

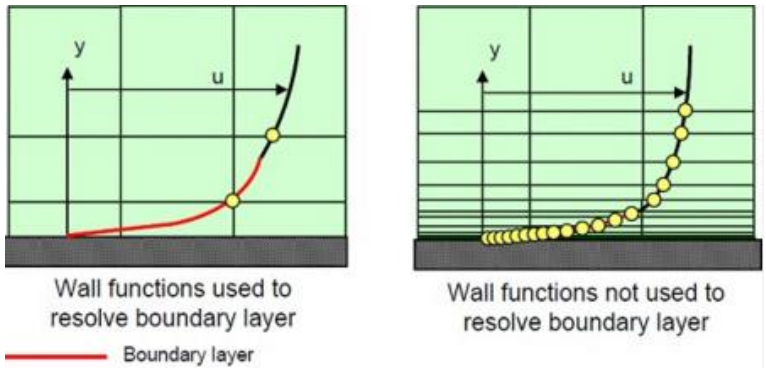

Figure 36: Boundary layer mesh methods [17]

The ideal case is to solve the boundary layer using the cell by cell calculation, although then a super-extra refine mesh is needed on the boundary layer, in order to get a wall y+≤5. Due to the complexity and dimensions of our model to be meshed, to get a full mesh with a wall y+≤5 it is almost impossible with the resources available. To generate the refine mesh for the sensitivity analysis, we have created a mesh with a boundary layer as small as the CPU power available, ending with a mesh of 52.369.975 elements (Figure 35) and with an average wall y+ of 16.54.

9.2. Comparison

On the following table (Table 11) the difference on the results with the main mesh and the refine mesh are exposed.

Table 11: Comparion Table (Sensitivity Analysis)

Mesh	Main Mesh	Refine Mesh	Difference in % between the two different meshes
Software	FLUENT 18.0	FLUENT 18.0	
Mesh Type	Polyhedral	Polyhedral	
Mesh elements	6,659,315	52,369,975	
Solver	k-ω SST	k-ω SST	
P_in [bar]	3.36	3.25	3.27%
P_out [Pa]	0	0	0.00%
Vel_in [m/s]	3.17	3.16	0.32%

Max_vel [m/s]	9.81	9.83	0.20%
Mass Flow_in [kg/s]	4.5	4.5	0.00%
Mass Flow_out [kg/s]	4.5	4.5	0.00%
Avg Wall Y+	168.67	16.54	90.19%
Avg Temperature Water [◦C]	87.85	88.13	0.32%
Max Temperature Water [◦C]	131.19	138.55	5.61%
Avg Temperature DW SS [◦C]	143.01	142.43	0.41%
Max Temperature DW SS [◦C]	460.09	462.83	0.60%
Avg Temperature SS [◦C]	136.79	136.14	0.48%
Max Temperature SS [◦C]	434.53	433.39	0.26%
Avg Temperature CuCrZr [◦C]	119.17	120.17	0.84%
Max Temperature CuCrZr [◦C]	173.13	171.82	0.76%
Avg Temperature Inconel [◦C]	271.02	270.53	0.18%
Max Temperature Inconel[◦C]	389.7	387.87	0.47%
Avg Temperature Inlet [◦C]	70	70	0.00%
Avg Temperature Outlet [◦C]	84.27	83.83	0.52%

The average difference between the both meshes in the main results is 1%, meaning a 99% of similarity on the results.

In order to not only performed a quantitative comparison but also a qualitative comparison, the main contour plots of both meshes will be compere.

Table 12: Temperature contour maps on the solid part

Main Mesh	Refine Mesh
Temperature [ºC]	Temperature [ºC]
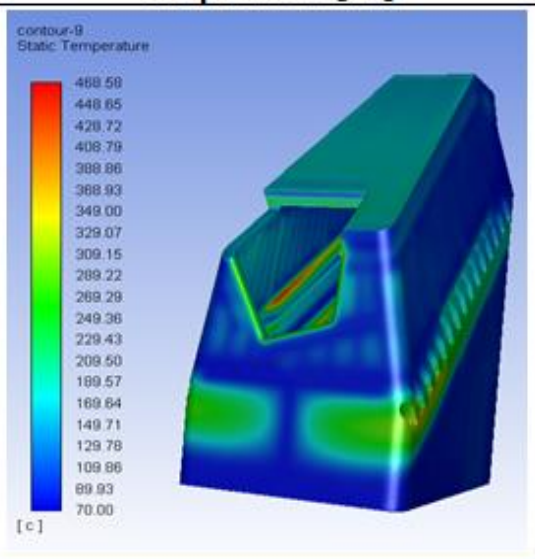	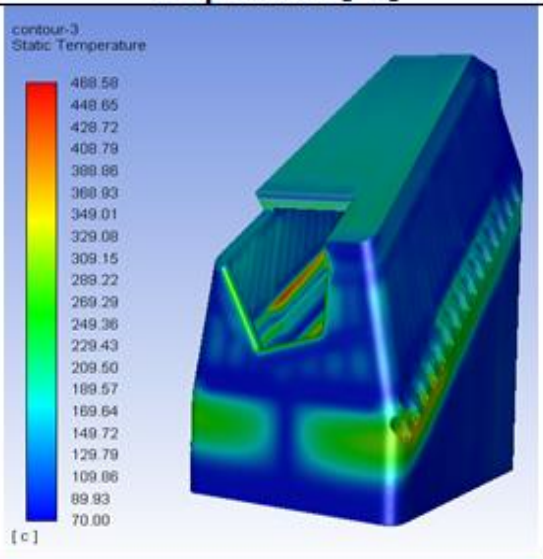
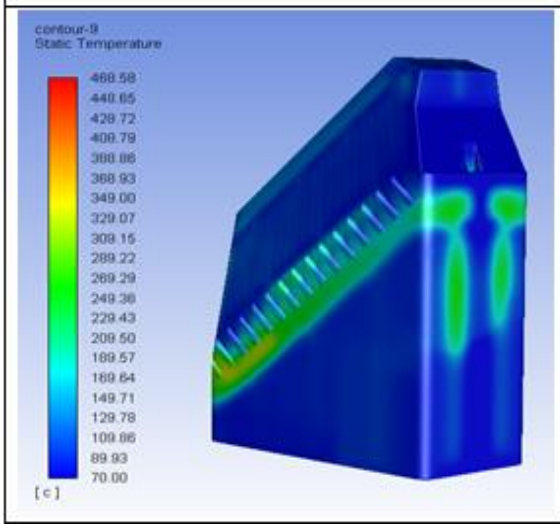	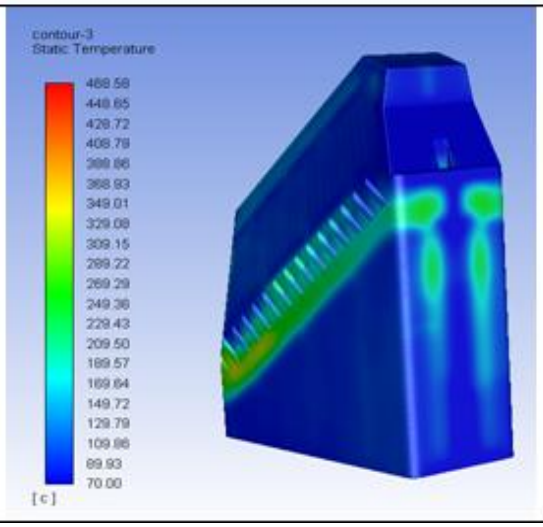
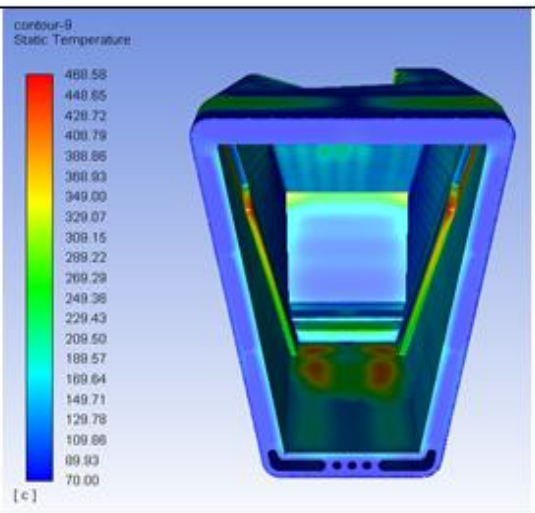	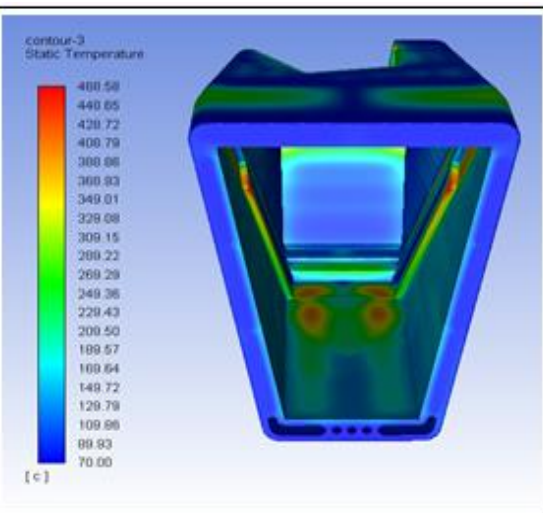

In relation with the temperature distribution on the outside walls, no important differences can be observed.

Table 13: Hydraulic contour maps on the hydraulic part

Main Mesh	Refine Mesh
Pressure [Pa]	Pressure [Pa]
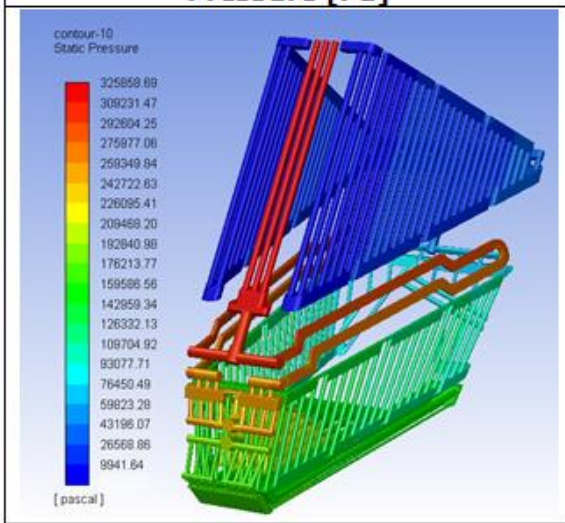	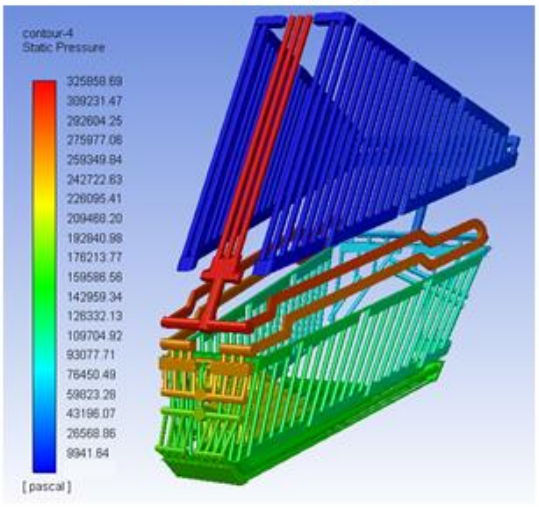
Wall Y+	Wall Y+
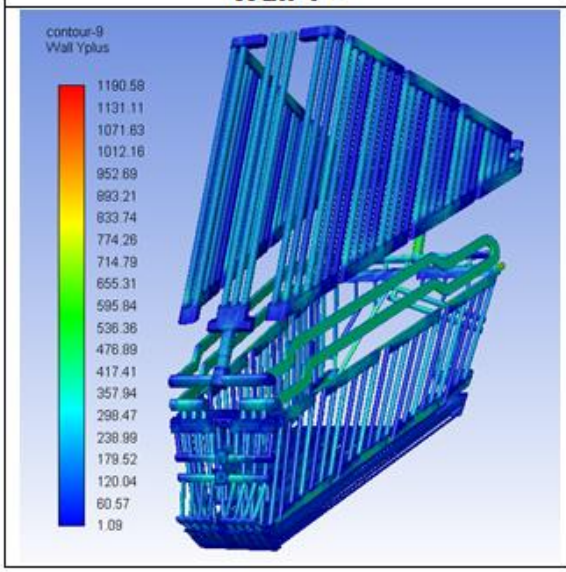	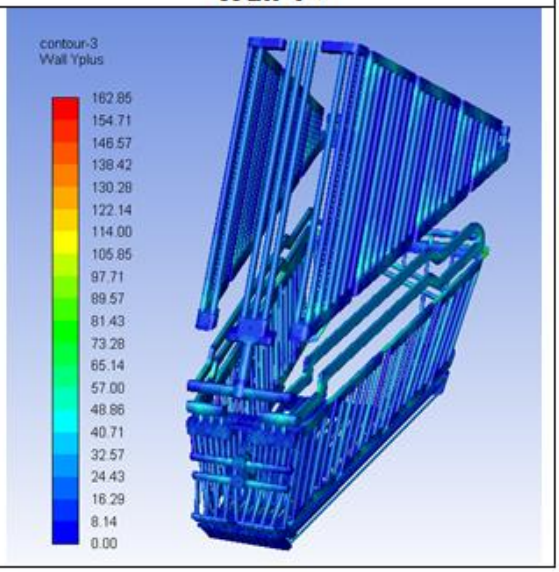

We can check that with the new mesh we are fully inside the wall y+ that Ansys Fluent recommend when using the k-ω STT turbulence model (y+≤300), the average wall y+ on the water walls is 16.54, meaning that in plenty of places we are with a y+≤5, where a cell by cell calculation takes place on the boundary layer, meaning that the boundary layer is solved in a more realistic way.

Table 14: Temperature contour maps on the hydraulic part

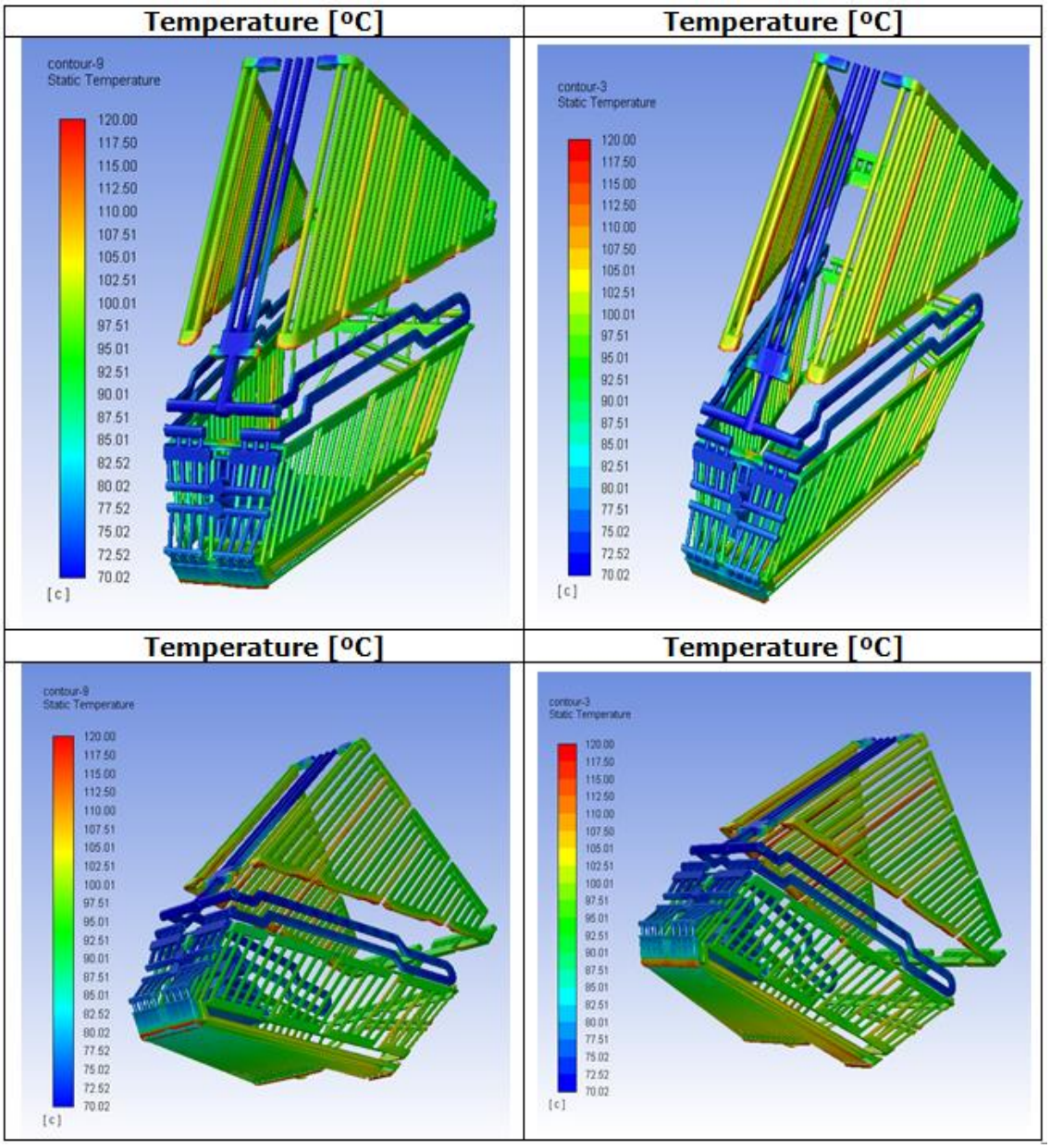

Comparing the temperature distribution on the water walls, it is observed that the results are equivalent.

For the internal planes (Annex 15.2), the differences are minimum or indistinguishable. The bigger difference is that we are getting slightly higher values of velocity inside some pipes on the refine mesh, although we are just speaking of differences less than 5%. However, where the bigger concerns are is on the temperature distribution, and we can conclude that the difference between the two meshes is fully inside the limits. Meaning, that the main mesh is validated and its results completely independent with the mesh used. Therefore, there is no need to use a complex mesh with boundary layer mesh, which implies much more CPU needs and computational time.

CHAPTER 10: MECHANICAL TRANSIENT ANALYSIS

10.1. Mechanical Transient Analysis

The goal of this analysis is to study the Electron Cyclotron Upper Launcher BSM cooling performance along time, during the ITER inductive operation. The main issues to be studied on a transient operation is to detect the presence of temperature inertia due to a pulsed operation and to verify that using an steady state analysis the results are similar and inside an affordable difference.

The software that has been used for this analysis is Ansys Mechanical 18.0.

10.2. Case Studied

On Table 15 it is shown the CAD model and the mesh of the BSM that has been analysed, are exactly the same that the one used for the thermal-hydraulic CFD analysis (Section 5).

The only differences is that we are performing a mechanical analysis, meaning that we will not simulate the water, instead of solving the fluid part we have assumed a heat transfer coefficient on the water walls, extracted from the steady-state CFD simulation, to simulate the cooling effect of the water. Therefore, the CAD part of the model that represents the water has been delate of the analysis.

Table 15: BSM CAD model and polyhedral mesh used on the mechanical transient analysis

BSM CAD Model	Polyhedral Mesh (6.659.315 elements)
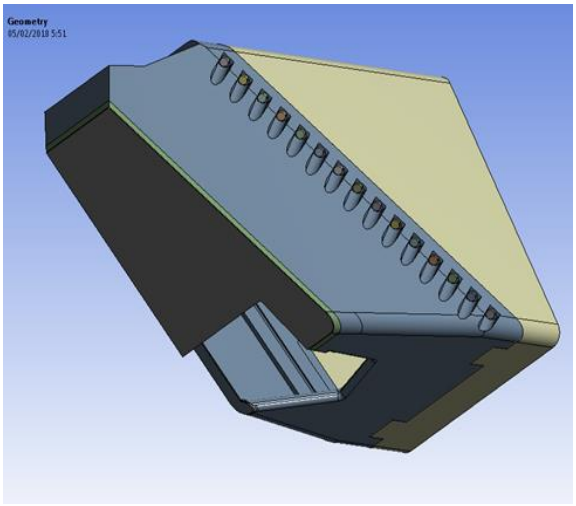	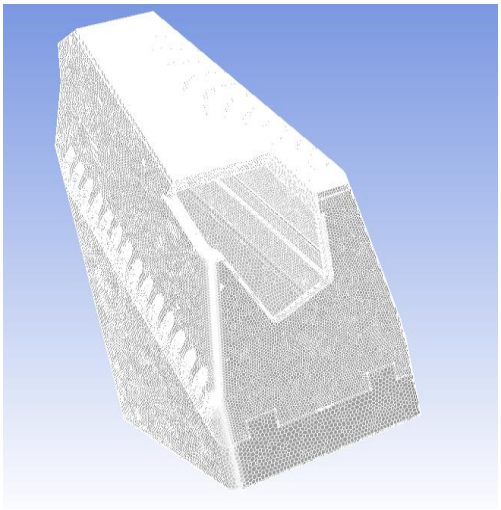

10.3. Boundary Conditions

The boundary conditions are exactly the same that the ones used for the thermal-hydraulic CFD analysis (Section 6):

Nuclear Heating

Nuclear volumetric heating (Figure 37).

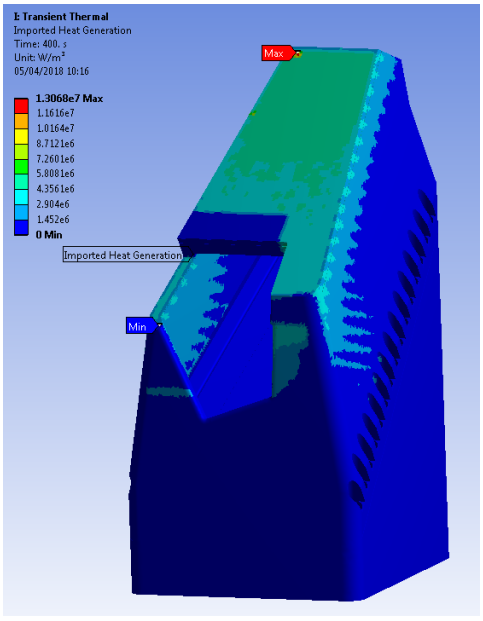

Figure 37: Nuclear Heating

Surface Loads

Surface Thermal loads (Figures 38 and 39) calculated using the Plasma View Factor (ANSYS Radiosity).

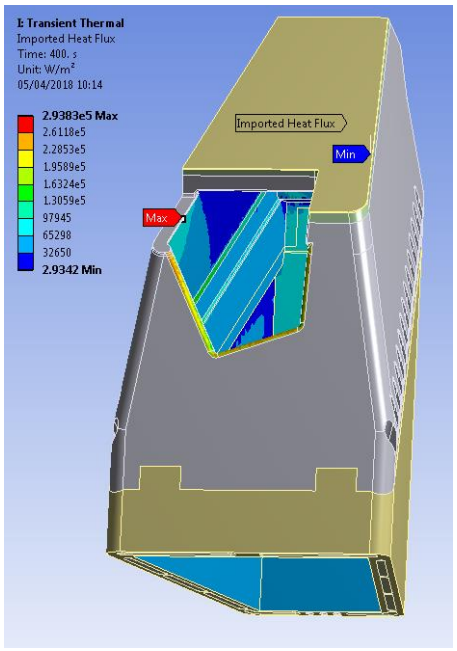

Figure 38: Internal surfaces Thermal Load

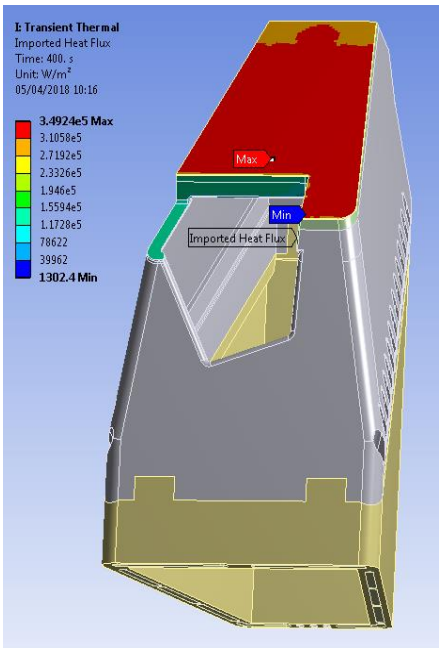

Figure 39: External surfaces Thermal Load

Heat Transfer coefficient

A HTC equal to 20000 W/m2°C and a bulk temperature of 70°C has been applied on the water walls in order to represent the water cooling (Figure 40). Do not forget that this is an important assumption, considering an equal HTC in all the water walls, although this analysis in not intended to extract exact results, is just a first and fast simulation to understand which can be the behaviour of the BSM in a transient analysis and which are the differences between an steady-state one.

The rest of the solid walls of the BSM, they have been considered adiabatic walls.

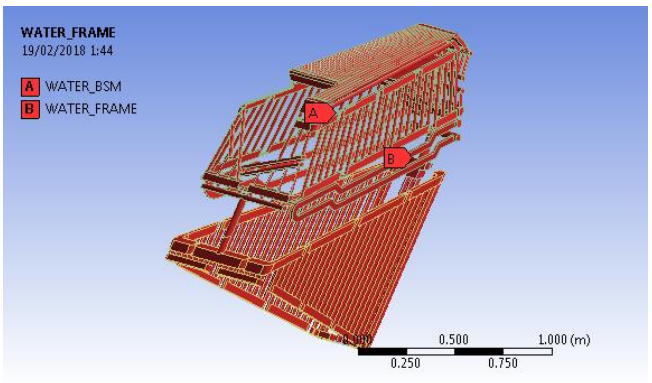

Figure 40: Application of the HTC

Inductive Operation

Scenario	Fusion Power [MW]	tON [s]	tOFF [s]
A) Inductive operation	500	400	1400
B) Hybrid operation	400	1000	3000
C) Non-inductive operation	356	4000	9000

Table 3.1 - ITER thermal scenario

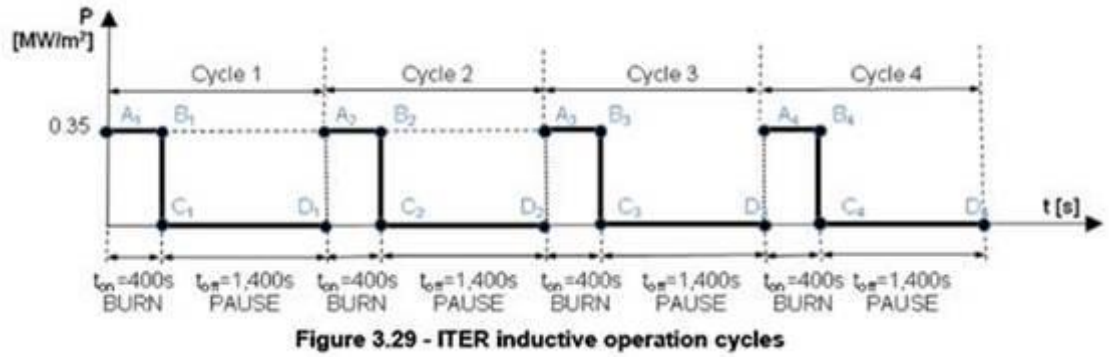

Figure 3.29 - ITER inductive operation cycles

Figure 41: ITER Inductive Operation

The inductive operation is the working operation that ITER is supposed to work, it is a pulsative operation, where the rector will be operating for 400s, thermal loads coming from the plasma are activated, and 1400s of pause, thermal loads coming from the plasma are desactivated.

10.4. Analysis Results

The results of the transient mechanical analysis are shown below:

All the images of contour maps that will be shown on this section are taken in the worst time step of the transient simulation, when the maxim temperatures are reached, that is always at the end of the pulse.

Table 16: Temperature contour maps on the solid part

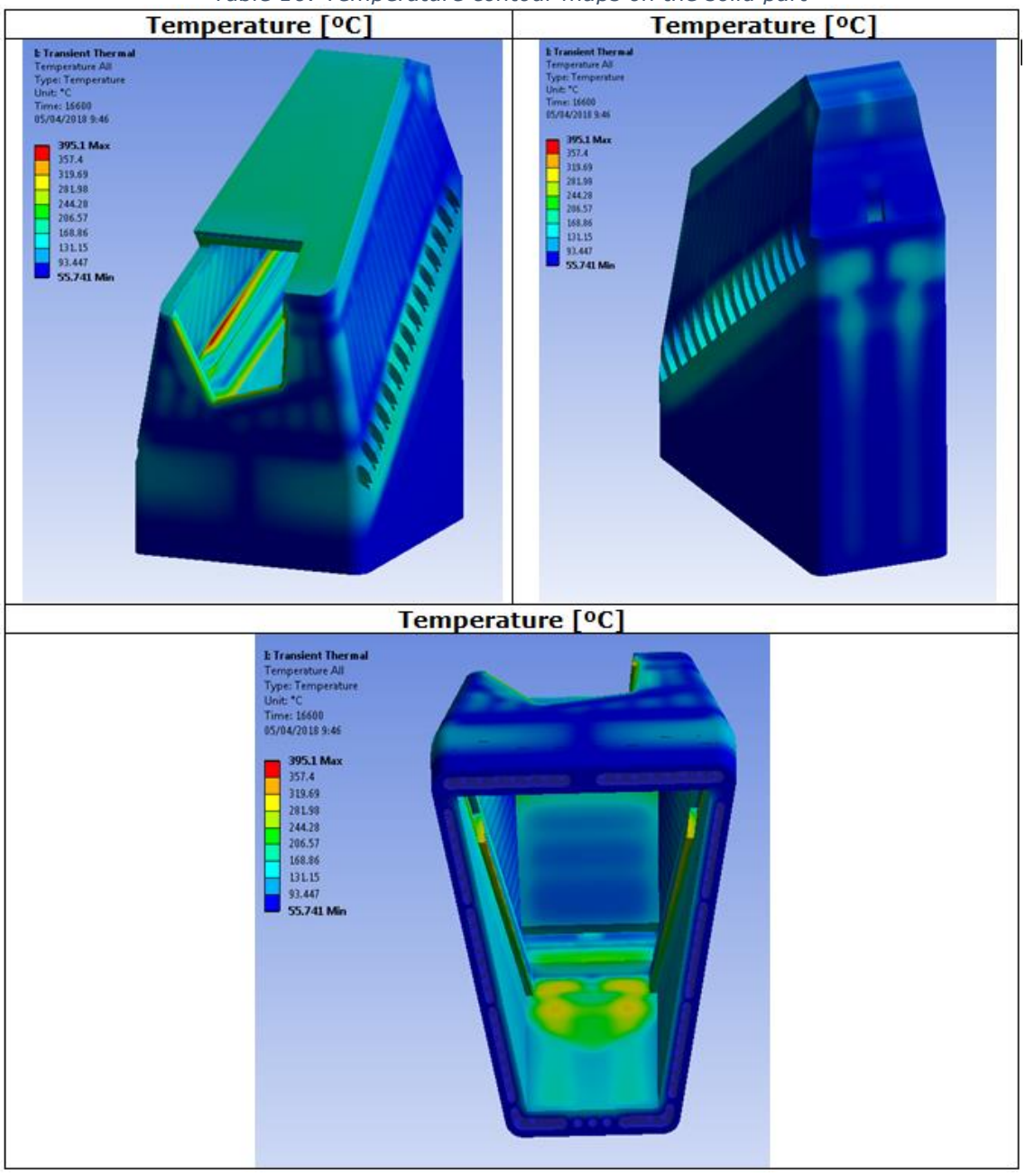

In order to obtain the temperature evolution, we tracked the temperature evolution of the different components of the model:

BSM Stainless Steel

Table 17: BSM Stainless Steel, temperature map distribution at its maximum time moment

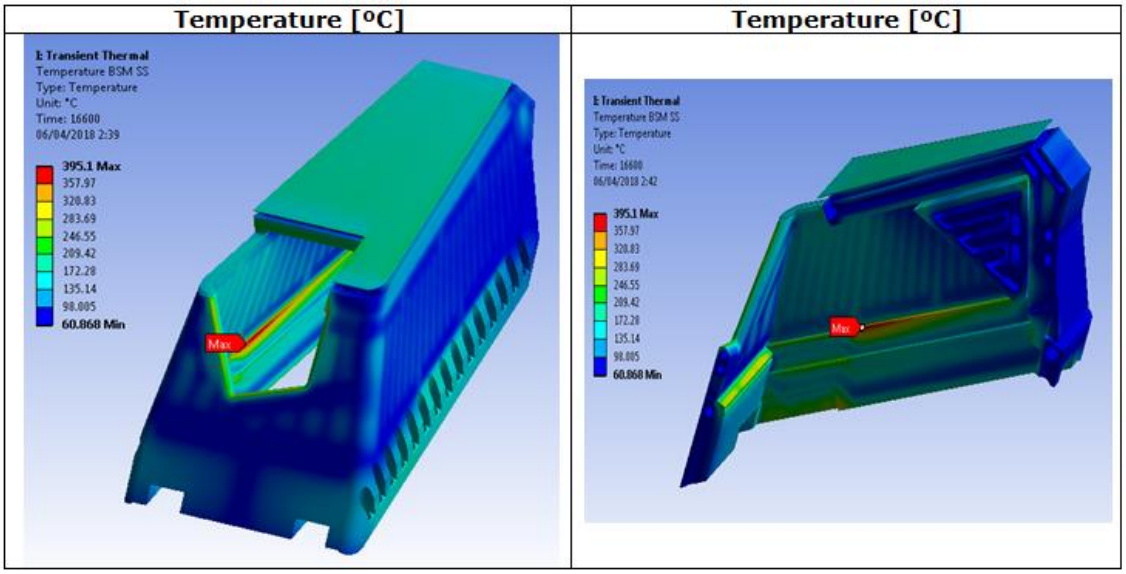

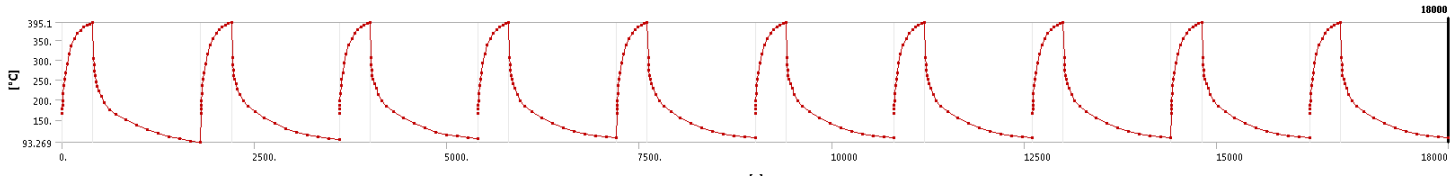

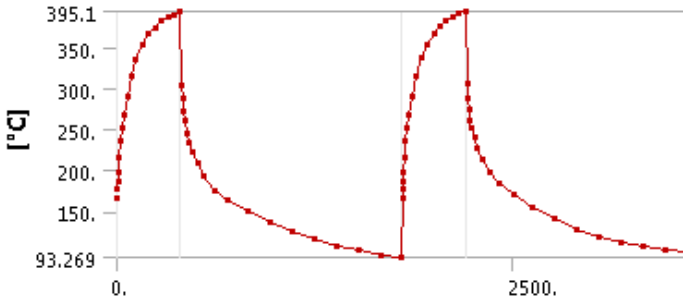

Figure 42: BSM Stainless Steel, temperature vs time

Frame Stainless Steel

Table 18: Frame Stainless Steel, temperature map distribution at its maximum time moment

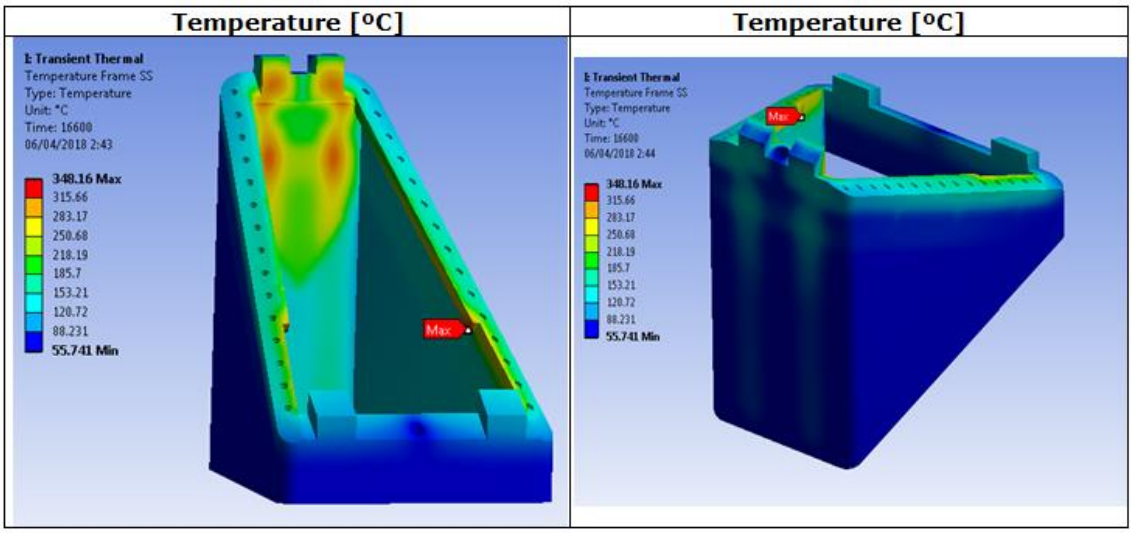

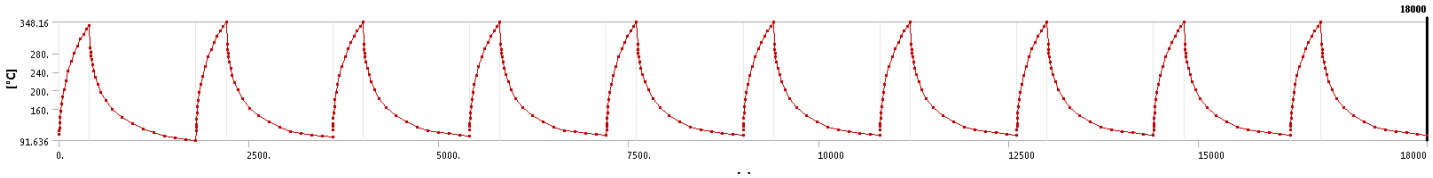

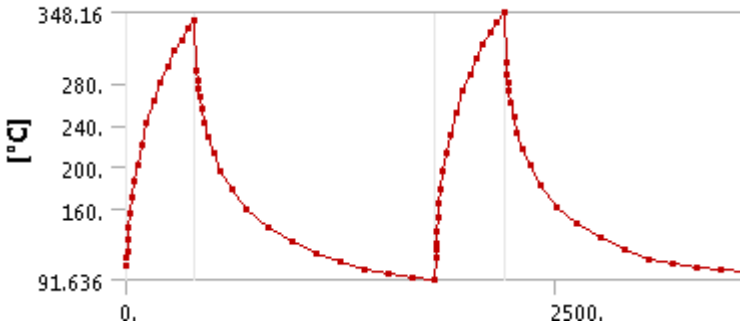

Figure 43: Frame Stainless Steel, temperature vs time

Inconel Bolts

Table 19: Inconel Bolts, temperature map distribution at its maximum time moment

Temperature [ºC]	Temperature [ºC]
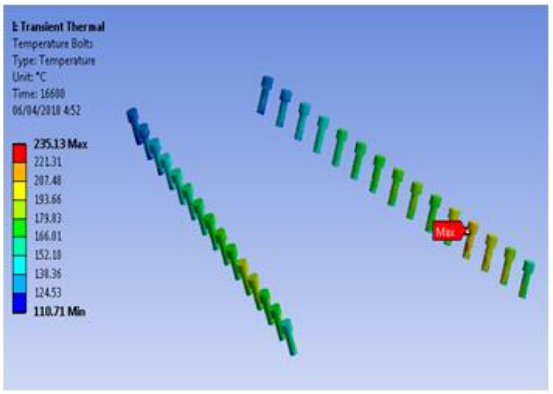	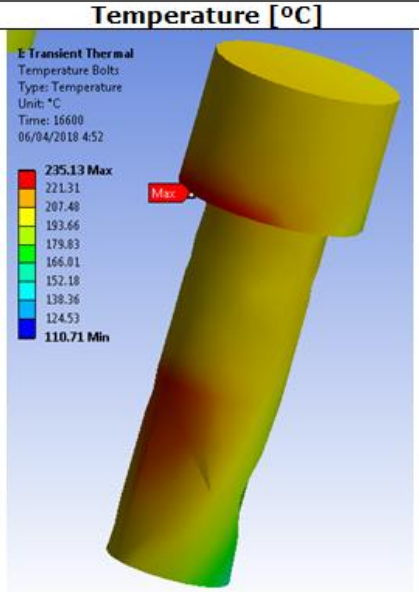

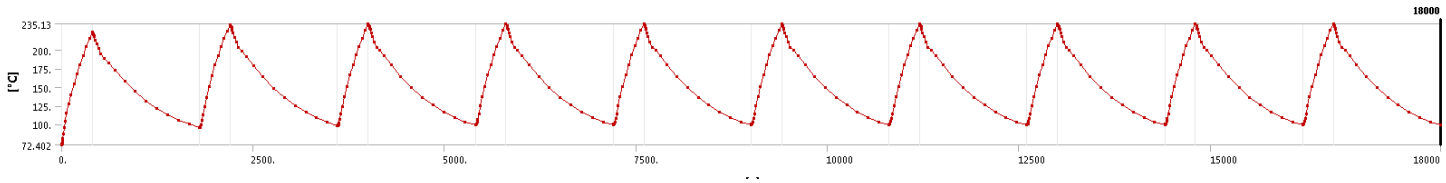

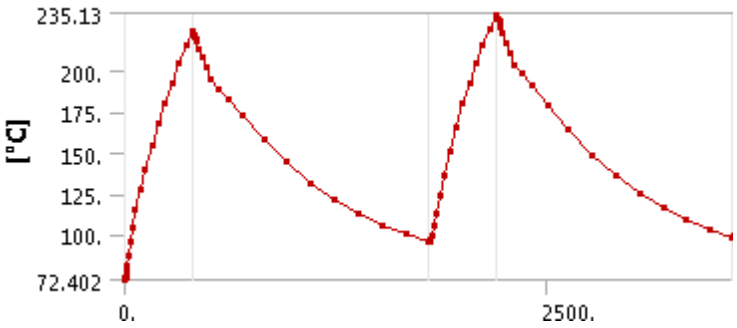

Figure 44: Inconel Bolts, temperature vs time

CuCrZr Heat Sink

Table 20: CuCrZr Heat Sink, temperature map distribution at its maximum time moment

Temperature [ºC]	Temperature [ºC]
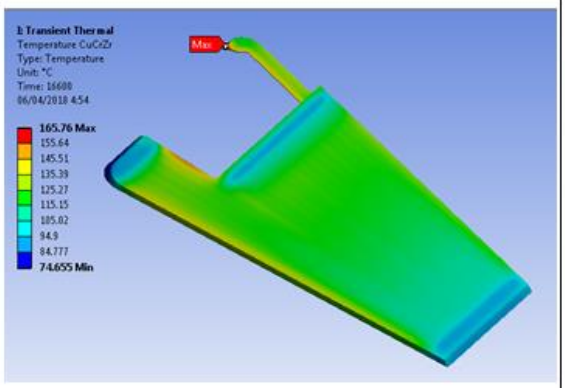	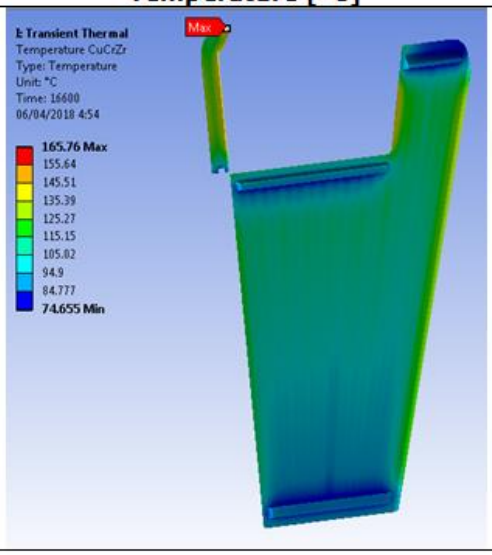

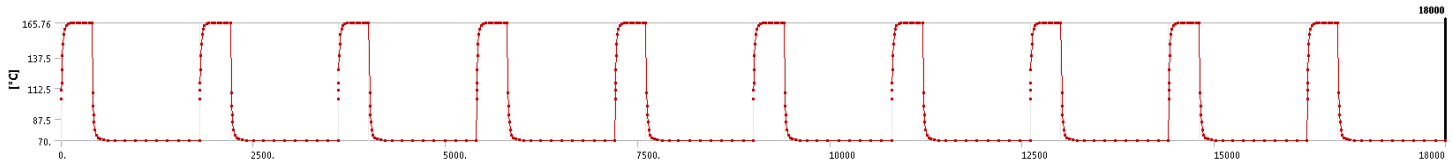

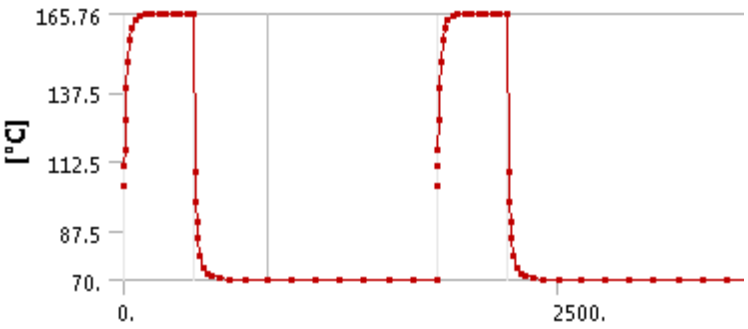

Figure 45: CuCrZr Heat Sink, temperature vs time

We can observe that there is no temperature inertia at any part of the BSM, and that after each pulse the temperature comes back to its initial value. And that the most critical situation is just after the pulses, where the maximum temperatures are reached.

CHAPTER 11: TRANSIENT VS STEADY-STATE

The main reason to perform a transient simulation is to detect inertia temperature problems in case of a pulsed operation, which has been verified on "Chapter 10". However, this transient analysis is also intended to verify that using a steady state simulation, is good enough to predict the temperature time response of the system. So, in this point we will discuss the differences between the results obtained with the steady state simulation vs the mechanical transient one.

Table 21: Steady state vs Transient results

Transient	Steady State
Temperature [ºC]	Temperature [ºC]
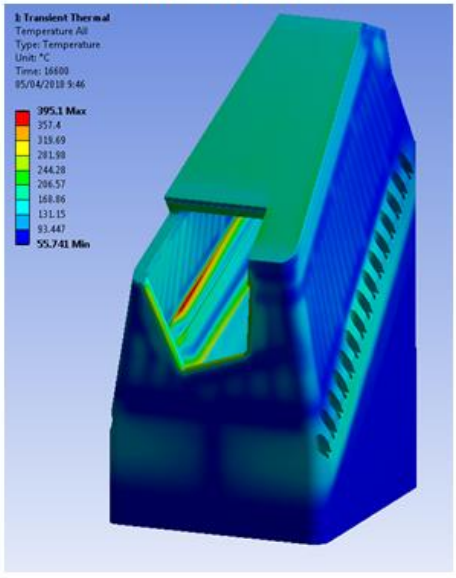	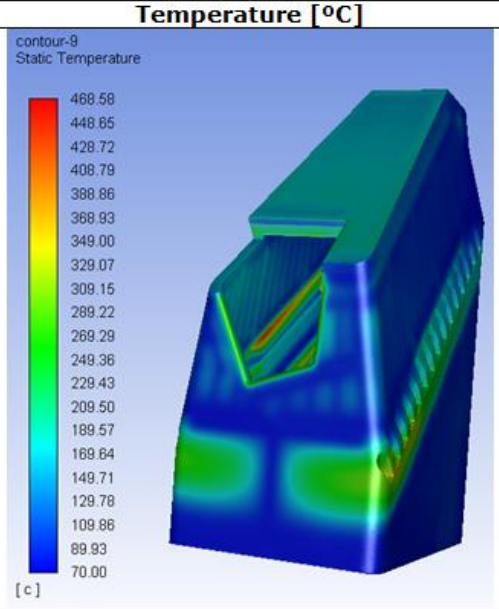

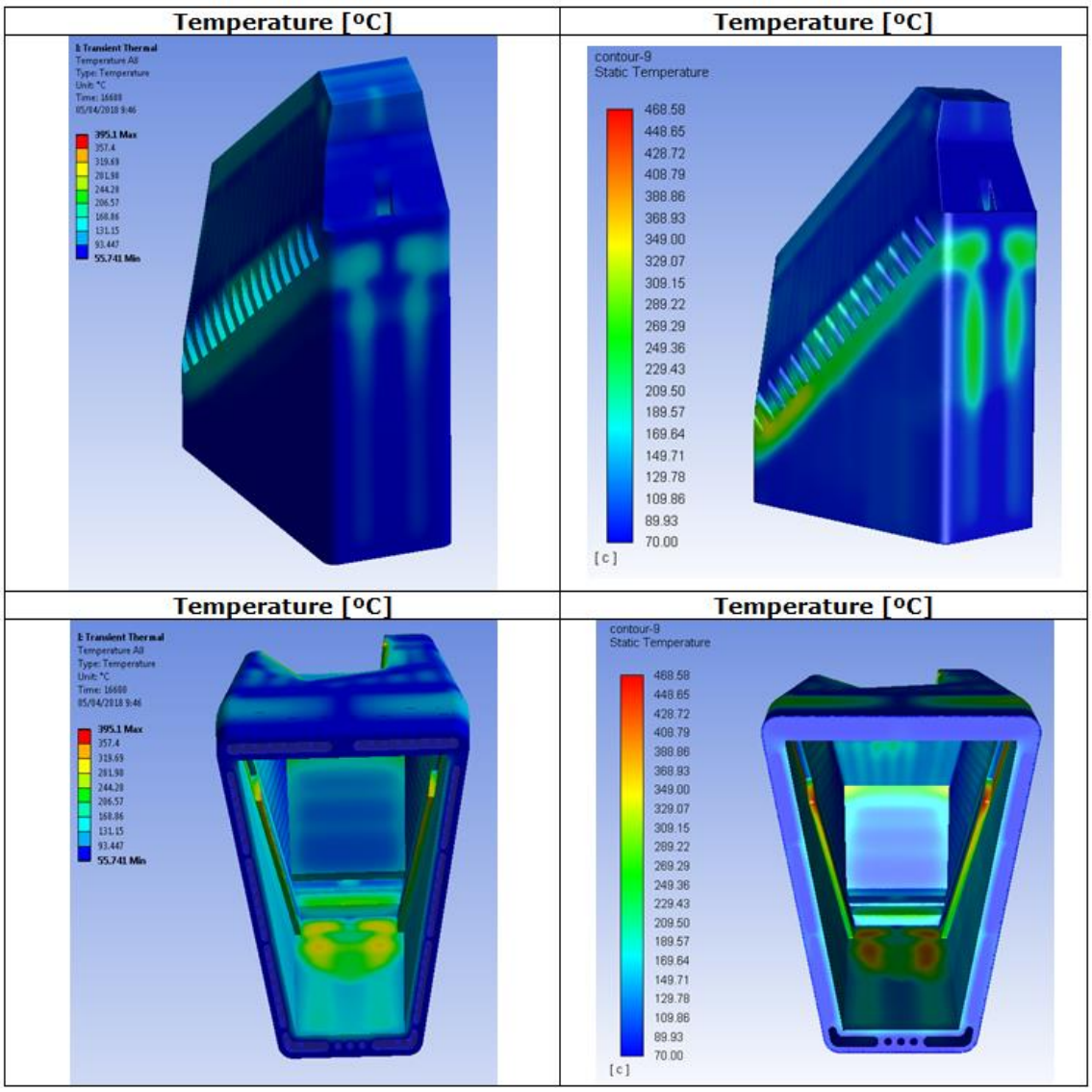

We can verify that in both cases we are at the same order of temperatures and with an equivalent temperature distribution. However, quantitatively speaking, we are getting lower temperatures on the transient simulation, meaning that the 400s of action of the inductive operation are not enough to reach the steady-state, meaning that the system is not yet in thermal equilibrium.

Therefore using a steady simulation we are predicting with good accuracy the temperatures distribution, and overestimating the reality in terms of temperature values.

CHAPTER 12: BUDGET

This chapter details the budget of a study similar to the one performed on this thesis, a thermal-hydraulic analysis for the assessment of a component.

It is an approximate budget made with the help of internet information, product catalogues and contacting experts and companies in the sector with the objective of determining the most reliable and representative price of the project.

This budget represents how it would be a budget for a company that wants to hire a study like the one carried out in this project. For its calculation four factors, personnel costs, machine use costs, software use costs, and industrial benefit will be taken into account.

In order to determine the personnel costs, it is assumed that the average price per hour of an engineer in Spain is approximately 25 €/h, and it has been tried to estimate the hours devoted to each section in order to obtain the total cost.

To calculate the costs of using software and machinery, the total value of the machinery and programs used is not taken into account, but rather the value proportional to the hours of use.

And finally, in relation to industrial profit, it is estimated at 7% of the total costs.

12.1. Software Cost

The software used to perform the analysis, has been ANSYS 18.0, which is considered one of the best softwares in the technical analysis sector. From this program, mainly three subprograms have been used:

- Ansys Meshing 18.0: to perform the mesh of geometry
- Ansys Fluent 18.0: to perform the steady-state CFD simulation
- Ansys Mechanical 18.0: to perform the transient mechanical simulation

An official half-year license to use all the Ansys programs described above has an approximate cost of 60,000€, this entails a cost of 14.88 €/h, in this project, it has been invested 2,016 hours of ANSYS 18.0 Software usage, which includes the time spent on the realization of all the meshes, the simulations set-up, the calculation time of the simulations and the post-processing time. All this adds up to a cost of software usage of **29,998.06€.**

12.2. CPU Cost

To be able to use a design and simulation program such as Ansys in a fluid way, it is necessary to have an important computing capacity; therefore it is essential to have high-performance computers. Throughout the project, a workstation of 150GB RAM and 24 CPU has been used, which can perfectly have a cost around 3,000€. If it is estimated that the project lasts for 6 months and that it is intended to amortize the computer in three years, the cost for its use, which has been half a year, it can be estimated in about **500€.**

12.4. Analysis Cost

12.4.1. Mesh Cost

The realization of several meshes, has meant an investment of 50 hours, and therefore represents an economic cost of **1,250€.**

12.4.2. Simulations Costs

The time devoted to the pre-processing and post-processing of the simulations and extraction of results involved a cost of 65 hours, which corresponds to an economic cost of **1,625€.**

12.6. Preparation of the documentation

12.6.1. Elaboration of the memory

The elaboration of the report of the thesis, which explains in detail the methodology followed, the results obtained and the conclusions extracted, a dedication about 50h is considered, which implies a cost of **3,750 €.**

12.6.2. Preparation of the presentation

Finally, the budget includes the time used to prepare a presentation, in order to expose in a summarize and visual way the work carried out in the project and conclusions obtained. It is estimated a dedication of 40h, which means a price of **1,000€.**

12.7. Total Budget

This section summarizes the different costs of the budget.

Table 22: Project Budget

Software Cost	
Software	€ 29,998.06

CPU Cost	
CPU	€ 500.00

Personnel Cost	
Analysis Cost	€ 2,875.00
Report and Presentation Elaboration Cost	€ 4,750.00
	€ 7,625.00

Total Costs	
Sofware Cost	€ 29,998.06
CPU Cost	€ 500.00
Personnel Cost	€ 7,625.00
	€ 38,123.06

Industrial Benefit (7%)	€ 2,668.61
	€ 40,791.67

IVA (21%)	€ 8,566.25
TOTAL	**€ 49,357.93**

12.8. Economic viability

The realization of a thermal-hydraulic study of the behaviour of the Upper-Launcher Antenna by computational simulations, requires an approximate cost of about 50,000 € from the point of view of the company that contracts the services.

It should be taken into account that studies of these characteristics carried out by professional engineering companies for customers could have a higher price that the one calculated on this project, because they can be more complex studies requiring more simulations, more studies, etc.

The question that we want to answer on this section is "Is it worth for a company to hire studies like the one carried out on this project?”

It is a fact that the cost that for a company implies to contract these types of analysis implies an important investment. However, the final purpose to perform computational simulations in that project is to validate the design and ensure its correct operability before the real operation starts when a failure is not affordable. Without computational simulations the only way to validate the component is by experimental test through prototypes. Which implies also an important cost, not only a specific test facility is needed, but also the construction of prototypes. Additionally, it should be taken into account that the experimental tests require a certain amount of time, with personnel costs to perform and control the tests.

However, to answer the question, it is necessary to compare the cost of the computational analysis with the expenses that the study would have had, did in an experimental way. An experimental study requires complex mechanical work on the machine to be test, such as the incorporation of sensors to measure and capture the changes in speed, pressure, etc., of the fluid. Additionally, it should be taken into account that the experimental tests require a certain amount of time, which implies having a machine stopped during the study, which for the company can mean an important cost, as well as the need of qualify personnel to perform and control the tests campaign. Computational calculations does not require any physical prototype, less personnel working on it, and a duration usually less than an experimental test, representing at the end an inferior cost.

However, it is important to emphasize that any study in computational simulations is not 100% reliable since simulating the reality requires the need of certain hypotheses to simplify the complexity of the calculation. Normally, these types of studies are carried out as a prior analysis, in order to have an idea of what is a good design and where the critical areas are located, in order to be able to perform after a more focused experimental study. In this way the costs of an experimental campaign are optimize and reliable with a good economic viability.

CHAPTER 13: CONCLUSIONS

This section presents the conclusions obtained during the realization of each phase of the project, as well as small conclusions of interest that have been detected.

Steady State CFD Analysis

Overall the cooling performance of the BSM seems to be good except for some peaks of ~460ºC at the internal part of the BSM (Figure 46). However this peaks are expected to be lowered with a new and improve view factor (surface thermal loads) calculation that has to be done with all the BSM internal elements as well as with the BSM external blankets elements.

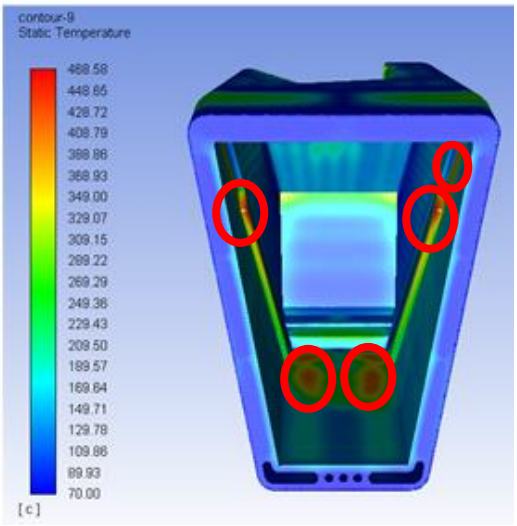

Figure 46: Critical zones due to over temperature

In relation with the lack of cooling on the region where the BSM is attached to the rest of the BSM (Figure 47), it is recommended in order to avoid any kind of thermal stresses, to introduce some extra cooling pipes on those regions, to enhance the cooling on the bolts region.

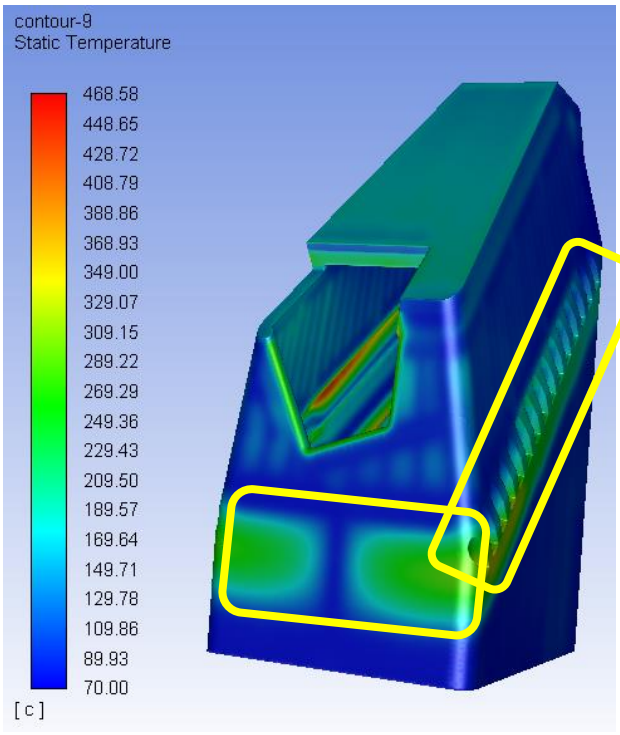

Figure 47: Lack of cooling

Another critical point, it is the ~360ºC on the Inconel Bolts (Figure 48). With the extra cooling pipes recommended on that region, a temperature decrease is expected. However, we highly recommend to change the material of the bolts from "Inconel" to "Stainless-Steel Grade 660". The bolts are under a constant stress condition, making them a high important part, due to its mission to keep the BSM joined to the rest of the Upper Launcher. So its failure can end-up to a major accident. The Grade 660 Stainless Steel is a precipitation hardening iron, base super alloy designed for applications requiring high strength up to ~700ºC.

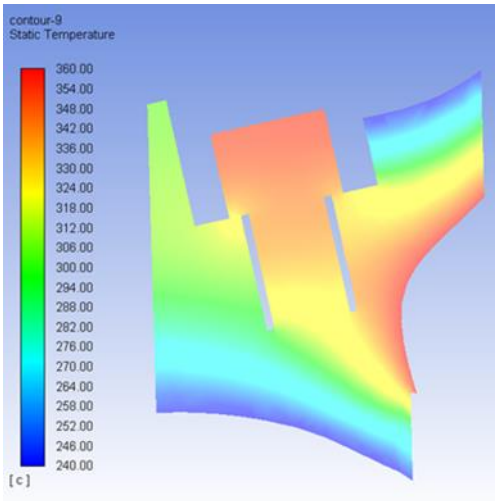

Figure 48: Critical Temperature on the bolts

Another undesirable effect, has been the not proper distributed flux inside the BSM Shell Side channels, which can end-up in internal thermal stresses due to high ΔT between channels. Figure 49, represents a section plane on the BSM Shell Side, where the solid part between channels has been colourised with the temperature and the water inside the channels has been colourised with the flux velocity, to detect easily that the channels where the velocity is almost 0m/s, the material around it have higher temperature than in the other channel with higher velocities ("in red circles on Figure 49"). However, in the worst case we are speaking of a maximum ΔT between channels of ~10ºC, which is not enough ΔT to generate critical thermal stresses.

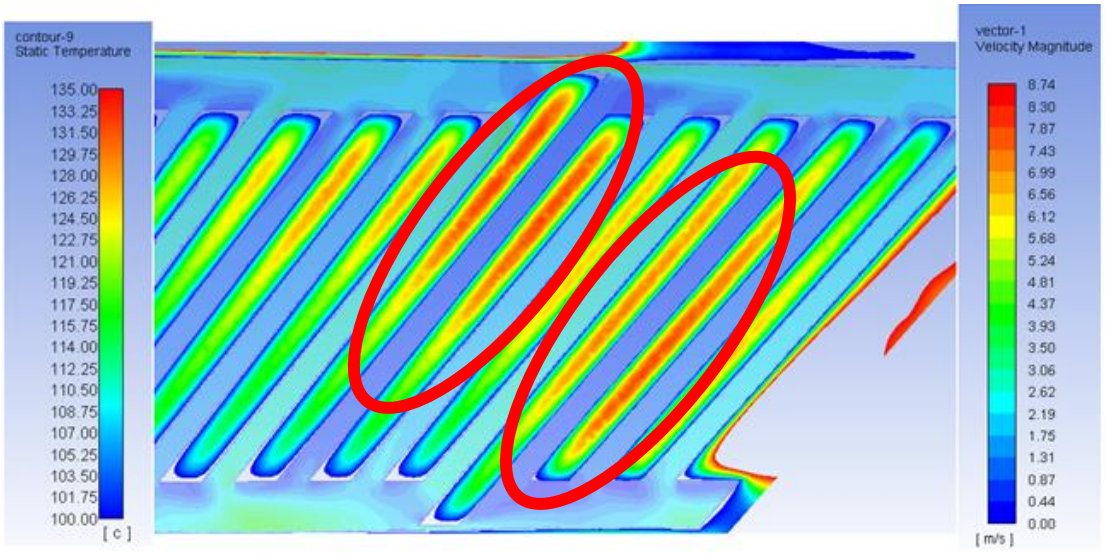

Figure 49:Not homogenous cooling on the BSM Shell side

Nonetheless, all this temperature distribution map of the BSM has to be used as an input for a mechanical stresses and displacements analysis, in order to completely verify and asses that we are always under the limits and that the ITER requirements are met.

Sensitivity analysis

On section 7 we have verified that the results shown on section 6 don't depend on the number of mesh elements, so for future analysis there is no need to use a refine mesh that will increase considerably the computational time and the CPU power needs. With the main mesh the results are practically the same with negligible differences compere with the refine mesh. The main difference is that using the main mesh the temperatures are a bit higher as maximum of 10 ºC, so by using the main mesh we are in a more conservative solution, which is in terms of safety quite good.

Mechanical transient analysis

The main issue to study with a transient is the possibility to get temperature inertia in a pulsative operation. This is not the case at any part of the BSM as we have observed on section 10 (Figure 50).

Moreover we have verified that a steady state simulation it is good enough due to we are predicting with good accuracy the temperatures distribution and slightly overestimating the reality, which is always good to have a conservative approach in terms of safety margins.

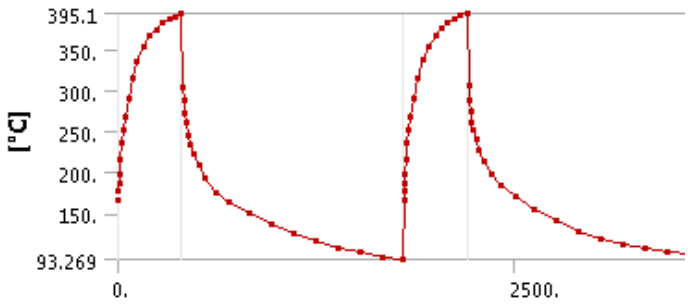

Figure 50: Maximum BSM Temperature evolution with time

Project future continuity

The next step will be to redesign the Antenna taking into account the results of that project, now it is known where are the critical parts, which are the main concerns, and a qualitative and quantitative idea about the Antenna cooling capabilities.

Once the redesign will be done, more thermal-hydraulic simulations and calculations will be needed in order to validate and asses the new model. All this will be repeated until the design will fully meet with ITER requirements.

However, a satisfactory outcome for the thermal-hydraulic analysis doesn't mean a satisfactory one for the mechanical-stresses and displacements. Even if the redesign comes from a different part that it is not the thermal-hydraulic one, another thermal-hydraulic validation will be needed, for example a material that is good for electromagnetic forces could not be good for cooling capabilities.

This project is just the first step or one part of the whole different analysis that a component needs to passed to be validated.

CHAPTER 14: BIBLIOGRAPHY

[1] What is Fusion? Last access May 25, 2018.
http://fusionforenergy.europa.eu/understandingfusion/

[2] ITER. Last access May 25, 2018.
http://fusionforenergy.europa.eu/understandingfusion/

[3] ITER Goals. Last access May 25, 2018.
https://www.iter.org/proj/inafewlines#1

[4] Plasma Heating. Last access May 25, 2018.
https://www.iter.org/sci/PlasmaHeating

[5] Electron Cyclotron Resonance Heating (Gyrotron). Last access May 25, 2018.
http://fusionforenergy.europa.eu/mediacorner/newsview.aspx?content=1218

[6] 'Cooling design and analysis of the ITER EC Upper launcher'
Authors: P. Spaeh, G. Aiello, A. Meier, T. Scherer, S. Schreck, D. Strauss, A. Vaccaro. Institute of Applied Materials KIT Karlsruhe, Germany
2015 IEEE 26th Symposium on Fusion Engineering (SOFE)

[7] CFD. Wangda Zuo. *Introduction of Computational Fluid* Dynamics.
[http://erivera-2001.com/MEC-2249/NAVIER_STOCKS_Zuo_paper.pdf]

[8] Navier-Stokes Equation. Last access May 25, 2018.
https://spaceflightsystems.grc.nasa.gov/education/rocket/nseqs.html

[9] Environmental Impact. Last access May 25, 2018.
https://www.iter.org/mach/safety

[10] The advantages of a polyhedral mesh. Milovan Peric, Stephen Ferguson. CD-adapco. *The advantage of polyhedral meshes.* [https://pdfs.semanticscholar.org/51ae/90047ab44f53849196878bfec4232b291d1c.pdf]

[11] Discretization Methods. Last access May 25, 2018. https://knowledge.autodesk.com/it/search-result/caas/CloudHelp/cloudhelp/2014/ITA/SimCFD/files/GUID-12A9AED8-2047-4D3A-BC80-82BE9CF47517-htm.html

[12] Solution Methods. Last access May 25, 2018. https://www.sharcnet.ca/Software/Fluent6/html/ug/node998.htm

[13] Wall Y+. Last access May 25, 2018. *https://www.cfd-online.com/Wiki/Dimensionless_wall_distance_(y_plus)*

[14] NIST. "Water Properties". Last access May 25, 2018. https://webbook.nist.gov/chemistry/fluid/

[15] Master on Nuclear Engineering academic material

[16] ITER Tokamak (Figure 1). Last access May 25, 2018. https://elperiodicodelaenergia.com/idom-desarrollara-el-diseno-de-diagnosticos-en-el-proyecto-iter-de-fusion-nuclear/

[17] Boundary Layer Mesh Methods (Figure 36). Last access May 25, 2018. https://www.computationalfluiddynamics.com.au/tips-tricks-inflation-layer-meshing-in-ansys/

CHAPTER 15: Annex

15.1 Coordinates of the Contours Planes

- FWP Back plate Pipes

	X	Y	Z
Point [m]:	6.609965	0.2	4.044804
Normal:	-0.606043	0	-0.795432

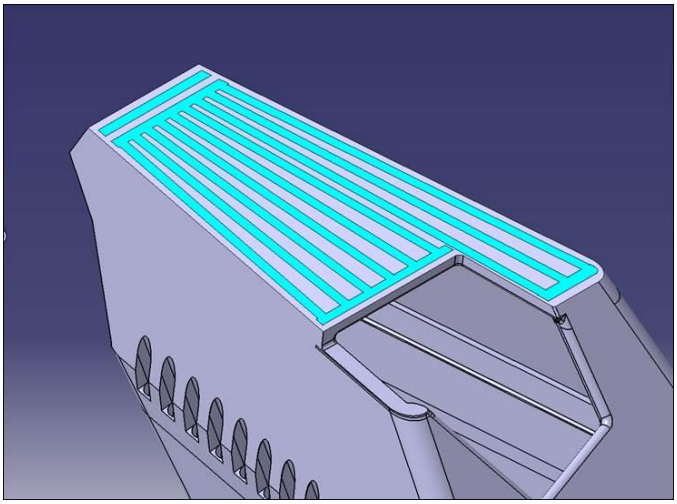

Figure 51: FWP Back plate Pipes

- BSM Shell Side

	X	Y	Z
Point [m]:	6.461848	-0.25496	4.214227
Normal:	-0.173648	-0.984808	0

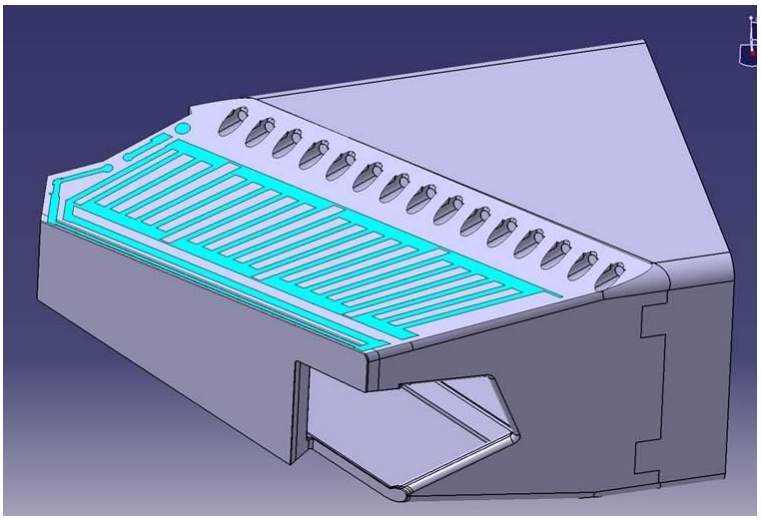

Figure 52: BSM Shell side

- BSM Shell Bottom

	X	Y	Z
Point [m]:	6.95893	-0.2257	4.038265
Normal:	0.190809	0	-0.981627

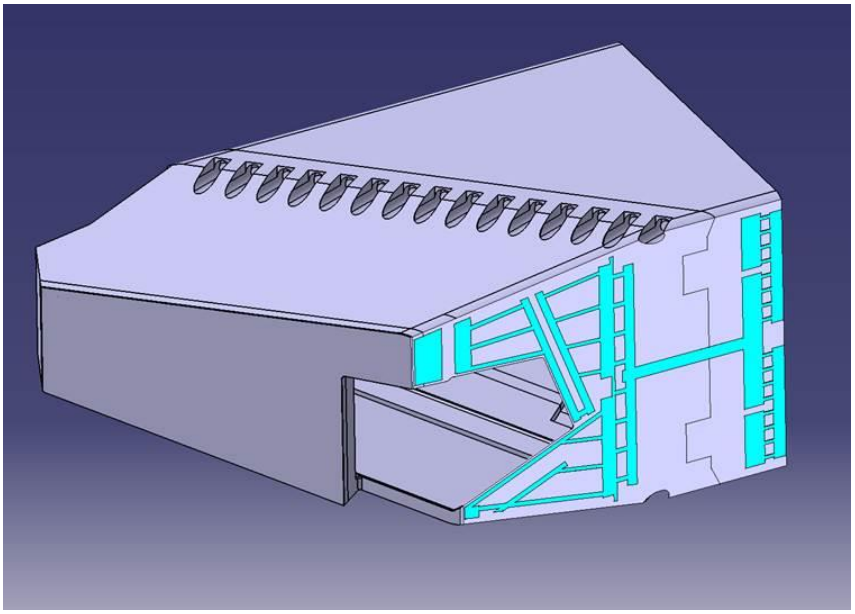

Figure 53: BSM Shell Bottom

- First Wall Panel front pipes

	X	Y	Z
Point [m]:	6.650117	-0.28626	3.971467
Normal:	0.606043	0	0.795432

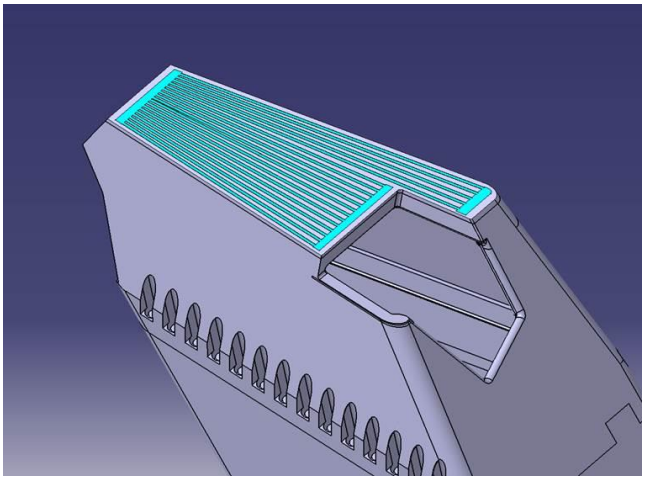

Figure 54: FWP front Ppies

- Central XZ plane:

	X	Y	Z
Point [m]:	5.807	0	4.596
Normal:	0	1	0

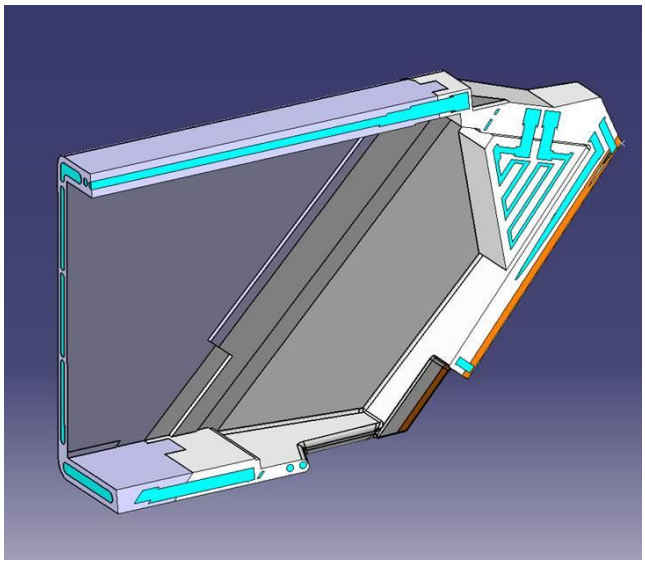

Figure 55: Central XZ plane

- Flange Perpendicular plane through bolt : (right side of the BSM looking form the plasma)

	X	Y	Z
Point [m]:	7.042	-0.365	4.380
Normal:	0.787912	-0.137175	-0.600314

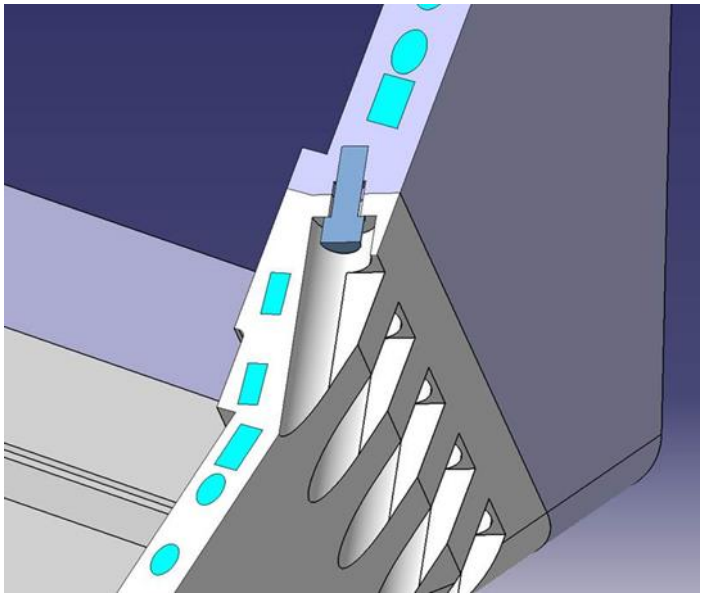

Figure 56: Flange Perpendicular plane through bolt

15.2 Internal Contour Maps – Sensitivity Analysis

Main Mesh	Refine Mesh
Temperature [ºC]	**Temperature [ºC]**
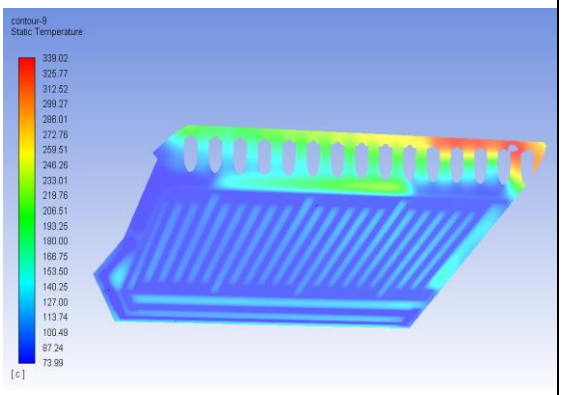	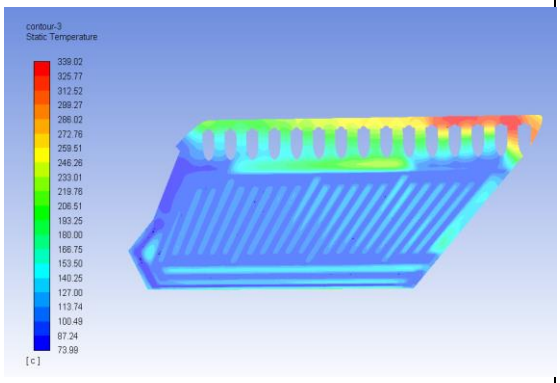
Temperature [ºC]	**Temperature [ºC]**
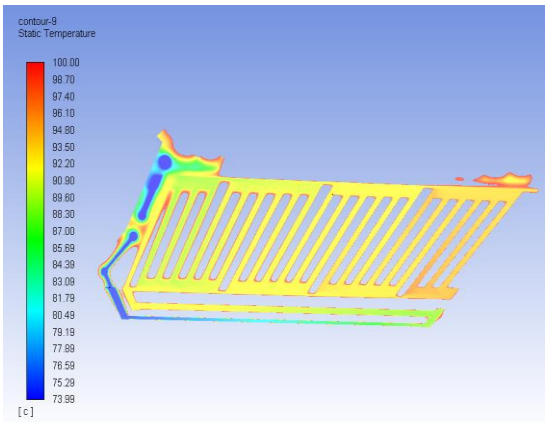	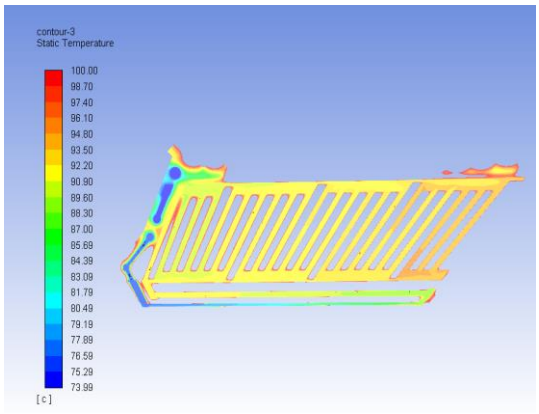
Velocity [m/s]	**Velocity [m/s]**
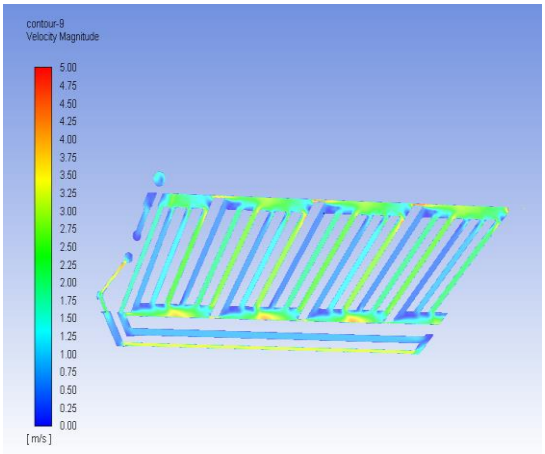	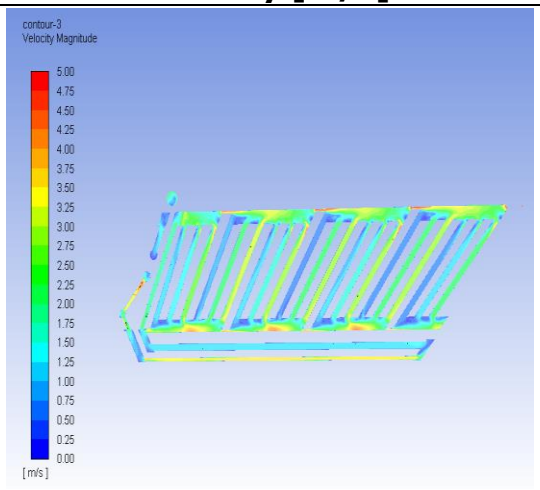

Pressure [Pa]	**Pressure [Pa]**
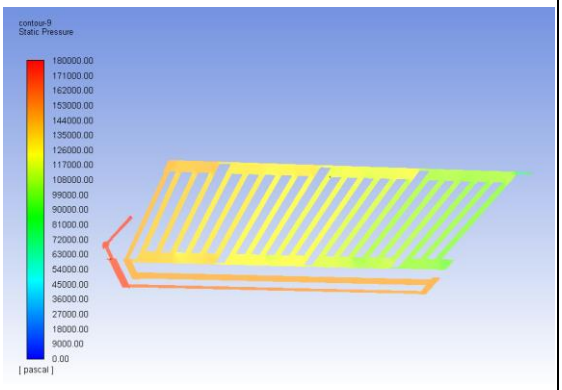	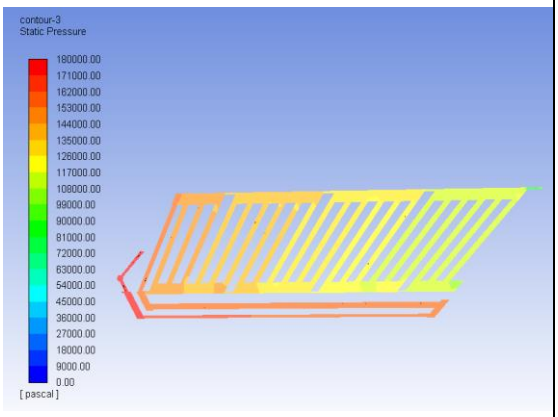
Temperature [ºC]	**Temperature [ºC]**
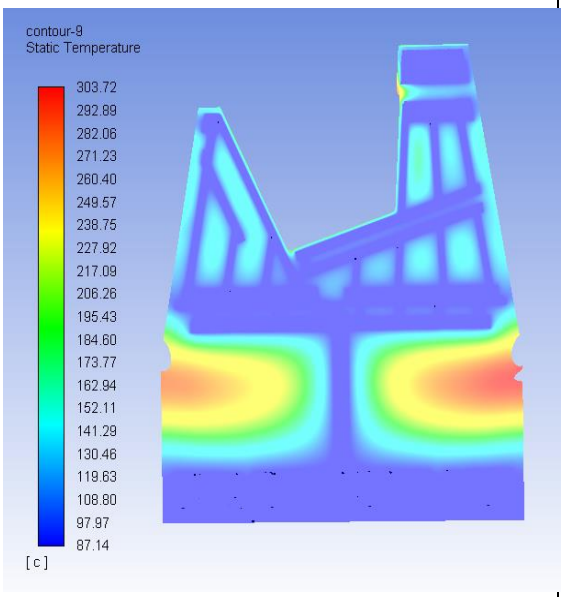	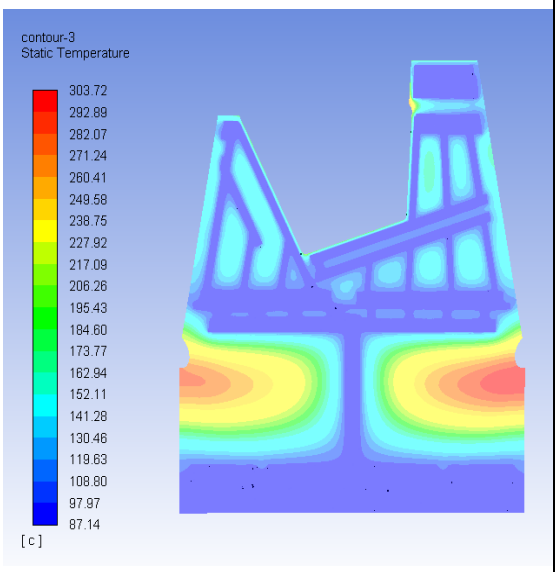
Temperature [ºC]	**Temperature [ºC]**
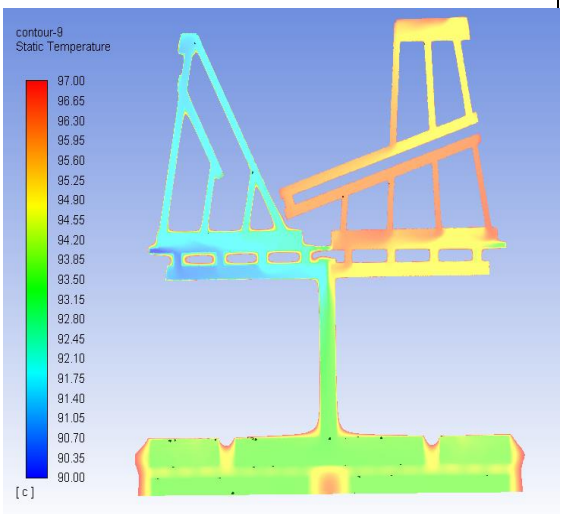	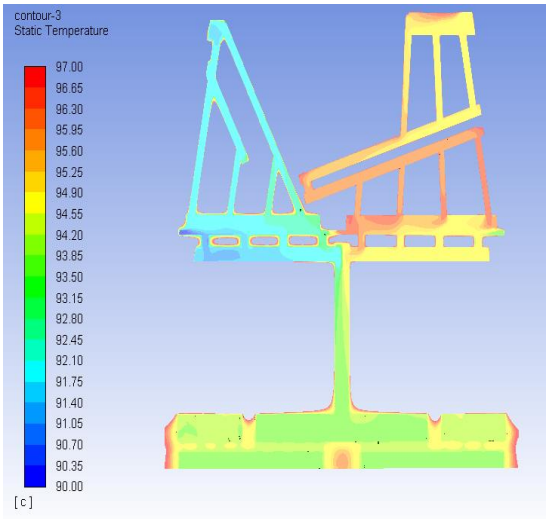

Velocity [m/s]	Velocity [m/s]
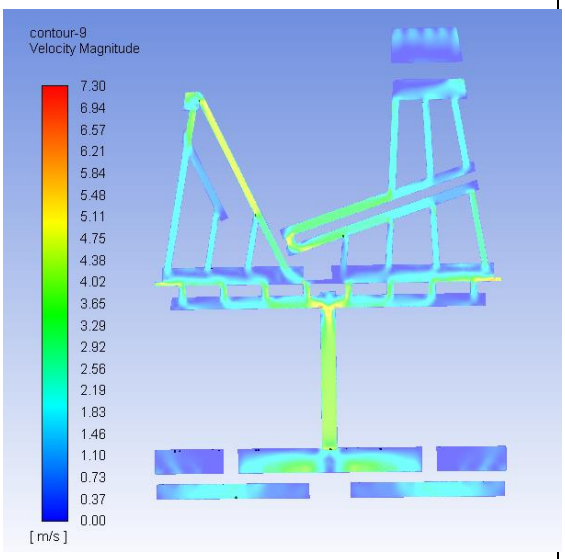	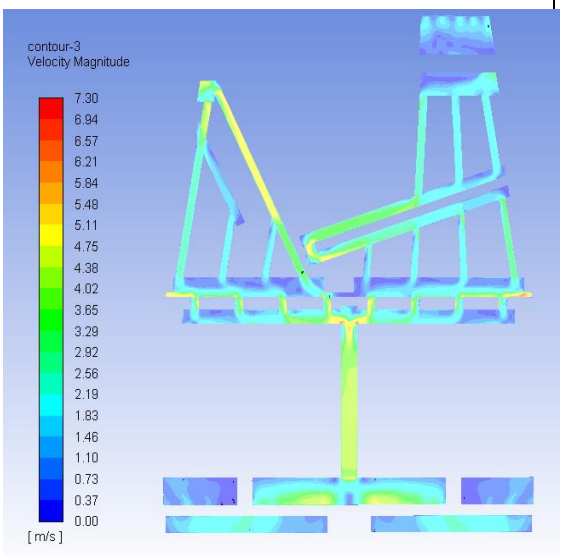
Pressure [Pa]	**Pressure [Pa]**
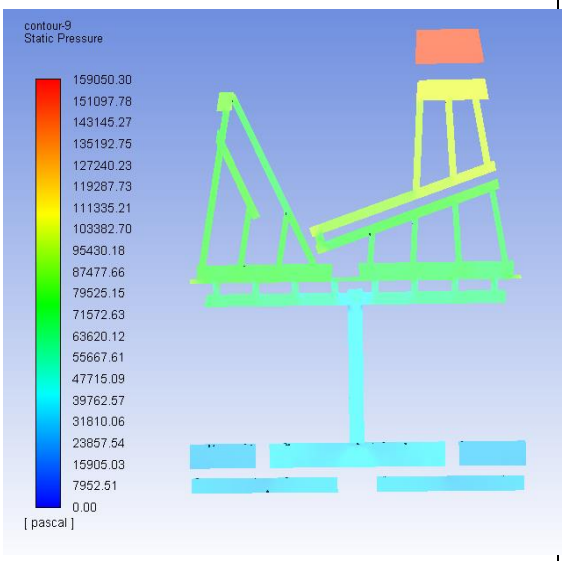	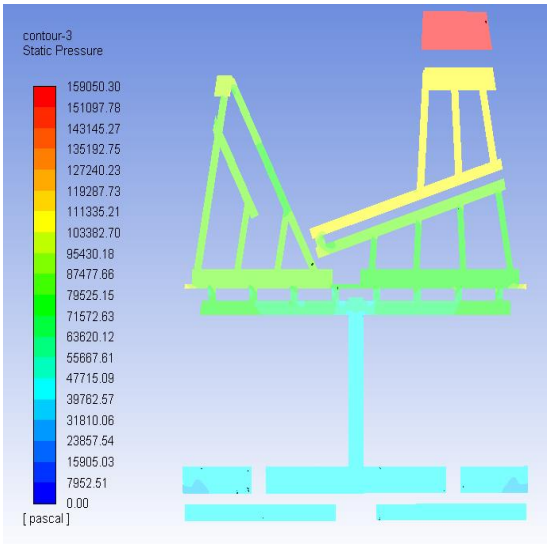
Temperature [ºC]	**Temperature [ºC]**
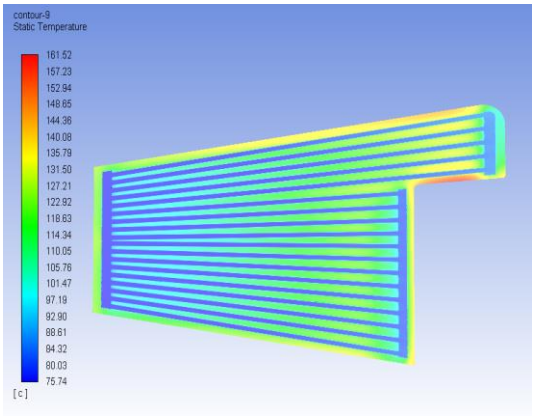	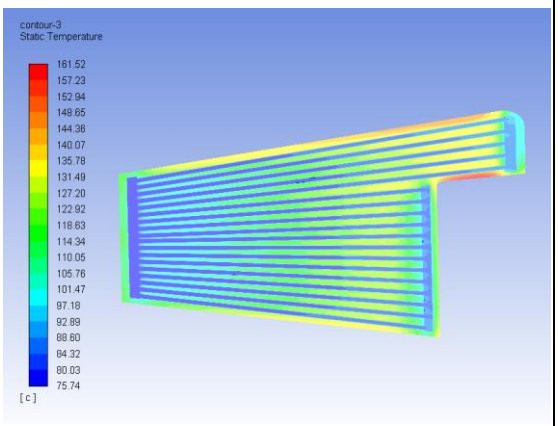

Temperature [ºC]	Temperature [ºC]
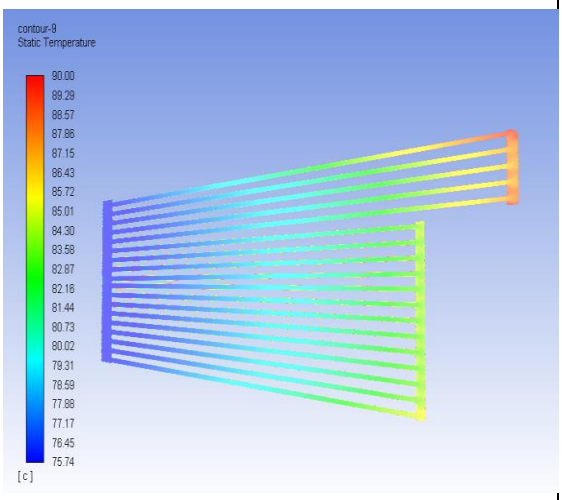	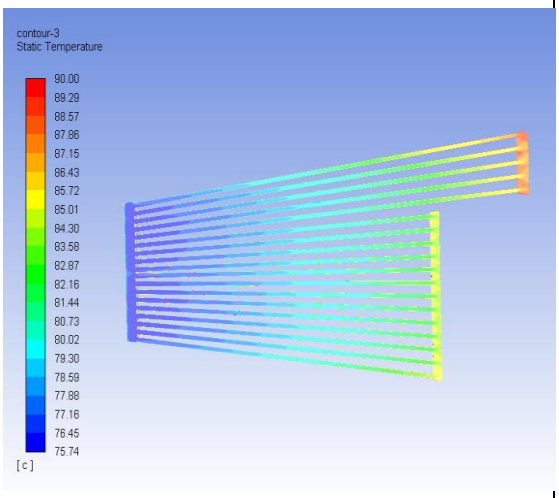
Velocity [m/s]	**Velocity [m/s]**
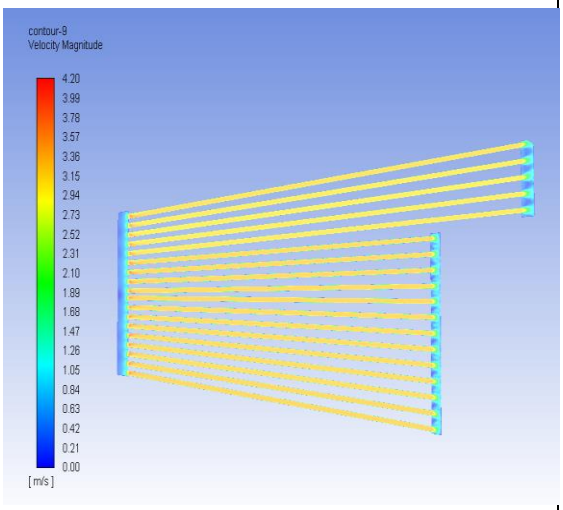	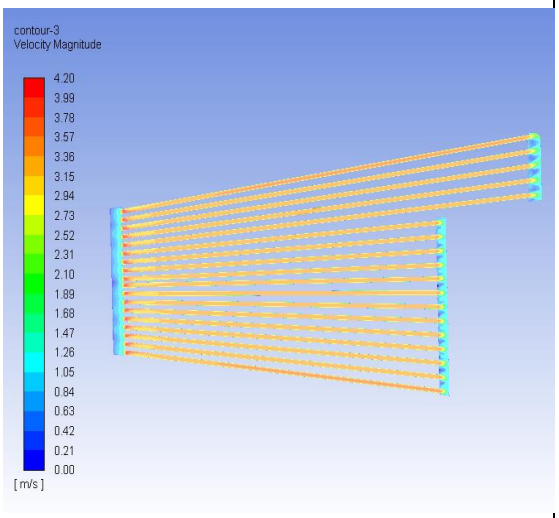
Pressure [Pa]	**Pressure [Pa]**
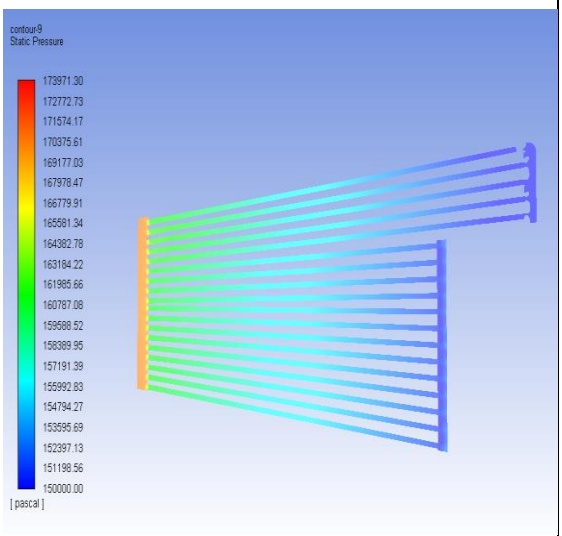	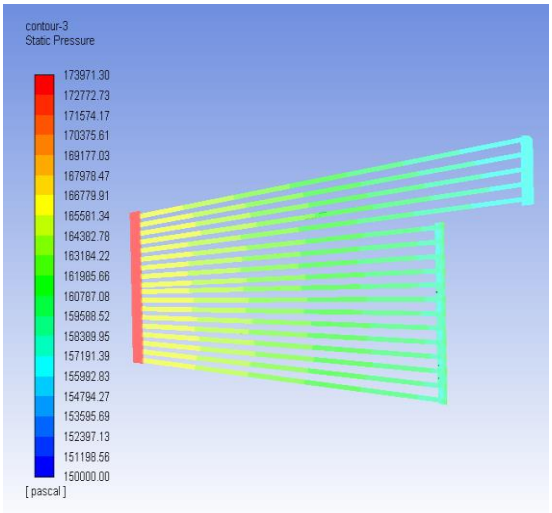

Temperature [ºC]	Temperature [ºC]
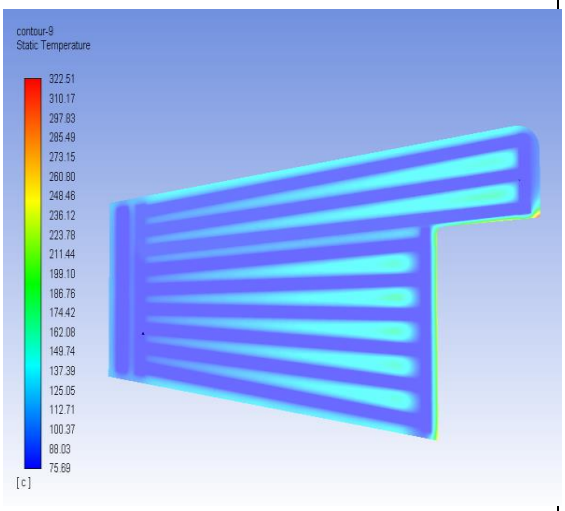	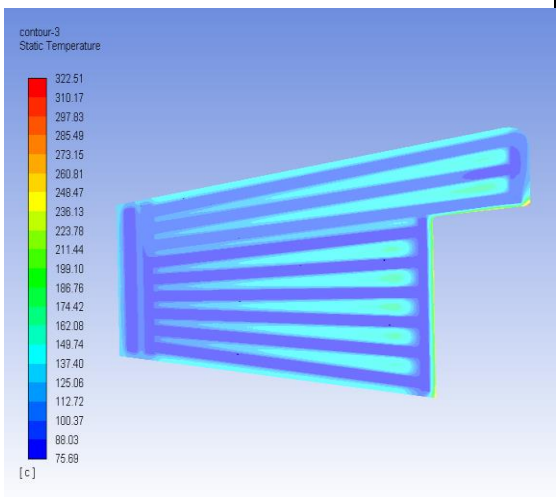
Temperature [ºC]	**Temperature [ºC]**
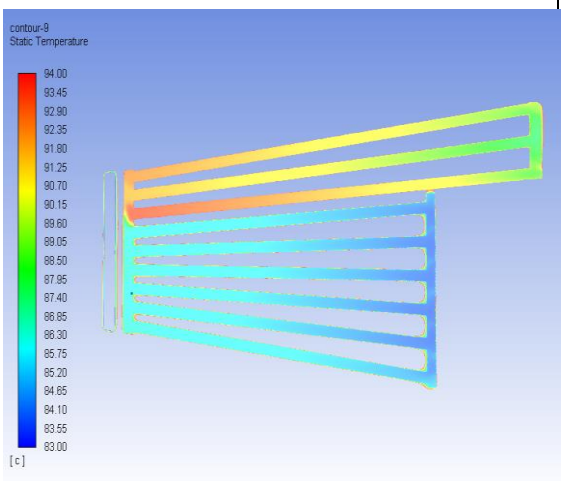	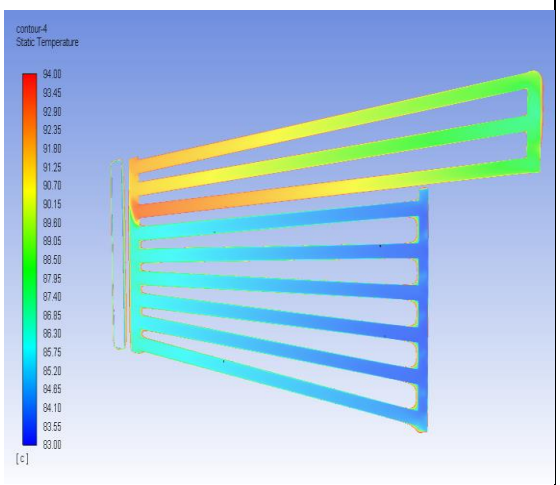
Velocity [m/s]	**Velocity [m/s]**
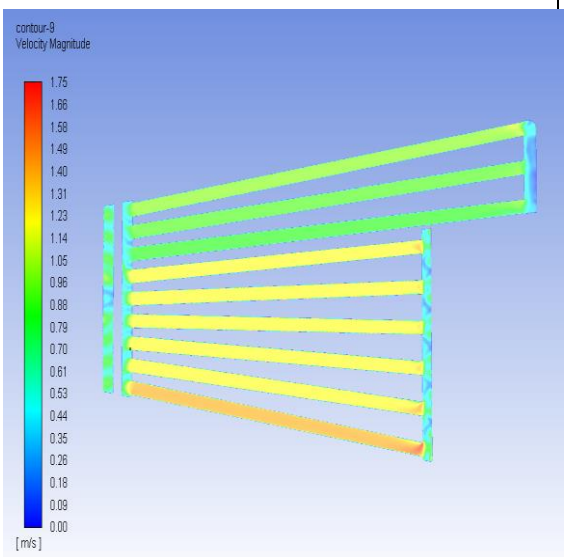	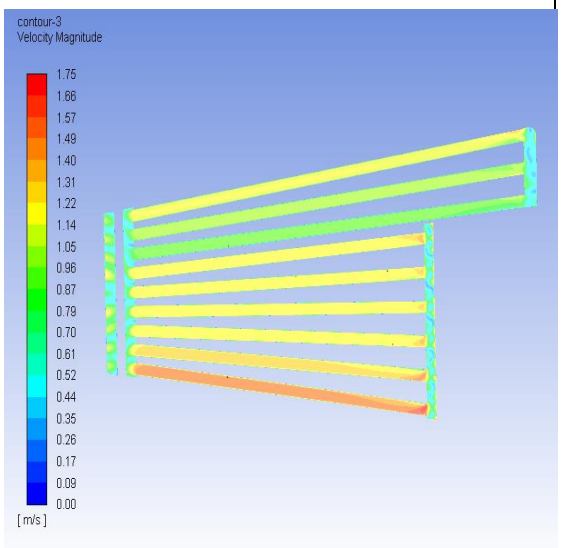

Pressure [Pa]	**Pressure [Pa]**
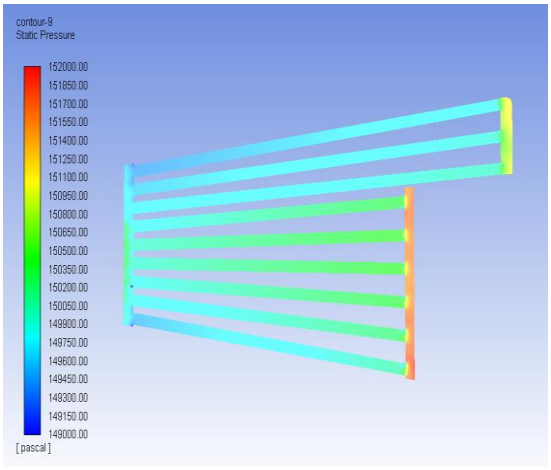	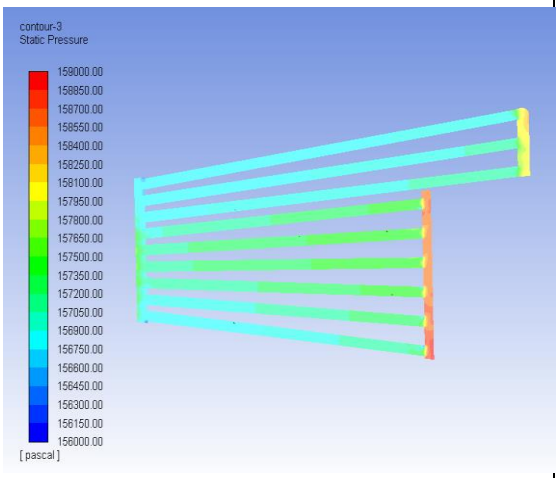
Temperature [ºC]	**Temperature [ºC]**
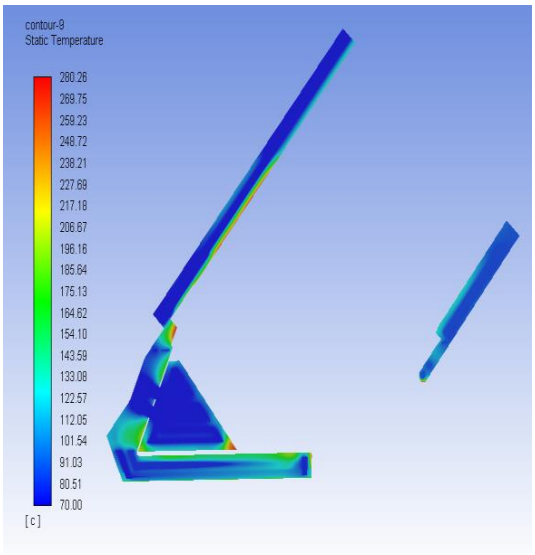	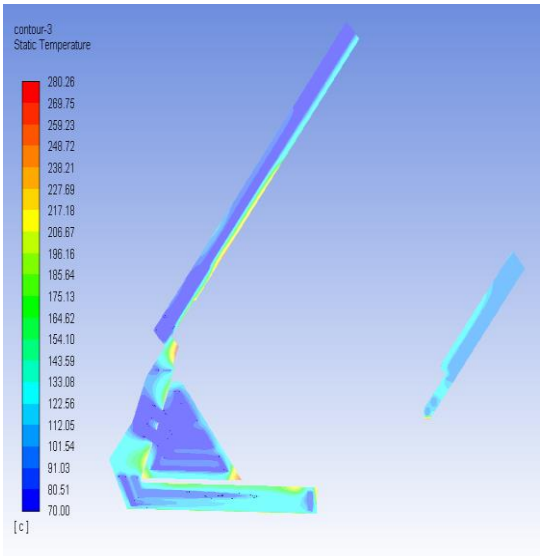
Temperature [ºC]	**Temperature [ºC]**
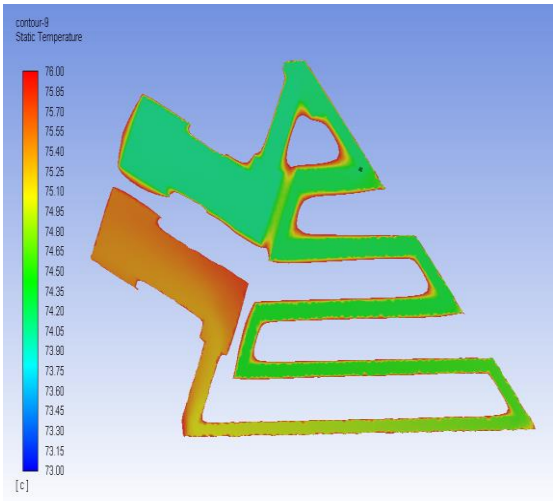	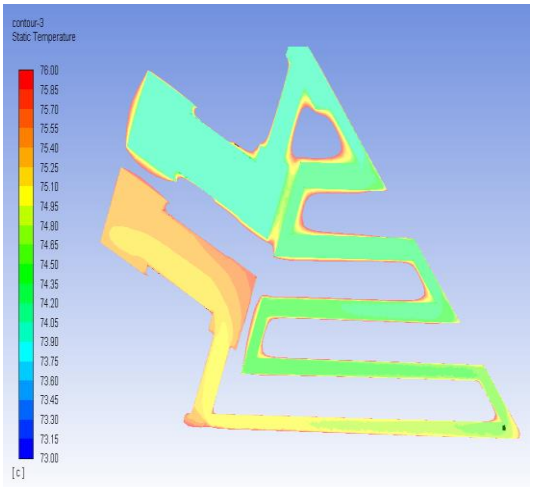

Velocity [m/s]	Velocity [m/s]
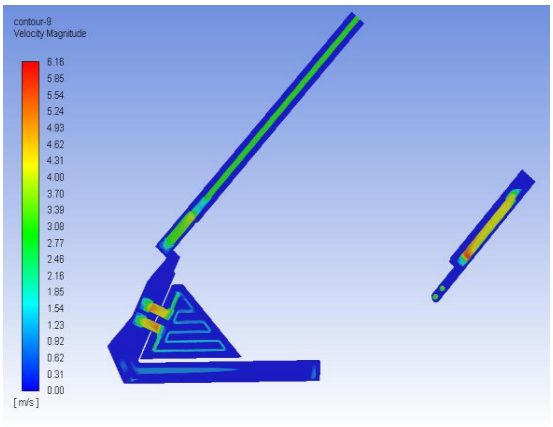	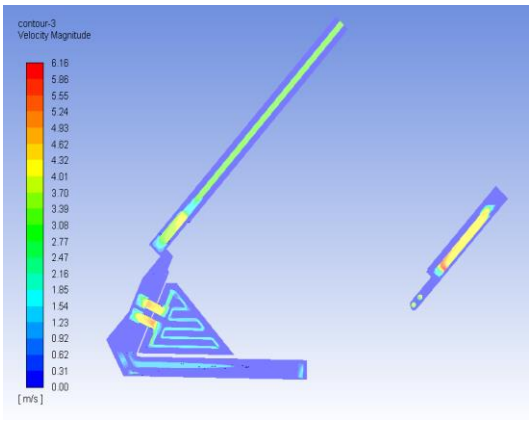
Pressure [Pa]	**Pressure [Pa]**
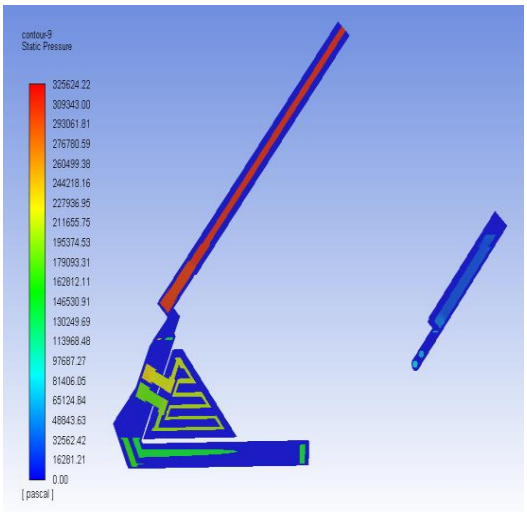	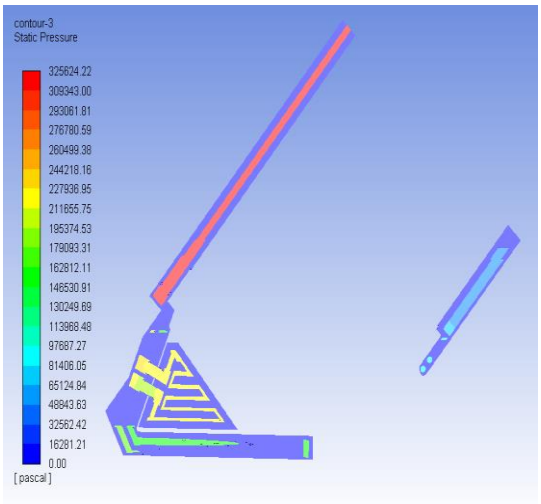
Temperature [ºC]	**Temperature [ºC]**
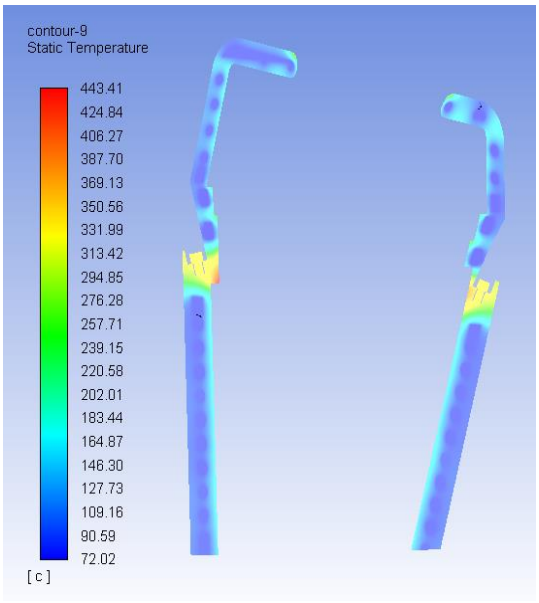	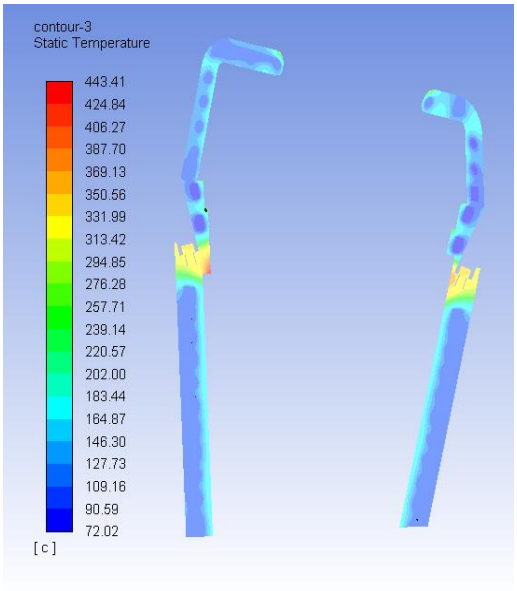

Temperature [ºC]	Temperature [ºC]
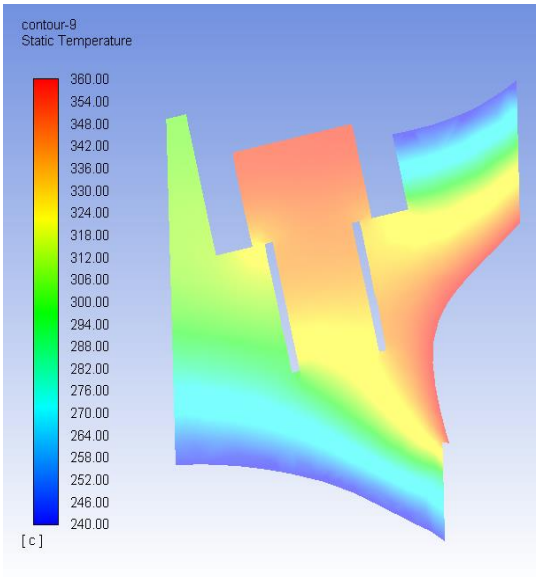	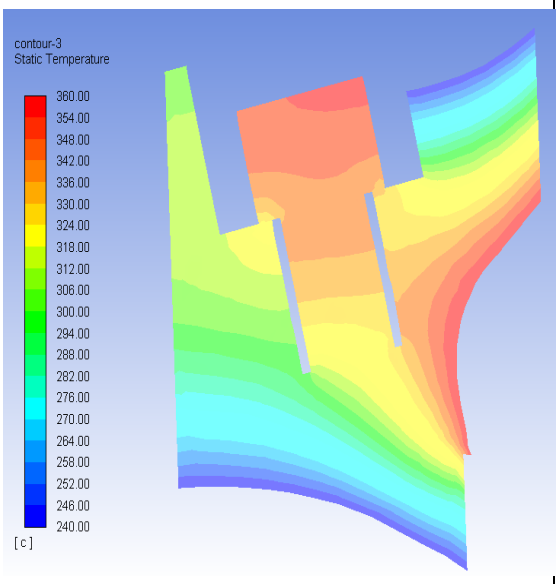

15.3 Use a vtk file as nuclear heating on Ansys fluent

In order to use a vtk. file to be interpolated as nuclear heating on Ansys Fluent, the following steps have been followed:

1. Open the *.vtk file on Paraview
2. Check if the *.vtk file use point data and not cell data, if this is not the case use the filter → Cell Data to Point Data
3. Check if the *.vtk file has the same coordinates and the same scale than the CAD model that will be use on Fluent. If this is not the case use the filter → Transform
4. Execute a python macro (for confidentiality issues this macro will not be shown) in order to convert the *.vtk file into a *.ip file. Use the filter → Programmable Filter. Copy the python macro and apply. (An *.ip can be read in Ansys Fluent a *.vtk file can not.)
5. Open Fluent
6. Build an UDF (Figure 57)
7. Read mesh or case
8. Add AT LEAST one User-Defined Scalar (UDS) and one User-Defined Memory (UDM)
9. On User-Defined Scalar (UDS) solution zone select the proper zone where we want to interpolate the nuclear heating, in our case the solid parts.
10. Set up your case as much as possible and Initialize the solution.
11. Load the UDF
12. Use File → Interpolate to interpolate the SOURCE data (*.ip filer) into UDS-0
13. Use Execute on demand (UDF name) to copy UDS-0 into the UDM-0

WARNING: If you initialize the solution, the UDM0 will be zeroed and this source term will be lost. You will have to reinterpolate the UDS0 and execute the DEFINE_ON_DEMAND function (copy_uds_to_udm) again to set the source term.

```
#include "udf.h"

DEFINE_ON_DEMAND(copy_uds_to_udm)
{

Domain* d = Get_Domain(1);
Thread* t;
cell_t c;

thread_loop_c(t,d)
{
begin_c_loop(c,t)
{
C_UDMI(c,t,0) = C_UDSI(c,t,0);
}
end_c_loop(c,t);
}

return;
}

DEFINE_SOURCE(my_source,c,t,dS,eqn)
{

real source;

dS[eqn] = 0.0;

source = 1e6*C_UDMI(c,t,0);

return source;

}
```

Figure 57: Fluent UDF to copy uds to udm